



Department of Precision and Microsystems Engineering

**Active Vibration Control of Smart Structures using
Fractional-order Control**

L. Marinangeli

Report no : MSD 2016.030
Coaches : Dr. S.H. HosseinNia, Dr. F. Alijani
Professor : Prof. Dr. Ir. J.L. Herder
Specialisation : Mechatronic System Design
Type of report : Master Thesis
Date : November 30, 2016

Active Vibration Control of Smart Structures using Fractional-order Control

by

Luca Marinangeli

For the degree of Master of Science in Mechanical Engineering
at Delft University of Technology,
to be defended publicly on Wednesday December 14, 2016 at 13:00 AM.

Student number: 4420144
Department : Precision & Microsystems Engineering (PME)
Project duration: January 11, 2016 – December 14, 2016

Thesis committee:	Prof. Dr. Ir. J.L. Herder,	TU Delft
	Dr. H. HosseinNia,	TU Delft, supervisor
	Dr. F. Alijani,	TU Delft, supervisor
	Dr. M. Abdalla,	TU Delft

An electronic version of this thesis is available at <http://repository.tudelft.nl/>.

Summary

In the past decades research on Active Vibration Control (AVC) has found increasing interest in control of flexible thin-walled structures, mainly made of new advanced materials such as composite carbon fibre. These types of composite structures combine high stiffness with good flexibility in achieving complex shapes, and are mostly used in automotive and aerospace applications where they are often subjected to undesirable vibrations. In the field of AVC, a new type of sensor and actuator have become popular by using so-called *smart materials*, such as piezoelectric materials. Given their distributed nature, they can be easily mounted on different types of structures, thus making them *smart structures*. State-of-the-art controllers, such as Positive Position Feedback (PPF), are very sensitive to spillover effect due to uncontrolled vibration modes, and therefore they are found to be difficult to tune in the case of multi-mode control. Another important aspect regarding the controller is that, apart from being able to reduce structural vibrations, it should ensure robustness and closed-loop stability for the controlled system. In this sense, careful positioning of sensors and actuators can have a great influence.

With the motivation of improving on the limitations of state-of-the-art controllers, in this thesis a novel AVC strategy based on fractional-order calculus is proposed, developed, and successfully applied in practice.

First, a fractional-order Positive Position Feedback (PPF) compensator is proposed to overcome the limitations of the commonly used integer-order PPF such as: frequency spillover, amplitude amplification in quasi-static region of the closed-loop response, and difficult tuning in multi-mode control. Tuning parameters of the controller are obtained by optimizing both magnitude and phase response of the controlled plant. Results are shown by comparing performances of the standard integer-order PPF and the optimized fractional-order PPF, both on a simple 1-DOF plant and on measured frequency response data from a rectangular carbon fibre/epoxy composite plate with free edges.

Secondly, a second version of the fractional-order PPF is proposed, and compared to the other controllers for the AVC of a rectangular carbon fibre/epoxy composite plate with free edges. The plate is excited orthogonally by a modal vibration exciter and controlled by Macro Fibre Composite (MFC) transducers. Vibration measurements are taken with a Laser Doppler Vibrometer (LDV) system. MFC actuator and sensor are positioned on the plate based on maximal modal strain criterion, in order to control the second natural mode of the plate. Both integer and fractional-order PPFs allow for the second mode to be effectively controlled, although the newly proposed fractional-order controllers are found to be more efficient in achieving the same performance with less actuation voltage, and more promising in reducing the spillover effect due to uncontrolled modes.

Dedicato alla mia famiglia

Preface

Since I was only a child, I have manifested a strong curiosity for technology and science in general. It is thanks to that curiosity that I decided I wanted to become an engineer, so I started my university studies in Rome. During my bachelor's degree I gained a lot of knowledge, but I was missing the hands-on experience that I have always thought an engineer should have. I wanted to make and work on something cool! So I moved abroad, to the Netherlands, to pursue my master degree at TU Delft, one of the best technical universities in the world.

I chose to study in the faculty of Mechanical, Maritime and Materials Engineering (3mE), in one of the most multidisciplinary and challenging master tracks such as PME. Here I could finally bridge the gap between theory and practice by choosing a very challenging and interesting graduation topic. In almost one year, I have been able to work on a fairly new theoretical subject such as fractional-order control, develop a control strategy never used before, and apply it both in simulations and experiments. And hopefully this will result in one, or maybe two, scientific publications. Looking back at all this, I must definitely say that I have worked on something very cool!

Luca Marinangeli
Delft, November 2016

Acknowledgements

Hereby I would like to express my gratitude to everyone who contributed directly or indirectly to this thesis.

Hassan HosseinNia Thank you for being my supervisor and introducing me to the world of control. At the beginning of my project, I was very sceptical about focusing too much on control. Nevertheless, with your extensive explanations I managed to extend my knowledge in this field, and I am glad to have done so.

Farbod Alijani Thank you for being my supervisor and spending an incredible amount of time to 're-build' the Engineering Dynamics lab. Thank you for giving me the possibility to work with such state-of-the-art equipment for vibration measurements.

Dennis de Klerk Thank you for helping me out with the PAK system and for the useful discussions about my experimental setup.

Jo Spronck Thank you for your interest in my project and for sharing your knowledge with me. Your discussions during the group meetings have been always very useful.

Rob Luttjeboer Thank you for the assistance in the lab and for ordering components.

Harry Jansen and Patrick van Holst Thank you for the fun times building my setup. I will never forget all your technical advices, discussions about football, and other fun topics!

Max Roest Thank you for the time spent in the lab learning together how use the laser vibrometer, and for telling me your enthusiastic stories about guitars.

Martijn Krijnen Thank you for the discussions about fractional-order control.

Marius, Anton, Stefan and Gijs Thank you for the fun time spent together in the office during the past year. A good working environment was essential to complete my project.

PME and MSD group Thank you for the constructive discussions during the group meetings.

Giovanni Ferrari Thank you for sharing your knowledge about AVC. It helped me a lot to quickly set up my experiments.

Vittorio Garofano Thank you for listening to my stories almost every day, and thanks for the feedback as a 'control guy'.

Giorgio Fagioli Thank you for all your 'technical' support during these 2 and half years we spent together in the Netherlands.

My family Thank you for your love and unconditional support. It's because of you that I could achieve my goals during the entire university career.

My Italian friends Thank you for coming (or at least having tried to come) all the way to the Netherlands to celebrate my graduation together.

My 'Dutch' friends Thank you for being the best part of this awesome journey!

Contents

Summary	i
Preface	v
Glossary	xiii
List of Acronyms	xiii
List of Symbols	xiii
1 Introduction	1
1.1 Background	1
1.2 Problem definition	2
1.3 Thesis objective	4
1.4 Research approach	4
1.5 Thesis Outline	5
2 Literature Review and Theory	7
2.1 Active vibration control of flexible structures	7
2.1.1 Spillover effect	9
2.1.2 Collocated modal control	10
2.1.3 Direct Velocity Feedback	11
2.1.4 Resonant Control	12
2.1.5 Positive Position Feedback	15
2.1.6 Controllers comparison	19
2.1.7 Other control algorithms	20
2.2 Smart materials and structures	21
2.2.1 Piezoelectricity & transducers types	21
2.2.2 Control of smart structures with piezoelectric sensors & actuators	23
2.3 Placement of piezoelectric sensors & actuators	24
2.3.1 Maximal modal force rule	24
3 A Fractional-order Positive Position Feedback Compensator	27
3.1 Introduction	28
3.2 Problem definition	30
3.3 Proposed method	31
3.4 Illustrative example	33
3.5 Conclusions	34

4	Active Vibration Control of a Carbon Fibre Composite Plate	37
4.1	Introduction	38
4.2	Control	39
4.3	Experimental Setup	43
4.4	Implementation of AVC	46
4.5	Conclusions	49
5	Discussion	53
5.1	Why PPF and Why Fractional-order control?	53
5.2	Fractional-order PPF #1 and #2	53
5.3	Spillover: from simulation to practice	54
5.4	Correction gain effect	54
6	Conclusions & Recommendations	57
6.1	General conclusions	57
6.2	Recommendations for future research	58
A	Appendix	59
A.1	Non-linear Vibrations	60
A.2	Modal Analysis software	61
A.3	Carbon fibre/epoxy plate production process	62
A.3.1	Material Properties	63
A.4	MFC transducer bonding procedure	63
A.5	High Voltage wires	63
A.6	COMSOL modelling	64
A.6.1	Carbon fibre/epoxy plate	64
A.6.2	MFC piezoelectric patch transducer	64
A.7	Signal conditioning piezoelectric sensors	64
A.8	Control system robustness against mistuning	65
A.9	Controlled time response	65
A.10	Effect of the long-time action of the piezoelectric actuator	66
A.11	CRONE implementation	67
A.12	Simulink model	67
A.13	Fractional-order PPF Optimization - MATLAB Code	68
A.13.1	Objective	68
A.13.2	Constraints	68
A.13.3	Optimization	69
B	Datasheets	71
B.1	Vibration Exciter	72
B.2	Impedance Head	73
B.3	Polytec LDV System	74
B.4	dSPACE System	75
B.5	Smart Material MFC	76
B.6	Carbon Fibre Properties	78
B.7	Epoxy Adhesive for transducers bonding	79
B.8	High Voltage Wires	80

List of Figures

1.1	Smart Structure [1].	2
1.2	Illustrative example of a smart structure with different transducers configurations.	3
2.1	Time and frequency domain visualization of vibration modes [2].	7
2.2	Role of active damping in (a) System poles and (b) Dynamic amplification ($1/2\xi$) [1].	8
2.3	Feedback control of flexible structure consisting of a large number of elastic modes [3].	8
2.4	In-bandwidth and out-of-bandwidth modes [1].	9
2.5	Pole-zero pattern in a collocated system. (a) Undamped (b) Lightly damped ($1/2\xi$) [1].	10
2.6	Collocated frequency response function [1].	11
2.7	Feedback control of vibration with a collocated piezoelectric actuator/sensor pair.	11
2.8	DVF feedback loop.	12
2.9	RC feedback loop.	13
2.10	Bode plot of RC controller tuned at 20 Hz.	13
2.11	Bode plot of $G(s)$ with 1 st mode controlled by RC.	14
2.12	Bode plot of $G(s)$ with 2 nd mode controlled by RC.	14
2.13	PPF feedback loop.	16
2.14	Bode plot of PPF controller tuned at 20 Hz.	16
2.15	Bode plot of $G(s)$ with 1 st mode controlled by PPF.	17
2.16	Bode plot of $G(s)$ with 2 nd mode controlled by PPF.	17
2.17	PZT transducer from PI [28]: (a) Transducer detail (b) Cutaway.	22
2.18	MFC transducer from Smart Material [27]: (a) Transducer detail (b) Cutaway.	22
2.19	PZT working principle [28]: (a) Lateral contraction (b) d_{31} effect.	22
2.20	MFC working principle [27]: both d_{33} and d_{31} are available as operational modes.	23
2.21	Piezoelectric actuator bonded on the surface of a plate structure [34].	25
2.22	Surface elastic strain energy density plots of the first four mode shapes of a rectangular plate with all-edges-free boundary conditions: the red areas indicate maximum strain and can be considered as optimal locations for actuator placement.	25
5.1	2 nd mode at 38.5 Hz controlled by integer-order PPF and fractional-order PPF #1 and #2. In (a), correction gain $\gamma = 2.5$ is used for fractional-order PPFs and $\gamma = 6$ for integer-order PPF. In (b), same correction gain $\gamma = 6$ is used for each controller. FRFs are measured at the center of the plate.	55

A.1	Non-linear vibration response around the 1 st natural frequency obtained using stepped-sine testing with different forcing loads.	60
A.2	Carbon fibre/epoxy plate production process.	62
A.3	Effect of filter mistuning on the closed-loop: (a) controlled natural frequency at 50 Hz and filters tuned at 45 Hz; (b) controlled natural frequency at 50 Hz and filters tuned at 55 Hz.	65
A.4	Time history of velocity response for sinusoidal excitation at second natural frequency (38.5 Hz): fractional-order PPF is activated at approximately 8.6 s	65
A.5	Average spectrum of carbon fibre plate both with control off and on: the long-time action of the piezoelectric actuator causes frequency shifts in the uncontrolled modes.	66
A.6	Simulink block diagram.	67
B.1	Polytec Scanning Vibrometer system, [40].	74

List of Tables

2.1	Controllers comparison.	19
A.1	Polytec PSV software acquisition settings.	61
A.2	Carbon fibre/epoxy plate material properties.	63
A.3	Natural frequencies and damping ratios comparison for active and inactive control. . .	66
B.1	Scanning Head.	74
B.2	Vibrometer Controller.	74
B.3	dSPACE system.	75

Glossary

List of Acronyms

TU Delft	Delft University of Technology
3mE	Mechanical, Maritime and Materials Engineering
PME	Precision & Microsystems Engineering
MSD	Mechatronic System Design
AVC	Active Vibration Control
EMA	Experimental Modal Analysis
NLMA	Non-Linear Modal Analysis
DOF	Degree of Freedom
FRF	Frequency Response Function
SISO	Single-Input Single-Output
MIMO	Multi-Input Multi-Output
DVF	Direct Velocity Feedback
APF	Acceleration-Position Feedback
HMPVF	H_∞ Modified Positive Velocity Feedback
HMPPF	H_∞ Modified Positive Position Feedback
RC	Resonant Control
NPF	Negative Position Feedback
PPF	Positive Position Feedback
IRC	Integral Resonant Control
PZT	Lead Zirconate Titanate
MFC	Macro Fiber Composite
ADC	Analog-to-Digital Converter
DAC	Digital-to-Analog Converter
LDV	Laser Doppler Vibrometer
IFAC	International Federation of Automatic Control
JVC	Journal of Vibration and Control

List of Symbols

α	Fractional-order #1
β	Fractional-order #2
η	Controller modal coordinate
γ	Controller correction gain
λ	Variable of fractional-order characteristic polynomial
ω	Plant natural frequency
ω_f	Controller natural frequency
ξ	Plant modal coordinate
ζ	Plant damping ratio
ζ_f	Controller damping ratio
ζ_T	Closed-loop damping ratio
$C(s)$	Controller transfer function
$C_F(s)$	Fractional-order controller transfer function
f	Modal control force
g	Controller gain
$G(s)$	Plant transfer function
h	Objective function
k	Modal constant
$L(s)$	Open-loop transfer function
p	Penalization factor
P_1 & P_2	Half-power points
P_{\max}	Resonance peak magnitude
s	Laplace transform variable
S_G	Transfer function quasi-static gain
$T(s)$	Closed-loop transfer function
w_1 & w_2	Weighting parameters for objective function

1

Introduction

1.1 Background

Mechanical systems are often subject to undesired vibrations or dynamic loads which can alter their performance and operating conditions.

Mechanical vibrations can have detrimental effects of various natures: they might cause structural failure (e.g. mechanical parts undergoing fatigue, or building response due to earthquakes), or affect the comfort level in vehicles (e.g. noise and vibrations due to car suspensions), or limit the operating conditions of precision devices where even small sources of vibrations are to be restricted (e.g. optical systems). Design changes are thus often required to limit the effect of vibrations while maintaining an acceptable system performance.

As clearly explained by A. Preumont [1], *Vibration Suppression* can be achieved in different ways, depending on the specific type of application, and the most common are: stiffening, damping and isolation. *Stiffening* (or more in general *structural re-design*) consists of shifting a particular resonance frequency outside the range of interest by the application of structural modifications and optimization techniques. *Damping* consists of reducing one or more resonance peaks by dissipating the vibration energy, and it can either be achieved by using additional damping materials or mechanisms (passive damping), or by using a set of actuators, sensors and a control algorithm (active damping). *Isolation* instead consists of preventing the transmission of noise and vibrations where they are undesirable for the correct operation of the system.

Active Vibration Control of Smart Structures

Among different classes of mechanical structures, in this work a particular focus is given to thin-walled structures. Thin-walled structures are extensively used in today's industry mainly in the automotive and aerospace sector, where a lightweight design is often an important requirement, especially when aspects like energy consumption, ease of handling and high-speed operation are concerned. Large space structures like antennas, robots, or satellites, as well as aircraft rudders or automobile panels are examples of such applications.

However, these types of structures are very flexible and thus prone to undesirable vibrations.

To mitigate these effects, a damping solution is generally preferred. Passive damping would not be effective when reduced weight is of main concern, since the use of an additional damping mechanism, or material, would considerably increase the total mass of the structure.

Active damping is instead preferred in this scenario, where the integration of a set of sensors, actuators and a proper control scheme would not only solve a specific vibration issue, but it would make the full system adaptable to possible unknown disturbances and conditions.

The choice of sensors and actuators becomes crucial when an active damping solution is selected. In fact their size, performance and mode of operation are to be taken into account both for the integration with the structure to be controlled, and for the control scheme to be designed. In the past decades, in the field of Active Vibration Control (AVC) a new type of sensor and actuator have become popular by using so called *smart materials*, such as piezoelectric materials, shape-memory alloys, magnetostrictive, electroactive polymers etc. These materials are called *smart* because they are inherently capable of detecting or responding to changes in their environment, making them very suitable both for sensing and actuation purposes. Given their distributed nature, they can be easily mounted onto different types of structures, thus making them *smart structures* (see Figure 1.1). Nowadays, distributed piezoelectric sensors and actuators are extensively used for active vibration control of smart structures, because of their unique features such as: low cost, low mass, ease of integration and wide frequency range of control.

A thoroughly designed control scheme is also required to make sure that the full integration with the piezoelectric transducers and the flexible structure makes a robust, reliable and stable active vibration control system.

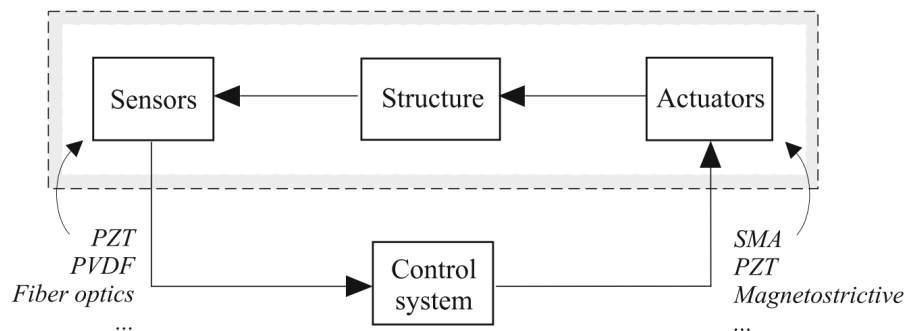


Figure 1.1: Smart Structure [1].

1.2 Problem definition

As mentioned before, from a control engineering perspective it is essential to have a controller which is, first of all, robust and stable from the theoretical design point of view, and secondly, applicable in practice while maintaining robustness and stability properties such that good performance in different conditions is guaranteed.

Spillover

When it comes to flexible structures, vibration control is often used to suppress specific modes of vibrations that are unwanted in a certain frequency range of operation; especially low to mid-frequency modes can be problematic because they usually occur with high amplitudes and have a rather simple shape, which is easy to trigger. Therefore, a lot of effort has been done to design controllers which can be *tuned* to suppress a specific or multiple resonance frequencies, so to directly target and solve the vibration issue as soon as it occurs without influencing other aspects of the dynamics of the system in question. However, this is not always the case, since the dynamics which are neglected can always have an influence on the performance of the controlled response by either limiting it or even causing instability.

This issue, in more technical terms, is known as *spillover effect* due to uncontrolled modes, which are those modes outside the bandwidth of the controller. Therefore, a main problem which is addressed in detail in this work is to limit spillover by a proper design of the control system.

Transducers' placement

However, spillover is not just a control-related issue, but it can also occur in practice when the controller interacts with the real structure via the sensing and actuation system.

For example, a sensor can measure the response caused by a vibration mode which is not intended to be controlled, or similarly the actuator can act on a mode which is not intended to be controlled. This cross-coupling between sensor and actuator will eventually result in the channelling of the control energy to the system dynamics which is neglected.

This problem is strictly related to the size, shape and placement of the distributed transducers equipping the smart structure. Therefore, another important issue which is covered in this thesis is the optimal size and placement of the piezoelectric transducers for spillover reduction and optimal control performance.

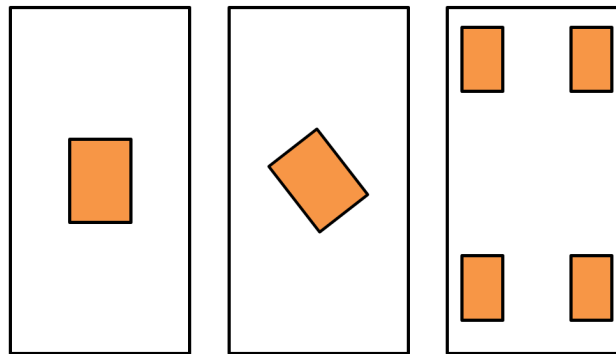


Figure 1.2: Illustrative example of a smart structure with different transducers configurations.

1.3 Thesis objective

The main goal of this thesis is a theoretical and experimental implementation of a novel active vibration control strategy. The aim is to suppress single/multiple vibration modes of a thin-walled flexible structure using optimal distributed actuation and sensing, paying particular attention to reduce the spillover effect caused by the dynamics of uncontrolled vibration modes.

Active vibration control with piezoelectric transducers has become very popular and an extensive literature is present. Most of the control techniques are now well established and they have been used for different types of applications, showing their advantages as well as their limitations. The fundamental motivation of this study is to tackle one of these limitations (spillover effect) under a different perspective, which has not extensively been addressed in current literature, in order to propose a novel approach and at the same time extend the know-how on a subject which still has plenty of room for future research.

1.4 Research approach

With the thesis objective defined, the research approach that has been chosen consists of the following tasks:

- ▶ Thorough literature study on active vibration control of flexible structure with piezoelectric transducers.
- ▶ Propose a novel control strategy to suppress single/multiple vibration modes on flexible structures.
- ▶ Analyse the proposed method theoretically and validate in simulations.
- ▶ Validate the proposed method experimentally by:
 - ▷ Performing Experimental Modal Analysis (EMA) on a flexible structure to be selected in order to identify its dynamic behaviour.
 - ▷ Identifying optimal placement for piezoelectric transducers.
 - ▷ Implementing the controller experimentally to suppress vibrations on the identified structure.

1.5 Thesis Outline

This report aims to guide the reader in the work I carried out for the completion of my master thesis. In particular, the entire work has been organized in different chapters.

Chapter 1 introduces the reader to the background and the most important aspects of active vibration control of flexible structures with smart materials.

In Chapter 2, a thorough literature review about the topic is presented. Readers who are not familiar with active vibration control principles and its applications are strongly advised to go through the content presented in this chapter.

Chapters 3 and 4 represent the main contribution of this thesis. Chapter 3 presents a novel fractional-order compensator for active vibration control, whereas in Chapter 4 its experimental application is discussed. Both chapters are written in scientific paper format to be submitted to the 20th World Congress of the International Federation of Automatic Control (IFAC) and to the Journal of Vibration and Control (JVC), respectively.

In Chapters 5 and 6, final discussions and conclusions about the outcomes of this work are explained.

Being that the topic of this thesis is very multidisciplinary, this report is written with a broad audience in mind. A reader with a general engineering background is intended to be able to go through the report entirely. Extensive appendices are included to leave future students the possibility to replicate, continue and extend this work.

2

Literature Review and Theory

In this chapter a brief literature review in the area of active vibration control of smart structures is presented. First the main control strategies are reviewed and the basic theory is shortly explained. Then smart materials for sensing and actuation are introduced, with particular focus on different types of piezoelectric materials, and some literature about active control with piezoelectric transducers is referenced. Finally a review about optimal placement criteria for piezoelectric sensors and actuators is presented.

2.1 Active vibration control of flexible structures

The basic idea of active vibration control of flexible structures is to suppress or reduce the dynamic response due to a particular vibration mode. In the time domain this can be easily visualized as if the vibrational oscillation amplitude decays faster when the control action is performed. But since structural control in general is conceived and targeted specifically to vibration modes, the effect of the active action of the controller is best seen in the frequency domain, rather than in the time domain, where the response due to different modes is best represented, Figure 2.1.

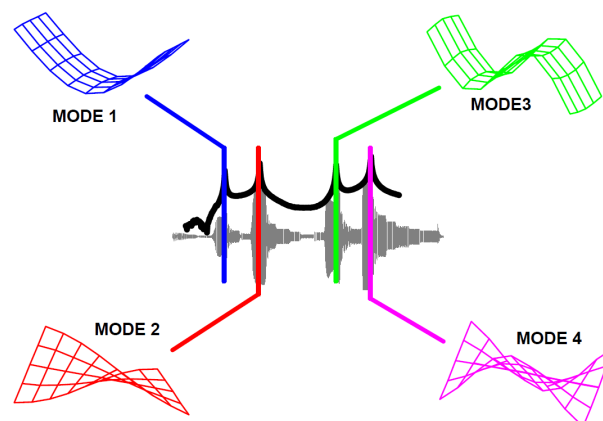


Figure 2.1: Time and frequency domain visualization of vibration modes [2].

The main objective of the controller is to provide active damping to the structure to be controlled (plant), which results in an attenuation of the resonance peak in the dynamic amplification and

an increase in the negative real part of plant poles. For a simple 1-DOF plant this concept is represented in Figure 2.2.

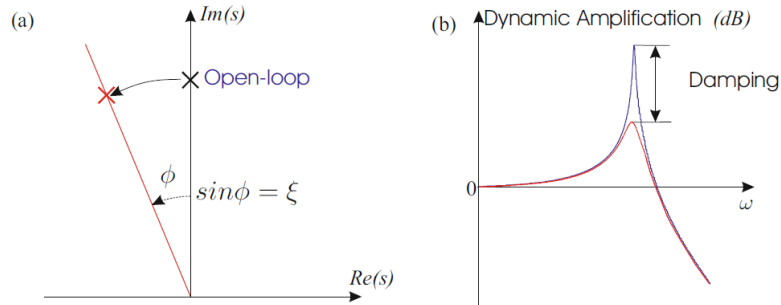


Figure 2.2: Role of active damping in (a) System poles and (b) Dynamic amplification ($1/2\xi$) [1].

The dynamics of flexible structures have very interesting properties. For example, because of their flexibility, they have a large number of elastic modes resulting in very high order transfer functions which are rather difficult to control. As already mentioned, controllers are designed to target only specific vibration modes in a restricted bandwidth of interest, and the fact that transfer functions are of high order means that there are out-of-bandwidth modes which are neglected but whose effect might influence the controlled response, or the so-called closed-loop system (see Figure 2.3). The effect of the uncontrolled, or out-of-bandwidth modes, is known in the literature as *spillover* and it is discussed in subsection 2.1.1.

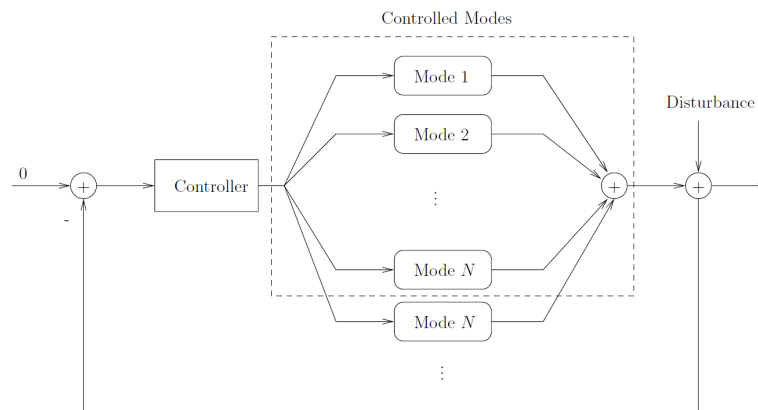


Figure 2.3: Feedback control of flexible structure consisting of a large number of elastic modes [3].

Another important aspect regarding the controller is that, apart from being able to reduce structural vibrations, it should ensure robustness and closed-loop stability for the controlled system. In this sense, careful positioning of sensors and actuators can have a great influence. For example, when actuators and sensors are positioned on the same degree of freedom (DOF) on the structure, the corresponding transfer function for that DOF is a *collocated* transfer function which has very interesting properties with respect to closed-loop stability. Collocated control is discussed in subsection 2.1.2.

2.1.1 Spillover effect

In general terms, spillover can be explained as the effect that modes which are outside the bandwidth of the controller have on the closed-loop system, Figure 2.4.

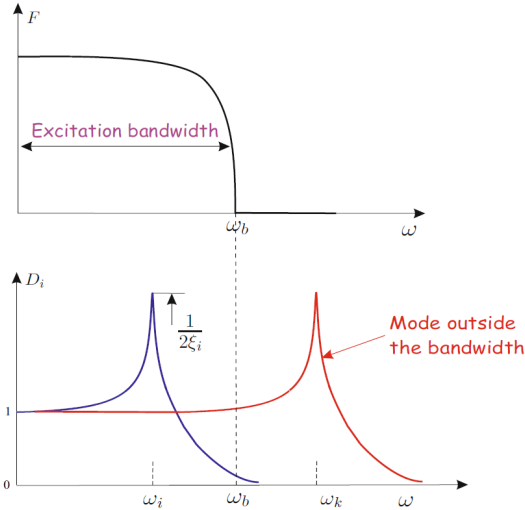


Figure 2.4: In-bandwidth and out-of-bandwidth modes [1].

It has been extensively investigated by M.J. Balas [4, 5], where two types of effects are defined: observation and control spillover.

- *Observation spillover* is when sensor outputs are contaminated by the measured response of residual modes.
- *Control spillover* is when residual modes are excited by the feedback control.

In his work, Balas developed a feedback controller for a finite number of modes of a flexible structure, and by deriving controllability and observability conditions of the full system (including a mathematical model of the structure), the combined effect of control and observation spillover could be studied with respect to closed-loop stability.

It is shown that, in absence of observation spillover, "*excitation of the residual modes can degrade the system response but it cannot destabilize the system*". Instead, when both control and observation spillover are present, even a small change in the poles of the system can lead to instability.

So, in general, even though instability is not a necessary consequence of the combination of control and observation spillover, "*all modal controllers have the potential to generate instabilities unless observation spillover can be eliminated*", assuming stability for the controller itself. If the latter case applies, a method to reduce the effect of control spillover must be devised in order to avoid unwanted excitation of the out-of-bandwidth modes and losses in control performance.

2.1.2 Collocated modal control

In structural dynamics, the equation of motion in modal coordinates of a generic 1-DOF system is simply expressed by a second order differential equation of the type:

$$\ddot{\xi} + 2\zeta\omega\dot{\xi} + \omega^2\xi = k^2 f \quad (2.1)$$

where ξ , ω , ζ are modal coordinate, natural frequency and modal damping of the system, respectively. The input force is f and k is a modal constant.

A control system, when sensors and actuators are related to the same DOF of the structure in question, is said to be *collocated*. If a force actuator and a displacement sensor are considered (as they will mostly be during this thesis), the corresponding open-loop collocated transfer function for that particular DOF takes the following form in the Laplace domain:

$$G(s) = \sum_{n=1}^{\infty} \frac{k_n^2}{s^2 + 2\zeta_n\omega_n s + \omega_n^2} \quad (2.2)$$

where n is indicating the mode number. A modal constant $k_n = \omega_n$ is assumed for simplicity throughout this thesis. Collocated systems have the property of having the phase always between 0° and -180° , meaning that poles and zeros interlace on the imaginary axis, where a zero corresponds to an anti-resonance in the frequency response. Equation (2.2) can thus be rewritten as:

$$G(s) = G_0 \frac{\prod_i (s^2 + 2\zeta_i z_i s + z_i^2)}{\prod_j (s^2 + 2\zeta_j \omega_j s + \omega_j^2)} \quad (\omega_k < z_k < \omega_{k+1}) \quad (2.3)$$

where z_i represents an anti-resonance. The pole-zero pattern and frequency response function (FRF) of a generic collocated system are represented in Figure 2.5 and Figure 2.6.

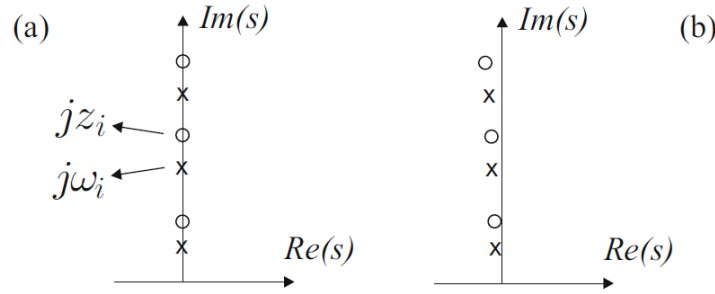


Figure 2.5: Pole-zero pattern in a collocated system. (a) Undamped (b) Lightly damped ([1]).

A generic feedback loop for vibration control with the assumption of a collocated piezoelectric actuator/sensor pair is illustrated in Figure 2.7, where $C(s)$ is the transfer function of the controller and $G(s)$ is the transfer function of the plant; v_s is the voltage from the sensor and v_a is the voltage to the actuator.

Collocation is a very interesting property that can be exploited when designing a feedback control scheme. In theory, collocated structures are always closed-loop stable with respect to out-of-bandwidth modes. As indeed described in subsection 2.1.1, collocation implies the elimination of observation spillover and thus guarantees stability, because the sensor can only measure the response from the same DOF of the actuator and not from other DOFs. However, in practice perfect collocation is never achievable, and when dealing with piezoelectric transducers the concept of *nearly-collocated* systems has to be introduced (see section 2.2). Stability is instead not guaranteed for *non-collocated* systems where observation spillover due to the non-collocation of sensors

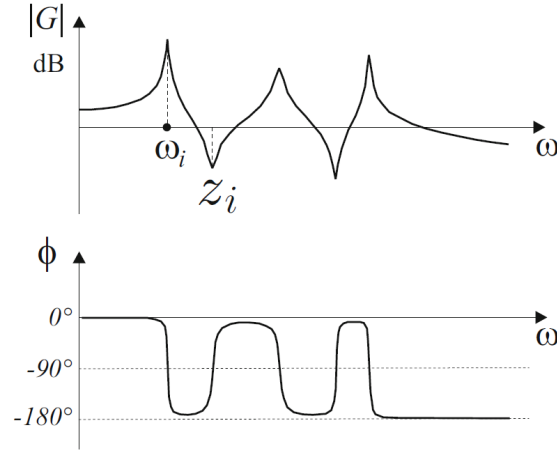


Figure 2.6: Collocated frequency response function [1].

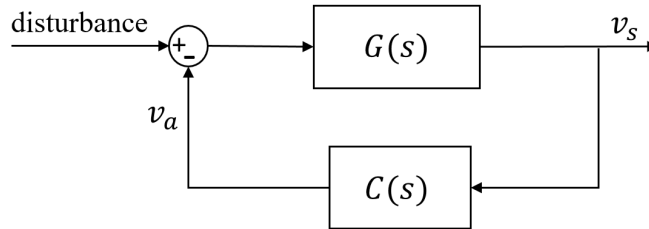


Figure 2.7: Feedback control of vibration with a collocated piezoelectric actuator/sensor pair.

and actuators can be present. Attention must be paid when designing a control scheme for a non-collocated system and different strategies can be used, but they will not be addressed in this thesis.

In the upcoming sections, the main control methods present in literature for AVC of flexible structures are explained. They are all defined as *modal* controllers because a modal description (rather than physical) of the dynamic structure is always considered for simplicity, where the dynamic behaviour can be described just as the linear combination (superposition) of many vibration modes. For each control method, modal displacement is considered to be measured by the piezoelectric sensor, although what is actually measured is strain which is proportional to the physical displacement. But since modal coordinates are proportional to the physical coordinates by the modal transformation matrix, it is possible to simply use the measured displacement signal in practical implementations.

2.1.3 Direct Velocity Feedback

A velocity feedback controller for vibration control, better known as Direct Velocity Feedback (DVF), is defined for a 1-DOF system as follows:

System:

$$\ddot{\xi} + 2\zeta\omega\dot{\xi} + \omega^2\xi = \omega^2 f \quad (2.4)$$

Control:

$$f = -g\dot{\xi} \quad (2.5)$$

where ξ , ω , ζ are modal coordinate, natural frequency and modal damping of the system, respectively; f is the modal control force and g is the feedback gain. Equation (2.4) and (2.5) can be combined and rewritten in the following form:

$$\ddot{\xi} + (2\zeta\omega + g\omega^2)\dot{\xi} + \omega^2\xi = 0 \quad (2.6)$$

where it is easy to notice that the velocity signal is directly feedback to the actuator with gain g and active damping is achieved. The corresponding feedback loop is shown in Figure 2.8.

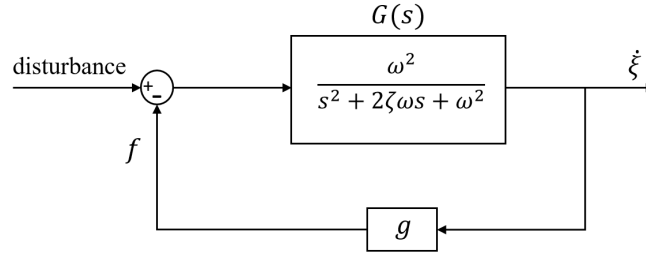


Figure 2.8: DVF feedback loop.

Direct Velocity Feedback does not prevent spillover effect from occurring, but unconditional closed-loop stability is guaranteed nevertheless for $g > 0$, as proven by Moheimani and Fleming [3]. Despite its stability properties, DVF shows important limitations that do not make it an appealing control scheme in the context of active control with piezoelectric transducers.

First of all, piezoelectric sensors (as better explained in section 2.2), measure strain in the structure, which can be considered as a displacement signal that would need to be differentiated first, before being feedback to the velocity controller $C(s)$. This means that the addition of a differentiator is required, but generally not preferred. Secondly, in order to make sure that the compensator rolls-off at high frequencies, some extra dynamics need to be added to it, although this could potentially cause instability. Furthermore, DVF has high control effort at all frequencies, and in this context of vibration control it is best to restrict the control effort in the frequency range of interest, to also prevent actuator saturation.

- These problems have been addressed by Kim [6] where a Direct Velocity Feedback and an Acceleration-Position Feedback (APF) have been used for the realization of an electrical damper and an electrical dynamic absorber, respectively, to suppress vibrations. It was demonstrated that an electrical dynamic absorber (APF) is more robust with respect to undesirable dynamics outside the control bandwidth than an electrical damper (DVF), due to its lower control effort both at low and high frequencies. Moreover, if both controllers are compared on the same setup, APF does not require an integrator to transform acceleration into velocity since an acceleration sensor can be directly used. More information on APF is provided in subsection 2.1.4.
- Omidi and Mahmoodi [7] instead used \mathbf{H}_∞ Modified Positive Velocity Feedback (HMPVF) to control multiple modes on a flexible collocated cantilever beam. A feed-through term was added to the model of the plant to simulate out-of-bandwidth dynamics, and the controller was designed with 2 parallel first and second-order compensators for each mode, of which the second-order one focuses on reducing a specific resonance peak and the first-order one reinforces the damping action.

2.1.4 Resonant Control

Resonant Control (RC) is a control technique which consists of the realization of an electrical dynamic vibration absorber. It is a second order high-pass filter compensator with negative

feedback, where the numerator dynamics convert the position feedback (from the piezoelectric sensor) to acceleration feedback. In modal coordinates RC is defined as follows:

System:

$$\ddot{\xi} + 2\zeta\omega\dot{\xi} + \omega^2\xi = \omega^2 f \quad (2.7)$$

Compensator:

$$\ddot{\eta} + 2\zeta_f\omega_f\dot{\eta} + \omega_f^2\eta = \ddot{\xi} \quad (2.8)$$

where ξ and η are the position coordinates of system and compensator; ω & ζ and ω_f & ζ_f are natural frequency and damping of structure and compensator; $f = -g\eta$ is the modal control force and g is the compensator gain. The corresponding feedback loop is shown in Figure 2.9.

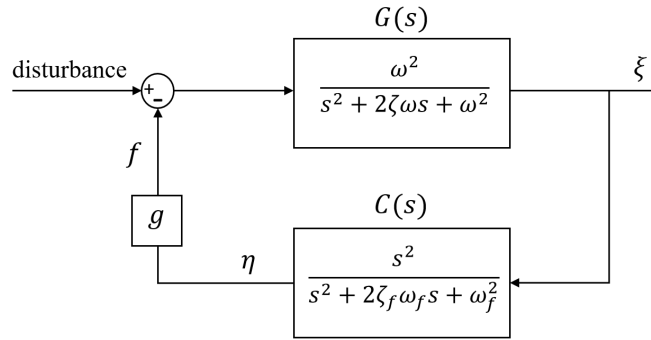


Figure 2.9: RC feedback loop.

The frequency ω_f is normally tuned to the same natural frequency of the structure of interest, and together with a proper choice for the parameters g and ζ_f vibration reduction can be achieved. Closed-loop stability is guaranteed for $g > 0$.

The bode plot of the filter $C(s)$ is shown in Figure 2.10, where a tuning frequency of 20 Hz is chosen.

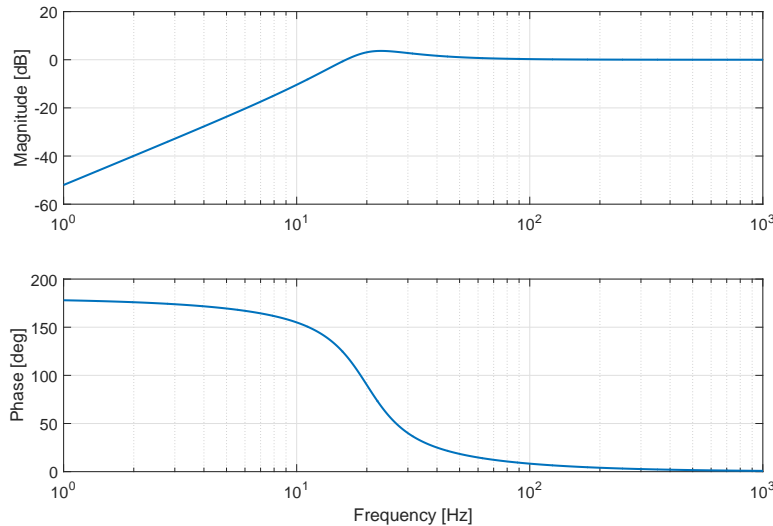


Figure 2.10: Bode plot of RC controller tuned at 20 Hz.

From the bode plot of $C(s)$ it is possible to understand the high-pass filtering characteristics of the controller. The +2 slope before the resonance frequency and the constant magnitude after

the resonance indicate that the action of the controller is seen mainly for frequencies around the resonance and higher, whereas any dynamics occurring below the resonance should be neglected. This can indeed be seen when the RC controller is applied to a generic plant $G(s)$. In Figure 2.11 and Figure 2.12 a simple collocated plant $G(s)$ with two modes, at 20 Hz and 100 Hz, is controlled with RC targeting 1st mode and 2nd mode, respectively.

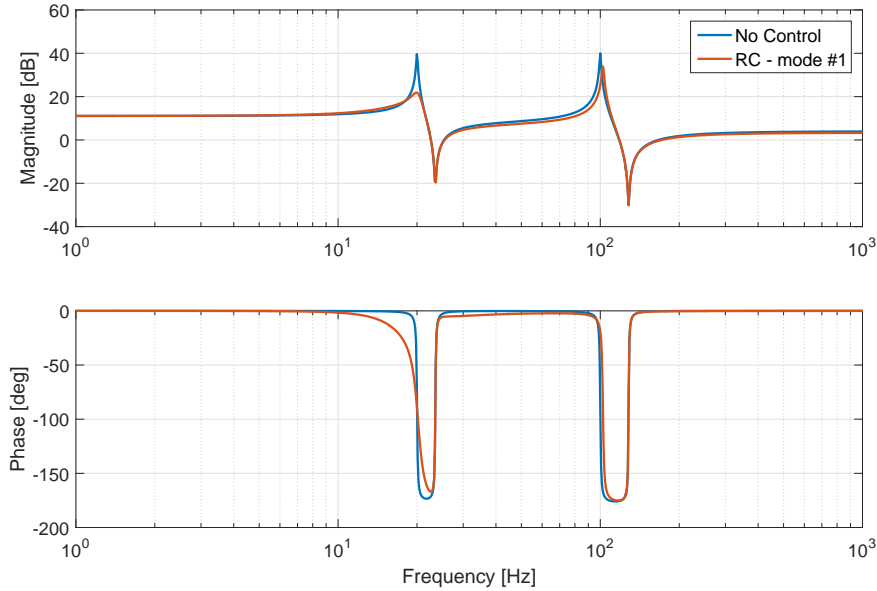


Figure 2.11: Bode plot of $G(s)$ with 1st mode controlled by RC.

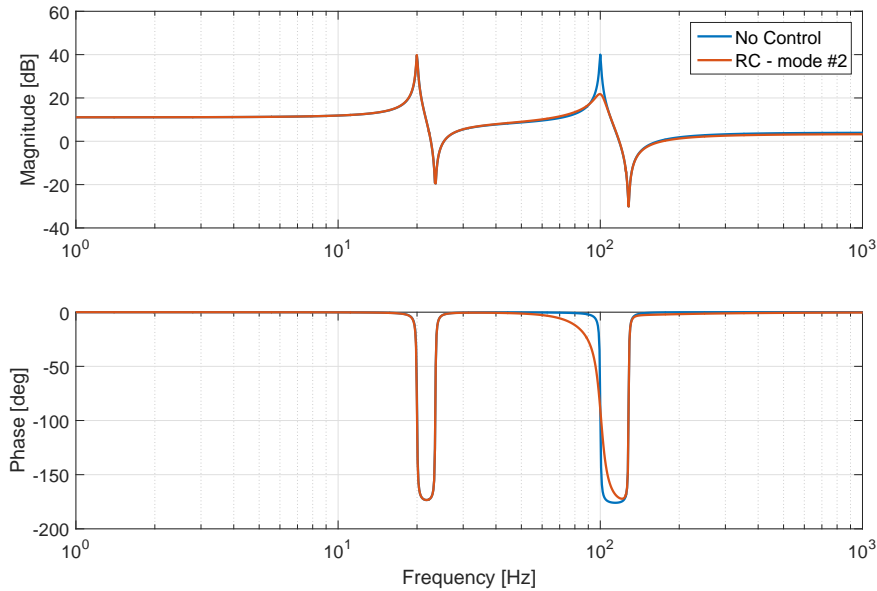


Figure 2.12: Bode plot of $G(s)$ with 2nd mode controlled by RC.

As clearly explained by Lüleci [8] with a similar example, from the bode plot of the closed-loop response some conclusions about the performance of the RC can be drawn:

- The high-pass filter characteristics cause the RC to affect the response on the 2nd mode when targeted to suppress the 1st mode. The 2nd peak is indeed shifted in frequency and changed in magnitude. This effect can be regarded as *spillover effect* due to the presence of uncontrolled dynamics.
- Conversely, the response on the 1st mode is not affected when the filter is tuned to suppress the 2nd mode. Spillover effect is not present in this case because of the high-pass characteristics of the RC.
- When multiple modes need to be controlled at the same time, particular attention must be paid to tuning the different RC compensators in order to limit the spillover effect. In fact, a compensator targeting a low frequency mode should be tuned prior to the one targeting a mode at higher frequency.
- RC is not appealing for a practical implementation: actuators and sensors have generally high frequency dynamics which are not neglected by the high-pass filter of the RC and can therefore destabilize the closed-loop system.

This control method has been used in several studies. In particular S.H. Kim studied RC in different contexts:

- ▶ In [6], as already explained in the previous section, an equivalent version of RC, called Acceleration-Position Feedback (APF) because acceleration is measured instead of displacement, was compared to Direct Velocity Feedback (DVF) showing more robustness with respect to spillover and lower control effort both at low and high frequency.
- ▶ In [9], RC, which is called instead Negative Position Feedback (NPF), was compared to the classic Positive Position Feedback (PPF). NPF was proposed to demonstrate the implementation of an electrical dynamic absorber using a displacement sensor. More information on PPF is provided in subsection 2.1.5.

2.1.5 Positive Position Feedback

The main drawback of the RC is that it does not roll-off at high frequency, where the presence of higher order dynamics, either coming from the structure or from actuators and sensors, might jeopardize the control performance. A control method which solves these issues and became popular in the field of active vibration control is the Positive Position Feedback (PPF). This technique has been first proposed in 1983 by Goh and Caughey [10] to overcome the instability associated with finite actuator dynamics, and it was applied for the first time in 1987 by Fanson [11] to experimentally suppress vibrations in large space structures.

In modal domain, the two equations for a 1-DOF system and PPF compensator are:

System:

$$\ddot{\xi} + 2\zeta\omega\dot{\xi} + \omega^2\xi = \omega^2 f \quad (2.9)$$

Compensator:

$$\ddot{\eta} + 2\zeta_f\omega_f\dot{\eta} + \omega_f^2\eta = \omega_f^2\xi \quad (2.10)$$

where ξ and η are the position coordinates of system and compensator; ω & ζ and ω_f & ζ_f are natural frequency and damping of system and compensator; $f = g\eta$ is the modal control force and g is the compensator gain.

The corresponding transfer functions of system (plant) $G(s)$ and PPF compensator $C(s)$ are shown in Figure 2.13 where also the positive feedback is clearly indicated.

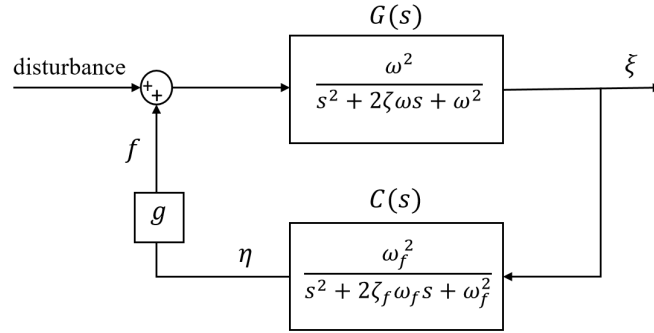


Figure 2.13: PPF feedback loop.

For this particular formulation given in 2.9 and 2.10, and which is found in most of the literature, the closed-loop stability condition [11] is simply given by:

$$g < 1 \quad \text{or equivalently} \quad \frac{K_f}{\omega^2} < 1 \quad (2.11)$$

where $g = \frac{K_f}{\omega^2}$, with gain K_f , is assumed to be positive since this method works with positive feedback. For a proper performance, ω_f is tuned equal to ω and ζ_f is normally chosen to be bigger than ζ .

The bode plot of the 2nd order low-pass filter $C(s)$ is shown in Figure 2.14, where a tuning frequency of 20 Hz is chosen.

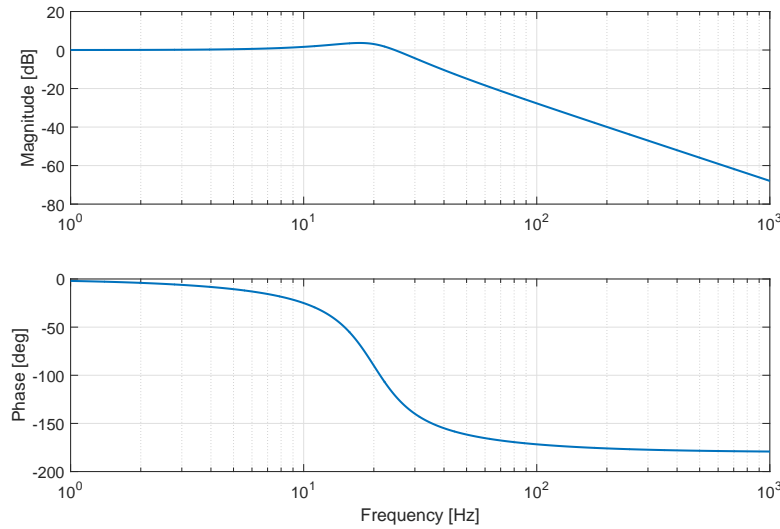


Figure 2.14: Bode plot of PPF controller tuned at 20 Hz.

In Figure 2.11 and Figure 2.12 a simple collocated plant $G(s)$ with two modes, at 20 Hz and 100 Hz, is controlled with PPF targeting 1st mode and 2nd mode respectively.

As clearly explained by Lüleci in [8] with a similar example, from the bode plot of the closed-loop response some conclusions about the performance of the PPF can be drawn:

- The low-pass filter characteristics cause the PPF to provide so-called active flexibility before

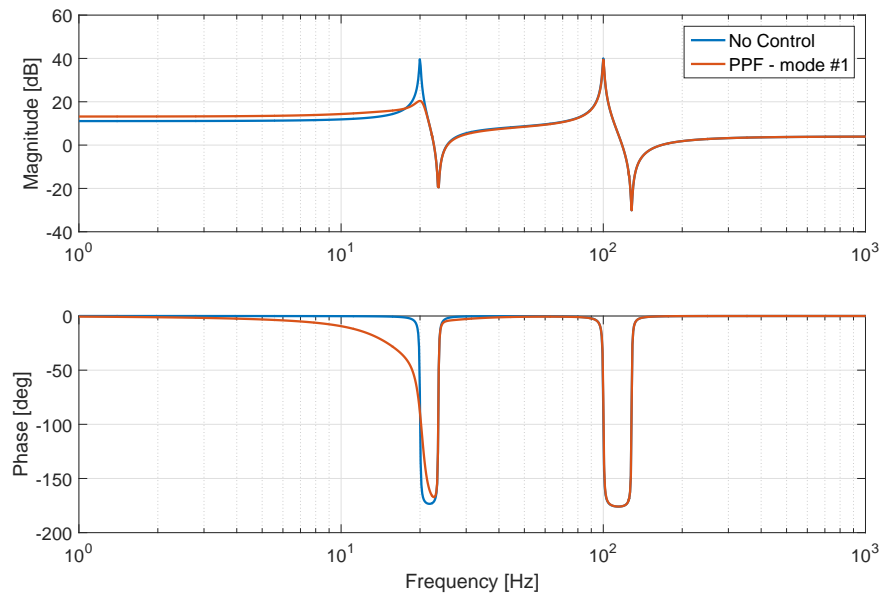


Figure 2.15: Bode plot of $G(s)$ with 1st mode controlled by PPF.

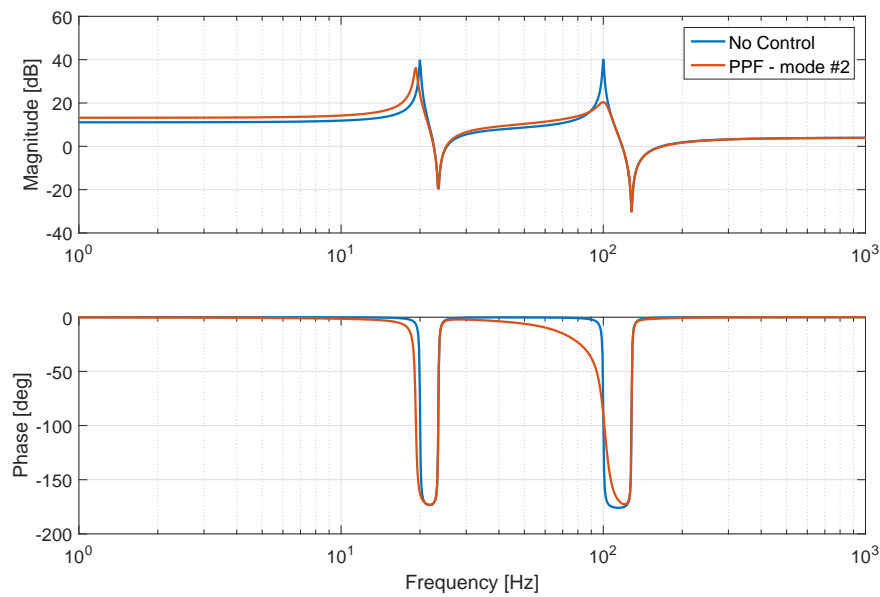


Figure 2.16: Bode plot of $G(s)$ with 2nd mode controlled by PPF.

the tuning frequency ω_f , active damping around ω_f and active stiffness for higher frequencies [12].

- PPF indeed does not affect the 2nd mode when targeted to the 1st mode, preventing high frequency spillover.
- The response on the 1st mode is affected instead when the filter is tuned to suppress the 2nd mode. Low frequency spillover is present and it can be seen both in the amplification of the

response in the quasi-static region and in the shift in frequency of the 1st resonance.

- When multiple modes need to be controlled at the same time, a compensator targeting a low frequency mode should be tuned later than a compensator targeting a mode at higher frequency in order to account for the frequency shift caused by the spillover effect.
- Spillover, as also seen for the RC, is strictly related to the phase behaviour of the closed loop: the more the phase of the closed-loop follows the phase of the plant, the less spillover is observed. **This relation between spillover and phase has not received much attention in literature and it is intentionally highlighted by the author in this work.**
- PPF does not necessarily require a model of the structure to be controlled, whereas other optimal control methods like LQR and LQG do require a model. When applied experimentally, the knowledge of the natural frequencies of the structure is often sufficient to successively apply PPF.

This control method has been very extensively studied and applied in many studies due to its appealing properties. Some of the main contributions in the literature of PPF are briefly presented here.

- ▶ Poh and Baz first applied the PPF as a 1st order filter and they proposed a "time sharing" strategy to control a large number of modes with a smaller number of actuators [13]; then they combined the Independent Modal Space Control (IMSC) with PPF [14].
- ▶ McEver and Leo [15] developed an autonomous vibration suppression algorithm based on PPF where an on-line identification is used to find the optimal design parameters.
- ▶ Song et al. [16] studied the robustness of the PPF with respect to possible unknown changes in the structural natural frequency to be controlled. Results showed that PPF performs well even when the natural frequency ω is not exactly known.
- ▶ Kwak et al. [17] studied for the first time very extensively the stability conditions, performance and design methodology for the PPF, both in Single-Input Single-Output (SISO) case and Multi-Input Multi-Output (MIMO) case.
- ▶ Kim [9], as already mentioned in the previous section, compared PPF to the Negative Position Feedback (NPF).
- ▶ Yuan [18] used a modified PPF which uses measured acceleration feedback and which they call Negative Acceleration Feedback (NAF). Unlike RC, and equivalent to APF, NAF also rolls-off at high frequencies like PPF because acceleration is directly measured and thus the s^2 term at the filter numerator is not required.
- ▶ El-Ganaini [19] studied PPF for suppression of non-linear system vibration at primary resonance and 1:1 internal resonance.

PPF variants

Besides the several fundamental studies, the Positive Position Feedback also presents different variants in the literature, where adaptive strategies or integration with other controllers are investigated.

- ▶ Smith [20] used a modified PPF in application to acoustic systems. Band-pass filters are used to limit spillover and phase interaction of adjacent modes in case of multi-mode control. An adaptive algorithm is used to tune the controller gain to proper levels for each mode.

- ▶ Creasy implemented an adaptive modified PPF for noise absorption in acoustic cavities [21] and payload fairings [22]. Butterworth low and high-pass filters are used in series with PPF filters for spillover reduction both at low and higher frequency.
- ▶ Mahmoodi [23] also made use of an adaptive modified PPF with both frequency and controller adaptation for active vibration control of structures.
- ▶ Orszulik and Shan [24] proposed a multi-mode adaptive PPF with an on-line parameter estimator using recursive least squares method with forgetting factor.
- ▶ Omidi and Mahmoodi [7] instead used \mathbf{H}_∞ Modified Positive Position Feedback (HMPPF), which they compared to the previously mentioned HMPVF, to control multiple modes on a flexible collocated cantilever beam. A feed-through term was added to the model of the plant to simulate out-of-bandwidth dynamics, and the controller was designed with 2 parallel first and second-order compensators for each mode, of which the second-order one focuses on reducing a specific resonance peak and the first-order one reinforces the damping action.

2.1.6 Controllers comparison

In this section the three control methods explained previously are summarized for clarity in Table 2.1.

Table 2.1: Controllers comparison.

Controller	Block diagram	Stability	Properties
DVF		Unconditional ($g > 0$)	<ul style="list-style-type: none"> • Direct addition of active damping. • Differentiator needed. • No roll-off at high frequencies. • High control effort at all frequencies.
RC		Unconditional ($g > 0$)	<ul style="list-style-type: none"> • 2nd order HP filter. • High frequency spillover. • No roll-off at high frequencies. • Difficult tuning in multi-mode control.
PPF		$0 < g < 1$	<ul style="list-style-type: none"> • 2nd order LP filter. • Low frequency spillover. • Roll-off at high frequencies. • Difficult tuning in multi-mode control.

System: $\ddot{\xi} + 2\zeta\omega\xi + \omega^2\xi = \omega^2 f$; $G(s) = \omega^2 / (s^2 + 2\zeta\omega s + \omega^2)$.

2.1.7 Other control algorithms

Besides the main control strategies introduced in the previous sections, active damping can be achieved also by means of other methods. Integral Resonant Control (IRC) is also often found in literature. IRC is a modified version of the Integral Force Feedback (IFF) method, which is developed for control systems where displacement actuators and force sensors are used [1]. This implies that the transfer function of the collocated system to be controlled should represent the dynamic stiffness, and not the receptance like in Equation (2.2). Hence, this collocated transfer function also shows pole-zero interlacing property but starts with a zero. IFF is thus modified by connecting a feed-through term to the collocated transfer function in order to convert a receptance type FRF to a dynamic stiffness FRF by the addition of a zero. The application of this technique however presents some limitations: it generally requires a model of the structure; modes cannot be treated separately; since the control gain decreases at higher frequencies this method is less effective for high frequency modes [8].

- ▶ Aphale [25] applied IRC on collocated smart structures. The addition of a feed-through term to the transfer function to be controlled is required such that zeros are followed by poles (and not vice versa) and integral feedback can be used. A bandpass filter is used as IRC.
- ▶ Russell [26] also used IRC for damping and tracking in nano-positioning systems. IRC is optimized to obtain a closed-loop Butterworth filter pattern, since the same response is optimal for positioning systems. Performance of IRC is compared with respect to other control methods.

The control methods explained so far can all be defined as classical collocated control methods. Traditional techniques such as LQG, H_2 and H_∞ have been also applied in this field, however they often require a more challenging implementation with respect to the classical methods [25]. These traditional techniques have not been addressed in this thesis, although they represent a valuable option for the active control of smart structures.

2.2 Smart materials and structures

Smart materials are inherently capable of detecting and responding to changes in their environment. This means that their properties can be changed by an external condition, such as temperature, light, pressure or electricity. This change is reversible and can be repeated many times, making them very suitable for sensing and actuation purposes. There are a wide range of different smart materials, and each offers different properties. The most common are: piezoelectric, shape-memory alloy and polymer, magnetostrictive, electroactive polymer, etc. Nowadays, distributed piezoelectric sensors and actuators are extensively used for active vibration control because of their unique features such as: low cost, low mass, ease of integration and wide frequency range of control.

In the next sections focus, is given to piezoelectric type of transducers. First, the piezoelectric phenomenon is explained, then two main types of transducers, which are lead zirconate titanate (PZT) and macro fiber composite (MFC), are introduced and finally some literature about active control with piezoelectric transducers is referenced.

2.2.1 Piezoelectricity & transducers types

Piezoelectricity is a phenomenon which relates mechanical stress and electricity and was discovered in 1880 by the French physicists Jacques and Pierre Curie. The so-called *direct piezoelectric effect* consists of an accumulation of electric charge in certain solid materials when they are subjected to mechanical stress, whereas the *converse piezoelectric effect* consists of a generation of mechanical deformation when an electric field is applied.

The general linear piezoelectric constitutive equations for transversely isotropic materials can be given in matrix form as:

$$\begin{bmatrix} \mathbf{S} \\ \mathbf{D} \end{bmatrix} = \begin{bmatrix} \mathbf{s}^E & \mathbf{d}^t \\ \mathbf{d} & \epsilon^T \end{bmatrix} \begin{bmatrix} \mathbf{T} \\ \mathbf{E} \end{bmatrix} \quad (2.12)$$

The field variables are the stress \mathbf{T} , strain \mathbf{S} , electric field \mathbf{E} and electric displacement \mathbf{D} , whereas the constants are the elastic compliance \mathbf{s} , piezoelectric strain constant \mathbf{d} and dielectric permittivity ϵ . The superscripts E and T denote that the corresponding constants are evaluated at constant electric field and constant stress, respectively, and the superscript t stands for the transpose.

PZT

The lead zirconate titanate (PZT) is a piezoceramic material with very good actuation properties but it is also very brittle and sometimes difficult to adapt to complex curved geometries. The standard design for a PZT transducer consists of a piezoceramic layer between two electrodes for electrical contact, together with a polymer structure for electrical insulation and mechanical stability (Figure 2.17b). The results is a module which is extremely robust and capable of both sensor and actuator functionality.

MFC

Differently from the monolithic design of PZT, piezocomposite transducers are made of an active layer which is composed of a mixture between epoxy resin and piezoceramic fibers. Advantages of piezocomposite traducers is the possibility of molding the anisotropic mechanical properties in order to optimize certain actuating directions. In 1996, NASA invented a specific type of transducer called macro fiber composite (MFC) which provides high performance, durability and a very good flexibility which makes these transducers a preferred option in case they have to be adapted to different structure geometries. Details of a MFC transducer built from Smart Material [27] is given in Figure 2.18a and 2.18b.

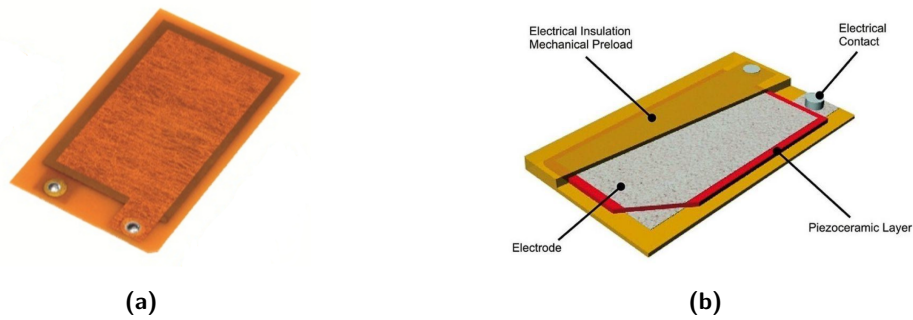


Figure 2.17: PZT transducer from PI [28]: (a) Transducer detail (b) Cutaway.

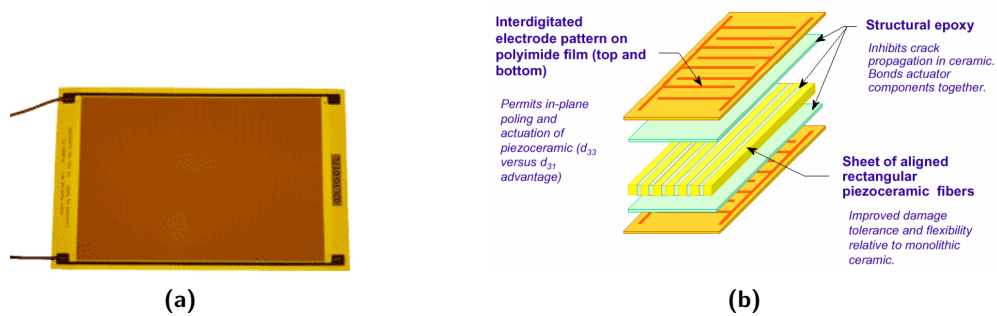


Figure 2.18: MFC transducer from Smart Material [27]: (a) Transducer detail (b) Cutaway.

Working principle

The working principle of the PZT used as an actuator resembles the one of a capacitor: the piezoceramic acts as a dielectric between the electrodes, and an electric field is created in the ceramic when a voltage is applied inducing a lateral contraction of the material in a direction perpendicular to the electric field, Figure 2.19a and 2.19b. This is known as d_{31} effect.

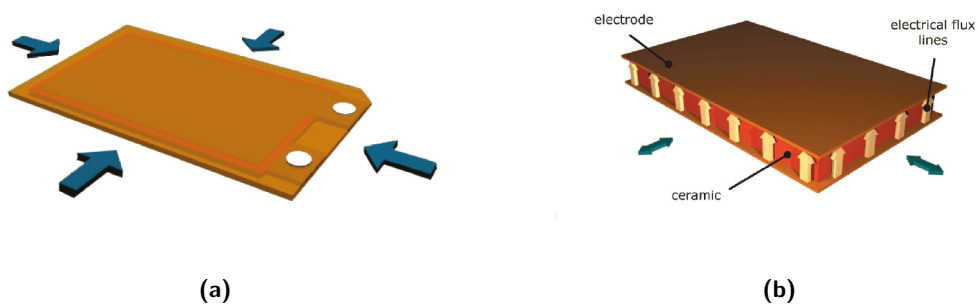


Figure 2.19: PZT working principle [28]: (a) Lateral contraction (b) d_{31} effect.

The MFC transducer instead, depending on the building type, can work either as an elongator with the d_{33} effect or as contractor with the d_{31} effect. The electric field that is generated is aligned with the direction of the fibers since they are perpendicular and interdigitated with the electrodes (Figure 2.20).

When an oscillating voltage is applied, each piezoelectric transducer oscillates at the same frequency of the input, making them suitable for vibration control purposes.

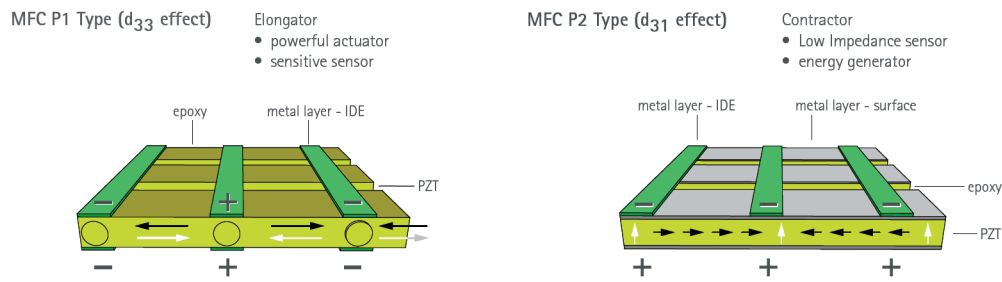


Figure 2.20: MFC working principle [27]: both d_{33} and d_{31} are available as operational modes.

2.2.2 Control of smart structures with piezoelectric sensors & actuators

As already mentioned, active vibration control is often applied in practice using piezoelectric transducers as sensors and actuators. Some of the main contributions in the literature are briefly presented here.

- ▶ Kwak and Heo [12] applied a MIMO PPF controller to control vibration of a smart grid structure equipped with PZT transducers. A new concept, the block-inverse technique, is proposed to control a higher number of modes than the number of actuators and sensors. Spillover effect due to application of MIMO PPF based on the block-inverse technique is also studied.
- ▶ Shin [29] investigated the active vibration control of clamp-clamped beams using PPF controllers with non-collocated sensor/moment pair actuator configuration to overcome the instability of DVF controller due to the phase shift at high frequencies.
- ▶ Zippo et al. [30] applied PPF for active vibration control of a composite sandwich plate using MFC transducers. Control was efficient in reducing vibration both in linear and non-linear regime.
- ▶ Ferrari and Amabili [31], as a continuation of the work of Zippo [30], applied non-collocated PPF both in SISO and MIMO.

2.3 Placement of piezoelectric sensors & actuators

Piezoelectric transducers can be easily mounted on different types of structures in the form of patches, but their size, orientation and location play a significant role when active control has to be performed. A badly positioned or misplaced sensor/actuator pairs can result in a poor control performance or even cause instability. For instance an unwise placement of a collocated sensor/actuator pair can make the control system unstable, whereas the wise placement of non-collocated sensor/actuator pair can make it stable [32].

The concept of perfect collocation, which holds in theory, has to be reconsidered in practice since both sensor and actuator can never be placed exactly on the same position or DOF, therefore it is better to talk about a *nearly-collocated* or *quasi-perfect collocated* system. Zippo et al. [30], for example, placed a piezoelectric sensor next to the actuator on the same face of a rectangular plate as a nearly-collocated system. Furthermore controllability, observability and also spillover effect are all factors that are related to the transducers' placement.

The location alternatives can be many and they also depend on the structure properties and geometry, therefore in order to maximize the performance of the full active vibration control system, an optimization criterion for the transducers' placement needs to be devised, and a suitable optimization technique has to be used to solve the optimality problem for a wide range of structures.

In literature, many different optimization algorithms have been proposed to solve different kinds of transducers' placement problems: univariate search method, genetic algorithm [33], simulated annealing, etc. are examples of algorithms that have been used in this context. However, more attention should be paid to the criterion rather than to the optimization itself.

Gupta et al. [32] have extensively reviewed in a unified way the various optimization criteria used by researchers for optimal placement of piezoelectric sensors and actuators on a smart structure. According to his technical review, the main optimization criteria are: (i) maximizing modal forces/moments applied by piezoelectric actuators, (ii) maximizing deflection of the host structure, (iii) minimizing control effort/maximizing energy dissipated, (iv) maximizing degree of controllability, (v) maximizing degree of observability, and (vi) minimizing spillover effects. Gupta et al. compared results from different studies where plates and beams with different boundary conditions were used as host structures.

Among the many optimization criteria, the maximization of modal forces/moments applied by piezoelectric actuators is found to be very interesting, since the final outcome of an optimization based on this criterion has been used as a rule-of-thumb in many studies [8, 30, 31].

2.3.1 Maximal modal force rule

Maximal modal force criterion has been first proposed by Bin [34] as a rule for optimal placement of piezoelectric actuators for plates. This rule is briefly explained as follows.

The transverse displacement w of a generic dynamic structure can be expressed in modal coordinates using the superposition principle:

$$w(x, y, t) = \sum_{j=1}^{\infty} \Phi_j(x, y) \eta_j(t) \quad (2.13)$$

where $\Phi_j(x, y)$ is the normalized modal function and η_j the modal coordinate. The structure equation of motion for mode j can thus be written as:

$$\ddot{\eta}_j + \omega_j^2 \eta_j = -z^0 abL[\Phi_j] \nu_j(t) \quad (2.14)$$

where the term on the right hand side is the modal control force $Q_j(t) = -z^0 abL[\Phi_j] \nu_j(t)$. By referring to Figure 2.21, it can be noticed that some of the terms of Q depend on the geometry

of structure and actuator: a and b are length and width of the piezo patch, $z^0 = \left(\frac{h+h_p}{2}\right)$ where h and h_p are thickness of structure and piezo. L is a functional operator and ν is the voltage to the piezo.

$$L = e_{31} \left\{ \left(\frac{\partial^2}{\partial x^2} \right) + \left(\frac{\partial^2}{\partial y^2} \right) \right\} \quad (2.15)$$

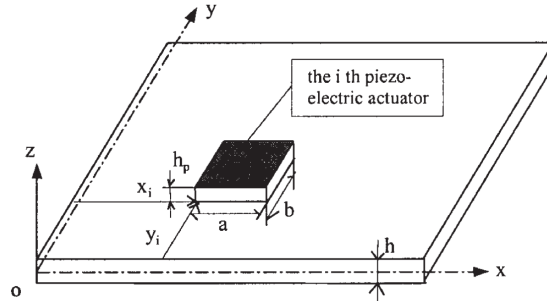


Figure 2.21: Piezoelectric actuator bonded on the surface of a plate structure [34].

When the absolute value of $L[\Phi_j]$ is maximum and voltage $\nu_j(t)$ is constant, then the control force $Q_j(t)$ will be maximum. Furthermore, when $Q_j(t)$ is maximum and the center of the piezo patch is located where $L[\Phi_j]$ is maximum, then the voltage $\nu_j(t)$ will be minimum. So it can be concluded that the piezoelectric patch actuator should be placed in locations where $L[\Phi_j]$ is maximum.

These locations are the regions of maximum modal strain in the host structure, so **the piezoelectric actuator should be placed where the strain is maximum for the specific vibration mode to be controlled.**

Mode shapes with modal strain energy distribution of a rectangular plate with all edge free boundary conditions are shown in Figure 2.22.

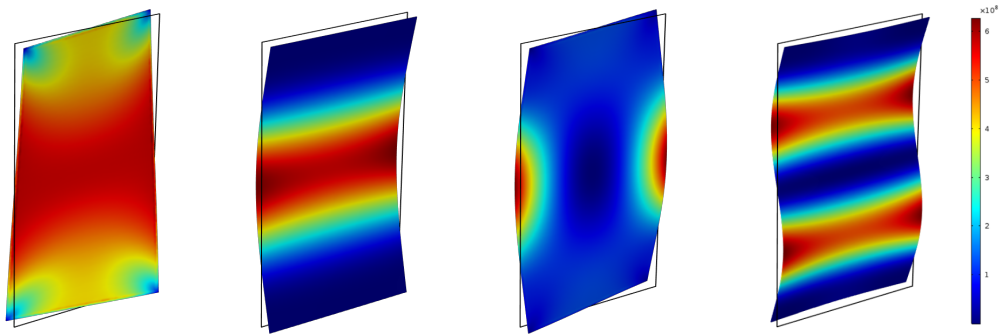


Figure 2.22: Surface elastic strain energy density plots of the first four mode shapes of a rectangular plate with all-edges-free boundary conditions: the red areas indicate maximum strain and can be considered as optimal locations for actuator placement.

The other optimization criteria reviewed by Gupta et al. [32] also propose optimal locations for actuator placement depending on the specific structure and boundary conditions, but as it has been pointed out by Lüleci in [8], these locations almost all coincide with regions of maximum modal strain, indicating that the actuator placement will be optimal not only for maximal modal force criterion but also for the other criteria. Therefore, it has been decided to use this approach in this thesis as a rule-of-thumb for optimal actuator placement.

3

A Fractional-order Positive Position Feedback Compensator

This chapter has been written in format of a scientific paper. A novel fractional-order Positive Position Feedback compensator for active vibration control is presented.

The aim of this paper is to show how the application of fractional control can improve on the limitations of the current active vibration control strategies.

The paper has been submitted to the 20th World Congress of the International Federation of Automatic Control (IFAC), taking place in July 2017 in Toulouse, France.

A Fractional-order Positive Position Feedback Compensator for Active Vibration Control

L. Marinangeli * F. Alijani * S.H. HosseinNia *

* *Department of Precision and Microsystems Engineering,
Delft University of Technology, Mekelweg 2, 2628 CD Delft,
The Netherlands (l.marinangeli@student.tudelft.nl; f.aliyani@tudelft.nl;
s.h.hosseinniakani@tudelft.nl)*

Abstract: In this paper a novel Active Vibration Control (AVC) strategy based on fractional-order calculus is developed. A fractional-order Positive Position Feedback (PPF) compensator is proposed to overcome the limitations of the commonly used integer-order PPF such as: frequency spillover, amplitude amplification in the quasi-static region of the closed-loop response, and difficult tuning in multi-mode control. Tuning parameters of the controller are obtained by optimizing both magnitude and phase response of the controlled plant. Results are shown by comparing performances of the standard integer-order PPF and the optimized fractional-order PPF, both on a simple 1-DOF plant and on measured frequency response data from a rectangular carbon fibre composite plate.

Keywords: Active Vibration Control, Spillover, Positive Position Feedback, Fractional-order control, Fractional-order filter, Experimental testing

1. INTRODUCTION

In the past decades research on Active Vibration Control (AVC) has found increasing interest in control of flexible thin-walled structures. These structures are often prone to undesirable vibrations, making AVC necessary particularly in industries where a lightweight design is of great importance. Piezoelectric transducers are often selected as sensors and actuators for the active control of flexible structures because of their unique properties including: low cost, low mass, ease of integration and wide frequency range of control. These types of transducers, when used as sensors, measure strain which is proportional to the physical displacement. In fact, control schemes specifically designed to use position as feedback signal have been extensively studied and applied in this context.

The main objective of the controller is to provide active damping to the structure (plant), which results in an attenuation of the resonance peak in the dynamic amplification. The dynamics of flexible structures have very interesting properties: because of their flexibility, they have a large number of elastic modes resulting in very high order transfer functions that are rather difficult to control. Controllers are designed to target specific vibration modes in a restricted bandwidth of interest, and the fact that transfer functions are of high order means that there are out-of-bandwidth modes which are neglected, but whose effect might influence the closed-loop response. The effect of the uncontrolled, or out-of-bandwidth modes, is known in the literature as *spillover* (Balas, 1978). Another important aspect regarding the controller is that, apart from being able to reduce structural vibrations, it should ensure robustness and closed-loop stability for the controlled system. In this

sense, careful positioning of sensors and actuators can have a great influence. The majority of the controllers studied in literature use a *collocated* configuration, where sensors and actuators are related to the same Degree of Freedom (DOF) of the structure. The phase of the open-loop collocated transfer function is always between 0° and -180° , meaning that poles and zeros interlace on the imaginary axis, where zeros and poles correspond to anti-resonances and resonances of the frequency response, respectively. Collocated systems have the property of being always closed-loop stable with respect to out-of-bandwidth dynamics (Preumont, 2011) and that is why most of the research involves collocation.

One of the most popular collocated modal control schemes is Positive Position Feedback (PPF), which has been first proposed in 1985 by Goh and Caughey (Goh and Caughey, 1985) to overcome the instability associated with finite actuator dynamics. This controller was applied for the first time in 1987 by Fanson (Fanson, 1987) to experimentally suppress vibrations in large space structures. PPF is a second order low-pass filter which rolls off quickly at high frequencies, making it very appealing against possible instability or performance losses due to out-of-bandwidth dynamics. Direct Velocity Feedback (DVF), Resonant Control (RC) (Moheimani, S.O.R. , and Fleming, 2006) and Integral Resonant Control (IRC) (Aphale et al., 2007) are also collocated control techniques which are popular in literature, but they present some limitations when used with piezoelectric transducers. In the field of AVC in general, apart from the aforementioned methods, many other different control strategies have been applied for several types of applications. Fractional-order calculus has been found to be a very effective tool in control (see

e.g. HosseinNia et al. (2014, 2013); Monje et al. (2004, 2008); Podlubny (1999)), however it has never found much room in the context of AVC and little research is present (Butler and de Hoon, 2013). In this paper, a fractional-order version of the PPF compensator is proposed to further improve its already appealing properties and to overcome some of its limitations such as low-frequency spillover, quasi-static gain amplification and difficult tuning in multi-mode control.

In the next section DVF, RC, PPF and IRC are elaborated and compared to justify the choice of PPF. Moreover, spillover effect has been introduced. In section 3 fractional-order PPF is developed and its parameters have been tuned using an optimization algorithm. An illustrative example is given in section 4, whereas final conclusions and remarks follow in section 5.

2. PROBLEM DEFINITION

2.1 Direct Velocity Feedback

Direct Velocity Feedback of a 1-DOF system is defined as follows:

$$\ddot{\xi} + 2\zeta\omega\dot{\xi} + \omega^2\xi = \omega^2 f \quad (1)$$

where ξ , ω , ζ are modal coordinate, natural frequency and modal damping of the structure, respectively; $f = -g\dot{\xi}$ is the modal control force and g is the feedback gain. Equation (1) can be rewritten in the following form:

$$\ddot{\xi} + (2\zeta\omega + g\omega^2)\dot{\xi} + \omega^2\xi = 0 \quad (2)$$

It can be noted that active damping in this case is achieved through direct velocity feedback signal with gain g . DVF does not prevent the occurrence of spillover effect, but unconditional closed-loop stability is guaranteed nevertheless for $g > 0$ (Moheimani, S.O.R. , and Fleming, 2006). Despite its stability properties, DVF shows important limitations that do not make it an appealing control scheme in the context of active control with piezoelectric transducers. First of all, piezoelectric sensors measure strain of the structure, which can be considered as a displacement signal that would need to be differentiated before being feedback to the velocity controller. Therefore, in using DVF a differentiator is required, but generally not preferred. Secondly, in order to make sure that the compensator rolls-off at high frequencies, extra dynamics needs to be added to it although this could potentially cause instability (Moheimani, S.O.R. , and Fleming (2006); Goh and Caughey (1985)). Furthermore DVF has high control effort at all frequencies, and in this context of vibration control it is best to restrict the control effort in the frequency range of interest also to prevent actuator saturation.

2.2 Resonant Control

Resonant Control consists of the realization of an electrical dynamic vibration absorber. It is a second order high-pass filter compensator with negative feedback, where the numerator dynamics convert the position feedback (from the piezoelectric sensor) to acceleration feedback. In modal coordinates RC is defined as follows:

System:

$$\ddot{\xi} + 2\zeta\omega\dot{\xi} + \omega^2\xi = \omega^2 f \quad (3)$$

Compensator:

$$\dot{\eta} + 2\zeta_f\omega_f\dot{\eta} + \omega_f^2\eta = \ddot{\xi} \quad (4)$$

where η , ω_f , ζ_f are modal coordinate, natural frequency and modal damping of the compensator, respectively; $f = -g\eta$ is the modal control force representing the negative position feedback. The frequency ω_f is normally tuned to the structure's frequency of interest, and together with a proper choice for the parameters g and ζ_f vibration reduction can be achieved. Here, closed-loop stability is guaranteed for $g > 0$. The high-pass filter characteristics prevent spillover at frequencies lower than the tuning frequency ω_f , but not at higher frequencies where spillover causes changes both in magnitude and frequency of higher vibration modes in the closed-loop response. Therefore, when multiple modes shall be controlled at the same time, multiple compensators can be applied in parallel, but particular attention must be paid to tuning the different RC filters in order to limit the spillover effect. In fact, a compensator targeting a low frequency mode should be tuned prior to the compensator targeting a mode at a higher frequency. It is worth noting that RC is not appealing for practical implementation since actuators and sensors have generally high frequency dynamics which are not neglected by the high-pass filter of the RC and can therefore destabilize the closed-loop system.

2.3 Positive Position Feedback

Unlike RC, Positive Position Feedback is a second order low-pass filter with position signal which is positively feedback to the plant. In modal domain, the two equations for a single DOF system and PPF compensator are:

System:

$$\ddot{\xi} + 2\zeta\omega\dot{\xi} + \omega^2\xi = \omega^2 f \quad (5)$$

Compensator:

$$\dot{\eta} + 2\zeta_f\omega_f\dot{\eta} + \omega_f^2\eta = \omega_f^2\xi \quad (6)$$

where in this case $f = g\eta$ is the modal control force representing the positive position feedback.

For this particular formulation, which is found in most of the literature, the closed-loop stability condition (Fanson, 1987) is simply given by:

$$g < 1 \quad \text{or equally} \quad \frac{K_f}{\omega^2} < 1 \quad (7)$$

where $g = \frac{K_f}{\omega^2}$, with gain K_f , is assumed to be positive since this method works with positive feedback. For a proper performance, ω_f is tuned equal to ω and ζ_f is normally chosen to be bigger than ζ . The low-pass filter characteristics cause the PPF to provide so-called active flexibility before the tuning frequency ω_f , active damping around ω_f and active stiffness for higher frequencies (Kwak and Heo, 2007). Therefore, it limits high-frequency spillover but it does not prevent low-frequency spillover which causes changes both in magnitude and frequency of lower vibration modes in the closed-loop response. When multiple modes need to be controlled at the same time, a compensator targeting a low frequency mode should be tuned after a compensator targeting a mode at higher frequency in order to account for the frequency shift caused by spillover effect.

DVF, RC and PPF are compared in Table 1.

Table 1: Controllers comparison.

Controller	Block diagram	Stability	Properties
DVF		Unconditional ($g > 0$)	<ul style="list-style-type: none"> • Direct addition of active damping • Differentiator needed • No roll-off at high frequencies • High control effort at all frequencies
RC		Unconditional ($g > 0$)	<ul style="list-style-type: none"> • 2nd order HP filter • High frequency spillover • No roll-off at high frequencies • Difficult tuning in multi-mode control
PPF		$0 < g < 1$	<ul style="list-style-type: none"> • 2nd order LP filter • Low frequency spillover • Roll-off at high frequencies • Difficult tuning in multi-mode control

System: $\ddot{\xi} + 2\zeta\omega\xi + \omega^2\xi = \omega^2 f$; $G(s) = \omega^2 / (s^2 + 2\zeta\omega s + \omega^2)$.

2.4 Integral Resonant Control

Another method that is often found in literature is Integral Resonant Control (Aphale et al., 2007). This method is a modified version of the Integral Force Feedback (IFF) method, which is developed for control systems where displacement actuators, and force sensors are used (Preumont, 2011). This implies that the transfer function of the collocated system to be controlled should represent the dynamic stiffness, and not the receptance which is used for the other controllers. Hence, a feed-through term is added to the collocated transfer function in order to convert its frequency response function from receptance to dynamic stiffness, allowing the use of integral feedback. This collocated transfer function also shows pole-zero interlacing property, but starting with a zero. The application of this technique however presents limitations: it generally requires a model of the structure; modes cannot be treated separately; the control gain decreases at higher frequencies causing it to be less effective for high frequency modes.

2.5 Spillover

In general terms, spillover can be explained as the effect that modes which are outside the bandwidth of the controller have on the closed-loop system. Spillover is classified as *observation spillover* when sensor outputs are contaminated by the measured response of residual modes, and *control spillover* when residual modes are excited by the feedback control (Balas (1978)). Observation spillover can be eliminated by the use of collocated configuration,

whereas the effect of control spillover strongly depends on the feedback control scheme used. In this work, observation spillover is assumed not to be present due to the use of collocation, and only control spillover (here simply referred as *spillover*) is treated.

The closed-loop system can become degraded or even destabilized due to the presence of out-of-bandwidth modes. The desired behaviour of the controller would be to target a specific mode and leave the response for the uncontrolled modes ideally unchanged, which in practice never happens because of spillover. Uncontrolled modes can indeed present a change in magnitude and a shift in the resonance frequency making the tuning of the controller more difficult when multiple modes are controlled at the same time. The control action also causes a magnitude amplification in the quasi-static region of the closed-loop response.

Spillover effect is strictly related to the phase behaviour of the closed-loop: the more the phase of the closed-loop follows the phase of the plant, the less spillover is observed, at the expense of a smaller reduction in magnitude of the controlled resonance peak (see Figure 1). This relation between spillover and phase has not received much attention in literature (Niezrecki and Cudney, 1997) and it is intentionally highlighted by the authors. Therefore, in the next section, a novel controller that improves both phase and magnitude response of the close-loop is proposed using fractional-order calculus.

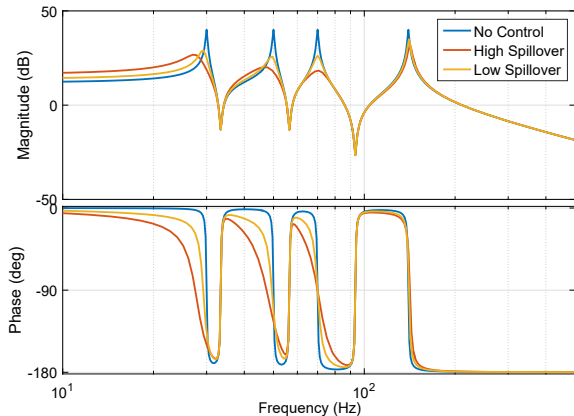


Fig. 1. Relation between spillover effect and phase of the closed-loop is shown by two differently tuned PPF compensators both used to suppress the 3rd mode of the plant: the more the phase of the closed-loop follows the phase of the plant the less spillover is observed, at the expense of a smaller reduction in magnitude of the controlled resonance peak. Quasi-static gain amplification is also caused by the control action.

3. PROPOSED METHOD

3.1 Fractional-order systems

As stated by Monje et al. (Monje et al., 2010), 'Fractional calculus can be defined as the generalization of classical calculus to orders of integration and differentiation not necessarily integer'. Fractional-order dynamic systems can be expressed by fractional-order transfer functions whose simplest form in Laplace domain is s^α where $\alpha \in \mathbb{R}$ and s is the Laplace transform variable. The benefit of fractional-order transfer functions comes from the fact that they have magnitude and phase response which are not representative of any integer-order transfer functions thereby providing in-between characteristics. In other words, fractional calculus allows for a trade-off between the phase lag of an integrator and the high frequency gain of a differentiator. Control engineering applications have found increasing interest in this concept, which has then been applied to different control systems like the classical PID (Podlubny, 1999; Monje et al., 2004; Tejado et al., 2012).

3.2 Fractional-order PPF

As seen in section 2, standard controllers for AVC present several limitations such as: quasi-static gain amplification, low and high frequency spillover, and difficult tuning in multi-mode control. Based on the already appealing properties of the PPF, a fractional-order PPF compensator is proposed to improve on these limitations. The integer-order PPF transfer function $C(s)$ shown in Table 1 is rewritten in Equation (8) as

$$C_F(s) = \frac{1}{\left(\left(\frac{s}{\omega_f} \right)^{2\alpha} + 2\zeta_f \left(\frac{s}{\omega_f} \right)^\alpha + 1 \right)} \quad (8)$$

where $1 < \alpha < 2$, $\alpha \in \mathbb{R}$ represents the fractional order. For $\alpha = 1$ the standard integer-order PPF is recovered.

In Figure 2 the bode plots of both integer and fractional-order PPF filters are compared.

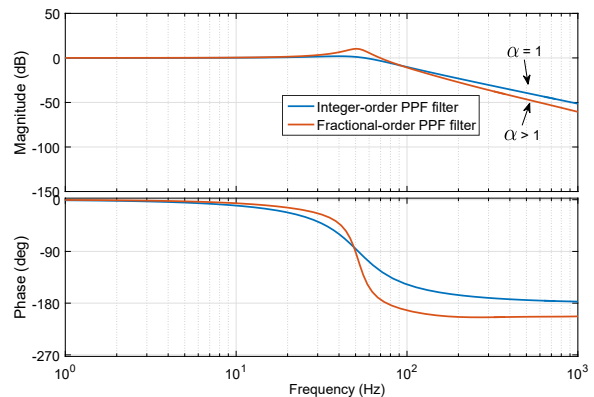


Fig. 2. Bode plots of integer and fractional-order PPF filters: fractional-order PPF with order $1 < \alpha < 2$ has a steeper roll-off after the tuning frequency ω_f .

The addition of another tunable parameter such as the fractional-order α , allows for the improvement of the limitations of the integer-order PPF, by providing a different magnitude and phase response of the filter $C_F(s)$, as seen in Figure 2. For example, the steeper roll-off after the tuning frequency ω_f indicates a greater filtering action at higher frequencies, thus limiting even more the high frequency spillover. Low frequency spillover is improved by the different phase change around ω_f , which allows the phase of the closed-loop response to be closer to the phase of the plant, as already highlighted in Figure 1. The quasi-static gain amplification S_G in the closed-loop $T(s)$ instead depends only on the controller gain g as shown in (9):

$$S_G = T(0) = \frac{G(0)}{1 - gC_F(0)G(0)} = \frac{1}{1 - g} \quad (9)$$

However, the fractional-order α allows the use of smaller values of g for the tuning of the controller, resulting in a lower closed-loop gain in the quasi-static region.

As a consequence, having less spillover and lower quasi-static gain allows for an easier tuning of multiple filters in case of multi-mode control, and an overall improved control performance.

The addition of α as a design parameter makes a full mathematical derivation of the effects of the fractional-order PPF very challenging to conduct. That is why an optimization approach is proposed to find the optimal filter parameters to actually improve on the aforementioned limitations. In section 4 an example is presented to show the expected performance of the new fractional-order controller.

3.3 Stability Analysis

The stability analysis for fractional-order PPF controller $C_F(s)$ can be explained as follows.

The roots of the denominator of $C_F(s)$ should all lie on the complex left-half plane to have a stable controller. By

mapping $\lambda = \left(\frac{s}{\omega_f}\right)^\alpha$, the characteristic equation of (8) can be rewritten as

$$\lambda^2 + 2\zeta_f\lambda + 1 = 0 \quad (10)$$

with roots

$$\lambda = -\zeta_f \pm \sqrt{\zeta_f^2 - 1} \quad (11)$$

Therefore, the condition to have a stable controller $C_F(s)$ is

$$\Re\{s = \omega_f \lambda^{\frac{1}{\alpha}}\} < 0 \quad (12)$$

or equally

$$|\arg(\lambda)| < \alpha \frac{\pi}{2} \quad (13)$$

where \Re indicates the real part of a complex number.

Controller stability for different values of α and ζ_f is depicted in Figure 3.

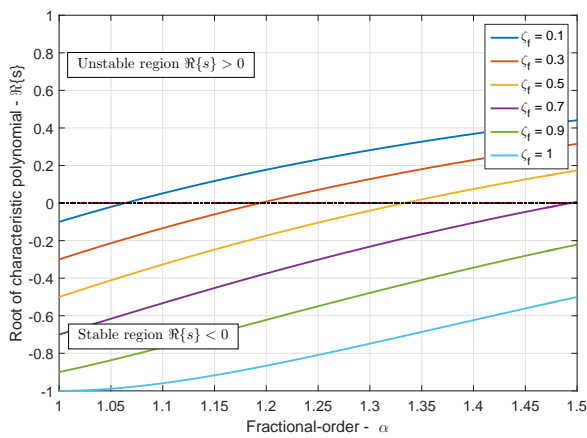


Fig. 3. Stability and instability regions for fractional-order PPF controller $C_F(s)$ for different values of ζ_f .

A closed-loop stability analysis is instead more difficult to conduct. Unlike the integer-order PPF, where the stability condition is simply given by $g < 1$, for the fractional-order PPF stability does not depend only on g , but also on the other parameters ζ_f and α . Thus, a full mathematical derivation of the stability condition is very extensive to obtain. Therefore, an alternative approach based on Nichols stability criterion is proposed.

The Nichols criterion states that closed-loop stability is guaranteed if the Nichols plot of the stable open-loop transfer function $L(s)$ does not intersect the line where $\angle L(s) = -180^\circ$ and $|L(s)| \geq 0$ dB. Therefore, by imposing this condition to the open-loop $L(s) = -gC_F(s)G(s)$, stability and instability regions for the closed-loop transfer function $T(s)$ can be depicted for different values of α , g and ζ_f (see Figure 4).

As represented in Figure 4, for a fixed value of ζ_f the stability region is defined by the relation between the fractional-order α and the gain g , where the curve indicates the stability limit. Values of $g = 0$ indicate that the controller $C_F(s)$ becomes unstable, as seen in Figure 3. For different values of ζ_f the stability region changes: as ζ_f increases, the stable region increases towards higher values of α ; moreover for $\alpha = 1$ the stability condition for the integer-order PPF is recovered ($g < 1$).

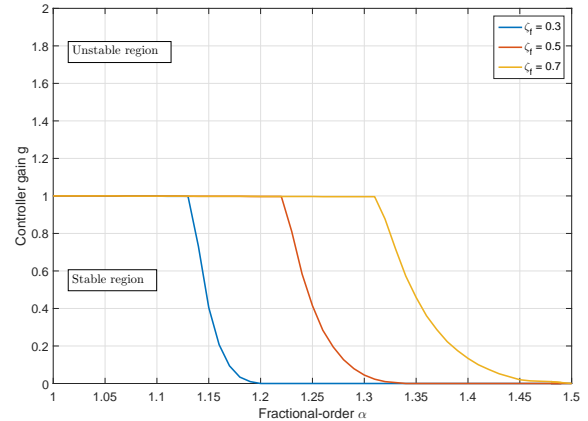


Fig. 4. Stability and instability regions for the closed-loop $T(s)$ for different values of ζ_f .

It is important to notice that the tuning frequency of the filter ω_f does not affect the stability analysis, since ω_f is assumed to be always tuned around the resonance frequency of the plant ω , whose value lies in the stable region of the closed-loop.

3.4 Filter Optimization

The fractional-order PPF filter of (8) has an additional design parameter with respect to the standard integer-order PPF, that is the fractional order α which provides more freedom for the choice of the other tuning parameters ω_f , ζ_f and g . Therefore, an optimality problem is defined to find the mentioned parameters for a fractional-order PPF filter which can limit spillover effect and quasi-static gain amplification. This is done by improving both phase and magnitude response of the closed-loop because of their direct relation with spillover, as already seen in Figure 1.

The objective function h to be minimized is:

$$h = w_1(P_{\max} - S_G) + w_2 \sum (\angle T(s) - \angle G(s)) \quad (14)$$

$$+ p \left(\max \left(0, \frac{P_1}{P_{\max}} - 1 \right) \right)^2$$

$$+ p \left(\max \left(0, \frac{P_2}{P_{\max}} - 1 \right) \right)^2$$

$$+ p \left(\max \left(0, \frac{S_G}{P_1} - 1 \right) \right)^2$$

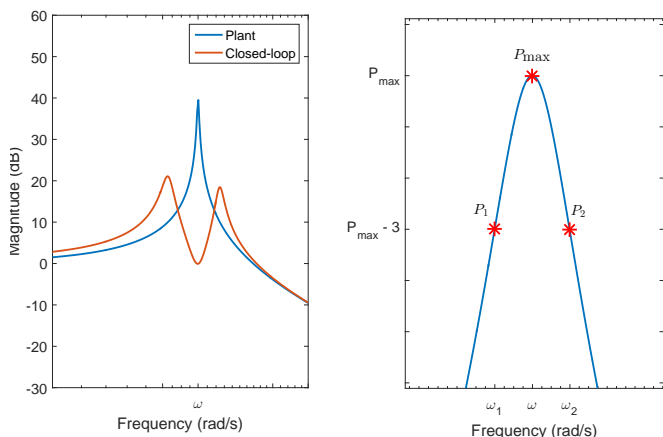
$$+ p \left(\max \left(0, \frac{S_G}{P_2} - 1 \right) \right)^2$$

$$+ p (\max(0, \zeta_T))^2$$

where the magnitude of the closed-loop $T(s)$, where $T(s) = \frac{G(s)}{1 - gC_F(s)G(s)}$, is optimized by the difference between the magnitude P_{\max} at the resonance ω and static gain S_G of the plant $G(s)$, so to impose maximal peak reduction; the phase is optimized instead by the minimization of the difference between phase of the closed-loop $T(s)$ and phase of the plant $G(s)$; two weights w_1 and w_2 are

used to give more importance either to the magnitude or phase optimization.

The objective is also enhanced by the addition of penalization functions, in order to make sure that the resonance peak is always reduced without creating two additional peaks around ω due to the presence of extra zeros in the closed-loop (Kwak, Moon K. and Han, Sang-Bo and Heo, 2004) (see Figure 5a). P_1 and P_2 are the so-called *half-power* points at 3 dB down from the resonance peak and are used to compute the closed-loop damping ζ_T at resonance with the Half-power Bandwidth method (see Figure 5b); p is the penalization factor. Closed-loop stability is also added as equality constraint by setting the number of unstable poles equal to 0.



(a) Closed-loop zero causing two extra peaks around resonance. This effect is limited by the addition of proper penalization functions. (b) Half-power points P_1 and P_2 at 3 dB down from the resonance peak. These points are used to compute the closed-loop damping ζ_T by the Half-power Bandwidth method: $\zeta_T = \frac{\omega_2 - \omega_1}{2\omega}$.

Fig. 5. Conditions for closed-loop damping ζ_T .

A Global-Search algorithm using a constrained non-linear optimization is chosen to solve the optimality problem because the objective h is highly non-linear and presents several local optima. The algorithm is implemented in MATLAB by means of the 'GlobalSearch' and 'fmincon' functions. The plant $G(s)$ is chosen to represent a simple 1-DOF system as in Equation (5), and the outcome of the optimization gives the four tuning parameters for the filter $C_F(s)$. Optimization results depend mainly on the choice of the two weights w_1 and w_2 , from which a filter $C_F(s)$ that has either a stronger effect on the magnitude or on the phase of the closed-loop can be obtained. In the next section some examples showing the potential benefit of using a fractional-order PPF rather than an integer-order PPF are presented.

4. ILLUSTRATIVE EXAMPLE

4.1 Simulation Results

Performances of the standard integer-order PPF and the optimized fractional-order PPF are compared first on a simple plant representing a 1-DOF system and then on

a plant representing a multi-DOF system. Comparison is made by tuning the integer-order PPF such that both compensators provide the same magnitude reduction of the resonance peak to be controlled. Tuning parameters for both filters are listed in Table 2. It is important to highlight that controllers are normally not tuned to achieve 100% peak reduction, and that is mainly done to avoid performance losses in multi-mode control.

Table 2: Tuning parameters for Integer and Fractional-order PPF filters, both providing same magnitude reduction of the resonance peak at ω .

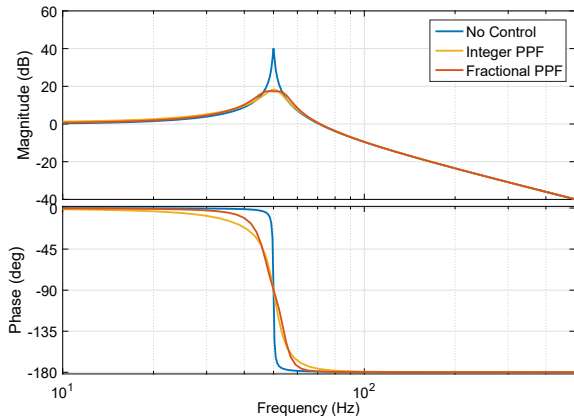
Parameter	Integer PPF	Fractional PPF
g	0.1	0.0365
ω_f	ω	1.0366ω
ζ_f	0.45	0.4227
α	1	1.1844

In Figure 6a, a simple plant with single resonance at 50 Hz is controlled by both integer-order and fractional-order PPF compensators. The same magnitude reduction is achieved for the two closed-loop responses, but the phase response is closer to the phase response of the plant when fractional-order PPF is used. In Figure 6b, the corresponding step response is shown, where it is clearly seen how the vibration is quickly damped out by both controllers although the steady state gain is closer to 1 in case of fractional-order PPF. This corresponds to a magnitude in the frequency response closer to the ideal behaviour at 0 dB.

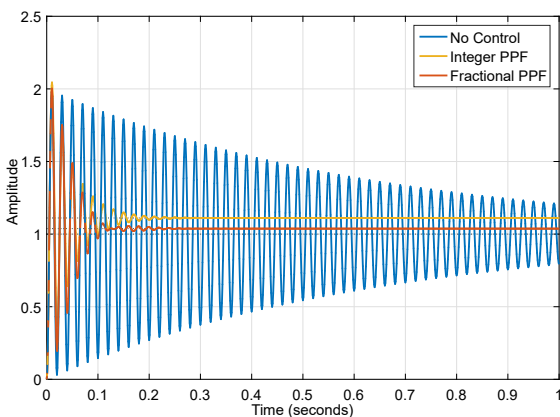
The real benefit of an improved phase behaviour is more evident in case of a multi-mode plant as shown in Figure 7. In Figure 7a, the 3rd mode is controlled and less spillover is present both at lower and higher frequencies than the controlled resonance when fractional-order PPF is used, since it maintains the phase response much closer to the plant response rather than what the integer-order PPF does. In Figure 7b, the 2nd and 4th modes are controlled simultaneously using two parallel PPF filters: again the spillover effect is much less in case of fractional-order PPF since the uncontrolled 1st and 3rd modes are less affected by the control action. Uncontrolled modes indeed present a smaller shift in frequency caused by spillover together with a largely reduced magnitude amplification in the quasi-static region, thus ensuring a better control performance and easier tuning of the filters especially when multiple modes are controlled at the same time.

4.2 Experimental Results

The same performance comparison of the two PPF filters is done on measured frequency response data. An experimental collocated transfer function has been obtained by performing modal tests on a rectangular carbon fibre composite plate. The plate was hung from four corners by nylon cords to simulate all edge free boundary conditions and an electrodynamic shaker was used to provide random excitation to obtain frequency response curves. An impedance head measures the force applied by the shaker and a Laser Doppler Vibrometer measures the velocity vibration response on the other side of the plate with respect



(a) Single-mode plant controlled.



(b) Step Response.

Fig. 6. Single-mode plant controlled by both integer and fractional-order PPF.

to the shaker (see Figure 8). The measured data is then imported into MATLAB as 'frd' object, velocity is converted to position, and PPF filters are applied similarly to what was done for the previous section. Tuning parameters of Table 2 are kept the same except for the gain g which has been adjusted according to the overall magnitude of the measured plant which is different from the one used in the previous section. In Figure 9, the measured plant response together with the controlled transfer functions are shown. In Figure 9a, the mode at 37 Hz is controlled and in Figure 9b, modes at 37 Hz and 108 Hz are controlled simultaneously. In both cases the spillover effect caused by the fractional-order PPF is found to be less both at low and high frequencies with respect to the standard integer-order PPF.

The experimental vibration setup of Figure 8 is proposed with the aim to eventually extend this work and implement the controller with piezoelectric sensors and actuators.

5. CONCLUSIONS

In this paper, a novel fractional-order compensator based on Positive Position Feedback has been proposed to limit the spillover effect caused by the dynamics of uncontrolled vibration modes. The strict relation between spillover ef-

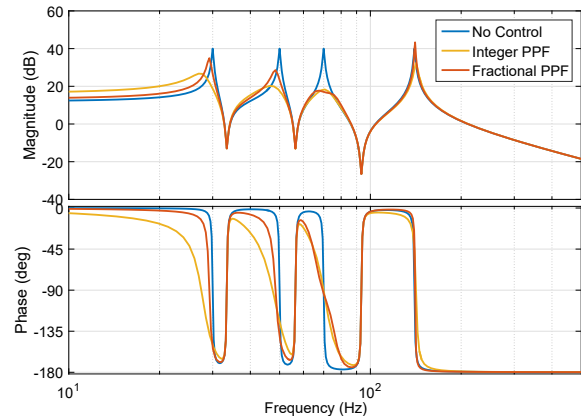
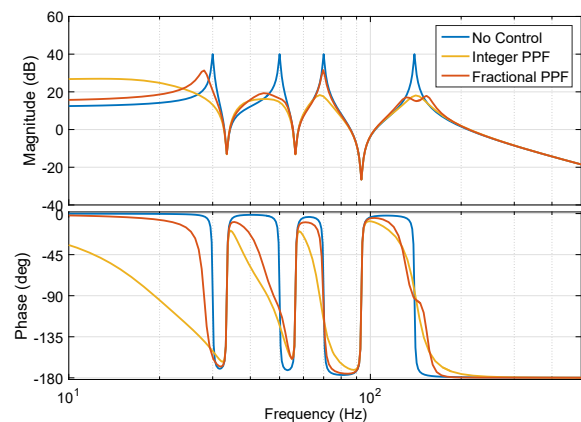
(a) 3rd mode controlled.(b) 2nd and 4th mode controlled.

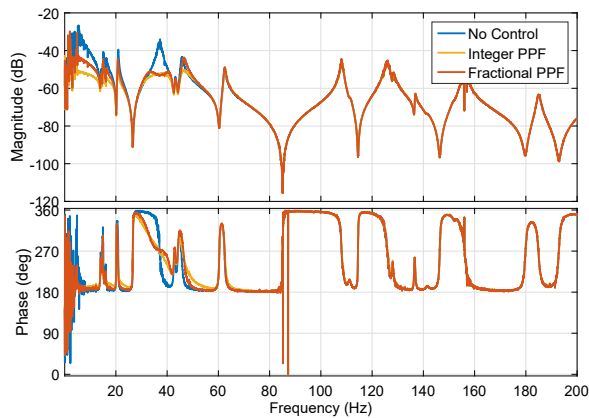
Fig. 7. Simple plant representing a multi-DOF system controlled by both integer and fractional-order PPF.



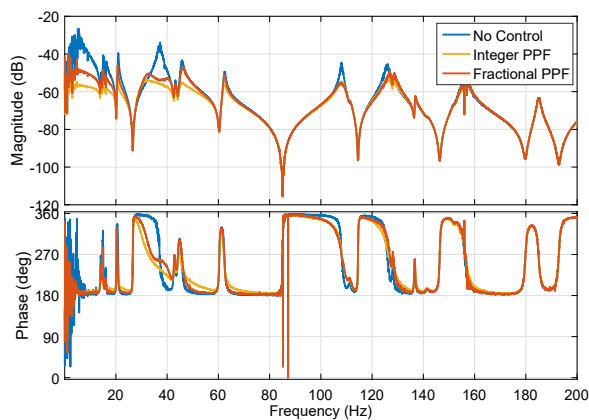
(a) Laser Doppler Vibrometer (b) Shaker and impedance head.

Fig. 8. Experimental vibration setup.

fect and closed-loop phase response has been highlighted and used for the controller optimization where both magnitude and phase response are optimized. A Global-Search algorithm using a constrained non-linear optimization has been used to obtain the tuning parameters. Performance of the fractional-order PPF filter has been verified by comparison with an integer-order PPF tuned such that



(a) Mode at 37 Hz controlled.



(b) Modes at 37 Hz and 108 Hz controlled.

Fig. 9. Effect of PPF on measured frequency response data.

both compensators provided the same magnitude reduction of the resonance peak. Results obtained both on simple plants, representing 1-DOF and multi-DOF systems, and experimental frequency response data have shown that fractional-order PPF improves the overall control performance with respect to the standard integer-order PPF by limiting the spillover due to uncontrolled modes both at high frequencies, by providing a steeper roll-off, and at low frequencies, by providing a better phase behaviour and limiting the magnitude amplification in the quasi-static region. It can thus be concluded that the use of fractional-order transfer functions is very promising to improve the performance of commonly used active vibration control strategies since they can provide in-between response characteristics that would not be achievable by standard integer-order transfer functions. Furthermore, an experimental implementation of the proposed fractional-order compensator needs to be performed to better validate its behaviour in a practical application.

REFERENCES

Aphale, S.S., Fleming, A.J., and Moheimani, S.O.R. (2007). Integral resonant control of collocated smart structures. *Smart Materials and Structures*, 16(2), 439–446.

- Balas, M.J. (1978). Feedback control of flexible systems. *IEEE Transactions on Automatic Control*, 23(4), 673–679.
- Butler, H. and de Hoon, C. (2013). Fractional-order filters for active damping in a lithographic tool. *Control Engineering Practice*, 21(4), 413–419.
- Fanson, J.L. (1987). *An Experimental Investigation of Vibration Suppression in Large Space Structures Using Positive Position Feedback*. Phd thesis, California Institute of Technology.
- Goh, C.J. and Caughey, T.K. (1985). On the stability problem caused by finite actuator dynamics in the collocated control of large space structures. *International Journal of Control*, 41(3), 787–802.
- HosseinNia, S.H., Tejado, I., Torres, D., Vinagre, B.M., and Feliu, V. (2014). A General Form for Reset Control Including Fractional Order Dynamics. *IFAC Proceedings Volumes*, 47(3), 2028–2033.
- HosseinNia, S.H., Tejado, I., and Vinagre, B.M. (2013). Fractional-order reset control: Application to a servomotor. *Mechatronics*, 23(7), 781–788.
- Kwak, M.K. and Heo, S. (2007). Active vibration control of smart grid structure by multiinput and multioutput positive position feedback controller. *Journal of Sound and Vibration*, 304(1-2), 230–245.
- Kwak, Moon K. and Han, Sang-Bo and Heo, S. (2004). The Stability Conditions, Performance and Design Methodology for the Positive Position Feedback Controller. *Transaction of the Korean Society for Noise and Vibration Engineering*, 14(3), 208–213.
- Moheimani, S.O.R., and Fleming, A. (2006). *Piezoelectric Transducers for Vibration Control and Damping*. Advances in Industrial Control. Springer-Verlag, London.
- Monje, C.a., Chen, Y.Q., Vinagre, B.M., Xue, D., and Feliu, V. (2010). *Fractional-order Systems and Controls. Fundamentals and Applications*.
- Monje, C.A., Calderon, A.J., Vinagre, B.M., Chen, Y., and Feliu, V. (2004). On Fractional PI^λ Controllers: Some Tuning Rules for Robustness to Plant Uncertainties. *Nonlinear Dynamics*, 38(1-4), 369–381.
- Monje, C.A., Vinagre, B.M., Feliu, V., and Chen, Y. (2008). Tuning and auto-tuning of fractional order controllers for industry applications. *Control Engineering Practice*, 16(7), 798–812.
- Niezrecki, C. and Cudney, H.H. (1997). Structural Control Using Analog Phase-Locked Loops. *Journal of Vibration and Acoustics*, 119(1), 104.
- Podlubny, I. (1999). Fractional-Order Systems and $PI^\lambda D^\mu$ -Controllers. *IEEE Transactions on Automatic Control*, 44(1), 208–214.
- Preumont, A. (2011). *Vibration Control of Active Structures*, volume 179.
- Tejado, I., HosseinNia, S.H. and Vinagre, B. M. (2012). Comparing fractional order PI controllers with variable gain and gain-order for the networked control of a servomotor. *IFAC Proceedings Volumes*, 45(3), 655–660.

4


Active Vibration Control of a Carbon Fibre Composite Plate

This chapter has been written in format of a scientific paper. It presents the active vibration control of a carbon fibre/epoxy composite plate using smart materials and fractional-order Positive Position Feedback compensator.

The aim of this paper is to show the experimental application of fractional control, which is for the first time done in the field of active vibration control of composite structures with smart materials.

The paper has been submitted to the Journal of Vibration and Control (JVC).

Fractional-Order Positive Position Feedback Compensator for Active Vibration Control of a Smart Composite Plate

Journal of Vibration and Control
XX(X):38–51
©The Author(s) 2016
Reprints and permission:
sagepub.co.uk/journalsPermissions.nav
DOI: 10.1177/ToBeAssigned
www.sagepub.com/


L. Marinangeli¹, F. Alijani¹ and S.H. HosseinNia¹

Abstract

In this paper Active Vibration Control (AVC) of a rectangular carbon fibre composite plate with free edges is presented. The plate is subjected to out-of-plane excitation by a modal vibration exciter and controlled by Macro Fibre Composite (MFC) transducers. Vibration measurements are performed by using a Laser Doppler Vibrometer (LDV) system. Two fractional-order Positive Position Feedback (PPF) compensators are proposed, implemented and compared to the standard integer-order PPF. MFC actuator and sensor are positioned on the plate based on maximal modal strain criterion, so as to control the second natural mode of the plate. Both integer and fractional-order PPFs allowed for the effective control of the second mode of vibration. However, the newly proposed fractional-order controllers are found to be more efficient in achieving the same performance with less actuation voltage. Moreover, they show promising performance in reducing spillover effect due to uncontrolled modes.

Keywords

Active Vibration Control, Fractional-order control, Positive Position Feedback, Spillover, Experimental Modal Analysis, Smart materials, Composite plates

1 Introduction

In the past decades research on Active Vibration Control (AVC) has found increasing interest in control of flexible thin-walled structures, mainly made of new advanced materials such as carbon fibre composites. These type of composite structures combine high stiffness with good flexibility in achieving complex shapes, and are mostly used in automotive and aerospace applications where they are often subjected to undesirable vibrations. In the field of AVC, a new type of sensor and actuator have become popular by using the so-called *smart materials*, such as piezoelectric materials, shape-memory alloys and electroactive polymers. These materials are called smart because they are inherently capable of detecting or responding to changes in their environment, making them very suitable both for sensing and actuation purposes. Given their distributed nature, they can be easily mounted on different types of structures, thus making them *smart structures*.

Piezoelectric transducers are often selected as sensors and actuators for the active control of smart flexible structures because of their unique properties including low cost, low mass, ease of integration and wide frequency range of control. In 1996 NASA invented a specific type of transducer called Macro Fibre Composite (MFC) which provides high performance, durability and a very good flexibility, making these transducers a preferred option in the case they shall be adapted to different structure geometries. Piezoelectric transducers in general, when used as sensors, measure strain which is proportional to the physical displacement. In fact, control schemes specifically designed to use position as

feedback signal have been extensively studied and applied in this context.

The main objective of the controller is to provide active damping to the structure (plant), which results in an attenuation of the resonance peak in the dynamic amplification. The dynamics of flexible structures have very interesting properties: because of their flexibility, they have a large number of elastic modes resulting in very high order transfer functions that are rather difficult to control. Controllers are designed to target specific vibration modes in a restricted bandwidth of interest, and the fact that transfer functions are of high order means that there are out-of-bandwidth modes which are neglected, but whose effect might influence the closed-loop response. The effect of the uncontrolled, or out-of-bandwidth modes, is known in the literature as *spillover* (Balas 1978). Another important aspect regarding the controller is that, apart from being able to reduce structural vibrations, it should ensure robustness and closed-loop stability for the controlled system. In this sense, careful positioning of sensors and actuators can have a great influence. The majority of the controllers studied in literature use a *collocated* configuration, where sensors and actuators are related to the same Degree of Freedom (DOF) of the

¹Department of Precision and Microsystems Engineering, Delft University of Technology, Mekelweg 2, 2628 CD Delft, The Netherlands

Corresponding author:

S.H. HosseinNia, Department of Precision and Microsystems Engineering, Delft University of Technology, Mekelweg 2, 2628 CD Delft, The Netherlands

Email: s.h.hosseinNia@tudelft.nl

structure. The phase of the open-loop collocated transfer function is always between 0° and -180° , meaning that poles and zeros interlace on the imaginary axis, where zeros and poles correspond to anti-resonances and resonances of the frequency response, respectively. Collocated systems have the property of being always closed-loop stable with respect to out-of-bandwidth dynamics (Preumont 2011) and that is why most of the research involves collocation.

One of the most popular collocated modal control schemes is Positive Position Feedback (PPF), which has been first proposed in 1985 by Goh and Caughey (Goh and Caughey 1985) to overcome the instability associated with finite actuator dynamics. This controller was applied for the first time in 1987 by Fanson (Fanson 1987) to experimentally suppress vibrations in large space structures. PPF is effective if tuned to suppress a chosen frequency and mode. It is a second order low-pass filter which rolls off quickly at high frequencies, making it very appealing against possible instability or performance losses due to out-of-bandwidth dynamics.

Applications of PPF with smart structures are also extensively studied in literature. Kwak and Heo (Kwak and Heo 2007) applied a Multi-Input Multi-Output (MIMO) PPF to control vibrations of a smart grid structure equipped with piezoelectric transducers. They proposed a new technique to control a higher number of modes than the number of actuators and sensors. Zippo et al. (Zippo et al. (2015)) applied PPF for active vibration control of a composite sandwich plate using MFC transducers. Ferrari and Amabili (Ferrari and Amabili (2015)), as a continuation of the work of Zippo, applied non-collocated PPF both in Single-Input Single-Output (SISO) and MIMO.

Direct Velocity Feedback (DVF), Resonant Control (RC) (Moheimani, S.O.R. , and Fleming 2006) and Integral Resonant Control (IRC) (Aphale et al. 2007) are also collocated control techniques which are popular in literature, but they present some limitations when used with piezoelectric transducers. In the field of AVC in general, apart from the aforementioned methods, many other different control strategies have been applied for several types of applications. Fractional-order calculus has been found to be an effective tool in control (see e.g. Hosseinnia et al. (2014); HosseinNia et al. (2013); Monje et al. (2004, 2008); Podlubny (1999)), however it has never found much room in the context of AVC and little research is present (Butler and de Hoon 2013).

Fractional-control has never been experimentally applied before in the field of AVC of smart structures, and it is for the first time presented in this paper. Two fractional-order versions of the PPF compensator are proposed, and compared to the standard integer-order PPF. Controllers are then implemented to control the 2nd mode of a carbon fibre/epoxy composite plate equipped with MFC actuator and sensor. A similar setup to the one used by Alijani and Amabili for similar studies (Alijani et al. 2013; Alijani and Amabili 2013) is built to test and control the plate with all edge free boundary conditions. These type of boundary conditions reduce the influence of temperature variations and other non-ideal boundary conditions which are generally associated with relevant changes in natural frequencies due to thermal stress. Therefore, completely free boundary

conditions have been chosen to perform experimental modal analysis on the composite plate. In the next section, integer and fractional-order PPF compensators are elaborated and compared. In section 3 the experimental dynamics setup and complete AVC setup are described in detail. In section 4 results are presented, whereas final remarks and conclusions follow in section 5.

2 Control

2.1 Positive Position Feedback

Positive Position Feedback is a second order low-pass filter with position signal which is positively feedback to the plant. In modal domain, the two equations for a single DOF system and PPF compensator are:

System:

$$\ddot{\xi} + 2\zeta\omega\dot{\xi} + \omega^2\xi = \omega^2 f \quad (1)$$

Compensator:

$$\ddot{\eta} + 2\zeta_f\omega_f\dot{\eta} + \omega_f^2\eta = \omega_f^2\xi \quad (2)$$

where in this case $f = g\eta$ is the modal control force representing the positive position feedback. The corresponding feedback loop is shown in Figure 1.

For this particular formulation, which is found in most of the literature, the closed-loop stability condition (Fanson 1987) is simply given by:

$$g < 1 \quad \text{or equally} \quad \frac{K_f}{\omega^2} < 1 \quad (3)$$

where $g = \frac{K_f}{\omega^2}$, with gain K_f , is assumed to be positive since this method works with positive feedback. For a proper performance, ω_f is set equal to ω and ζ_f is normally chosen to be bigger than ζ . The low-pass filter characteristics cause the PPF to provide the so-called active flexibility before the tuning frequency ω_f , active damping around ω_f and active stiffness for higher frequencies (Kwak and Heo 2007). Therefore it limits high-frequency spillover but it does not prevent low-frequency spillover which causes changes both in magnitude and frequency of lower vibration modes in the closed-loop response. When multiple modes need to be controlled at the same time, a compensator targeting a low frequency mode should be tuned later than a compensator targeting a mode at higher frequency in order to account for the frequency shift caused by spillover effect.

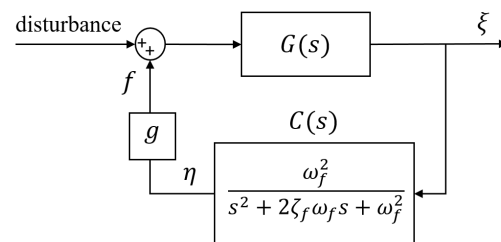


Figure 1. PPF feedback loop: $G(s)$ and $C(s)$ represent the plant and compensator transfer function, respectively.

2.2 Fractional-order Control

As stated by Monje et al. (Monje et al. 2010), 'Fractional calculus can be defined as the generalization of classical calculus to orders of integration and differentiation not necessarily integer'. Fractional-order dynamic systems can be expressed by fractional-order transfer functions whose simplest form in Laplace domain is s^α , where $\alpha \in \mathbb{R}$ and s is the Laplace transform variable. The benefit of fractional-order transfer functions comes from the fact that they have magnitude and phase response which are not representative of any integer-order transfer functions thereby providing in-between characteristics. In other words, fractional calculus allows for a trade-off between the phase lag of an integrator and the high frequency gain of a differentiator. Control engineering applications have found increasing interest in this concept, which has then been applied to different control systems like the classical PID (Podlubny 1999; Monje et al. 2004; Tejado et al. 2012).

2.2.1 CRONE approximation

Controllers with fractional-order transfer functions can only be implemented in hardware by means of integer-order approximation of fractional derivatives. Different approximations techniques are available, of which an overview is given by Vinagre et al. (Vinagre et al. 2000). In this work the most popular CRONE approximation proposed by Oustaloup in 1991 (Oustaloup 1991) is used. According to CRONE the approximation $\hat{F}(s)$ of $F(s) = s^\alpha$ is:

$$\hat{F}(s) = C_0 \prod_{n=1}^N \frac{1 + \frac{s}{\omega_{z_n}}}{1 + \frac{s}{\omega_{p_n}}} \quad (4)$$

where $\hat{F}(s)$ has N zeros ω_{z_n} and N poles ω_{p_n} in an interval of frequencies $[\omega_l; \omega_h]$.

Gain C_0 is adjusted so to have $|\hat{F}(s)| = 0$ dB at 1 rad/s. Zeros and poles are given by

$$\omega_{z_1} = \omega_l \sqrt{\psi}, \quad \omega_{z_n} = \omega_{p_{n-1}} \psi, \quad n = 2, \dots, N \quad (5a)$$

$$\omega_{p_n} = \omega_{z_{n-1}} \nu, \quad n = 1, \dots, N \quad (5b)$$

$$\nu = (\omega_h / \omega_l)^{\frac{\alpha}{N}}, \quad \psi = (\omega_h / \omega_l)^{\frac{1-\alpha}{N}} \quad (5c)$$

Outside the interval $[\omega_l; \omega_h]$ no fractional-like behaviour is present. Therefore, a frequency range of interest and a number N of poles and zeros must be defined before using this approximation.

2.3 Fractional-order PPF

Two fractional-order PPF filters are proposed to further improve performance and properties of the standard integer-order PPF already introduced in subsection 2.1.

2.3.1 Filter #1

The integer-order PPF transfer function $C(s)$ shown in Figure 1 is rewritten in Equation (6) as

$$C_{F_1}(s) = \frac{1}{\left(\left(\frac{s}{\omega_f} \right)^{2\alpha} + 2\zeta_f \left(\frac{s}{\omega_f} \right)^\alpha + 1 \right)} \quad (6)$$

where $1 < \alpha < 2$, $\alpha \in \mathbb{R}$ represents the fractional order. For $\alpha = 1$ the standard integer-order PPF is recovered.

In Figure 2 the bode plots of both integer and fractional-order PPF filters are compared.

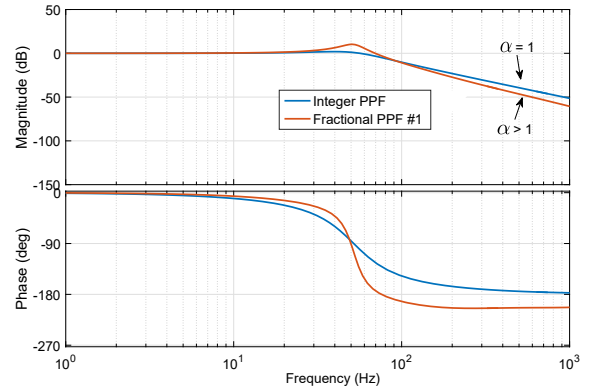


Figure 2. Bode plots of integer and fractional-order PPF #1 filters: fractional-order PPF #1 with order $1 < \alpha < 2$ has a steeper roll-off after the tuning frequency ω_f .

The introduction of an additional tunable parameter such as the fractional-order α , allows for the improvement of the performance of the integer-order PPF, by providing a different magnitude and phase response of the filter $C_{F_1}(s)$, as seen in Figure 2. For example, the steeper roll-off after the tuning frequency ω_f indicates a greater filtering action at higher frequencies, thus limiting even more the high frequency spillover. Low frequency spillover is improved by the different phase change around ω_f , which allows the phase of the closed-loop response to be closer to phase of the plant. This is because of the strict relation between spillover effect and phase of the closed-loop: the more the phase of the closed-loop follows the phase of the plant the less spillover is observed (see Figure 3). Moreover, the fractional-order α allows the use of smaller values of g for the tuning of the controller, resulting in a lower closed-loop gain in the quasi-static region.

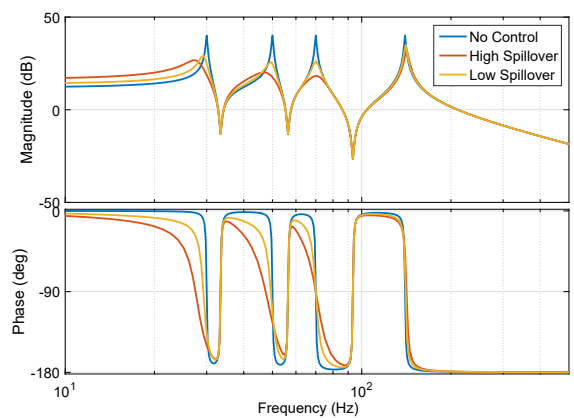


Figure 3. Relation between spillover effect and phase of the closed-loop is shown by two differently tuned integer-order PPF compensators both used to suppress the 3rd vibration mode of the plant.

As a consequence, having less spillover and lower quasi-static gain facilitates tuning of multiple filters in case of multi-mode control, and an overall improved control performance.

2.3.1.1 Stability Analysis

The stability analysis for fractional-order PPF controller $C_{F_1}(s)$ can be explained as follows: the roots of the denominator of $C_{F_1}(s)$ should all lie on the complex left-half plane to have a stable controller. By mapping $\lambda = \left(\frac{s}{\omega_f}\right)^\alpha$, the characteristic equation of (6) can be rewritten as

$$\lambda^2 + 2\zeta_f\lambda + 1 = 0 \quad (7)$$

with roots

$$\lambda = -\zeta_f \pm \sqrt{\zeta_f^2 - 1} \quad (8)$$

Therefore, the condition to have a stable controller $C_{F_1}(s)$ is

$$\Re\{s = \omega_f \lambda^{\frac{1}{\alpha}}\} < 0 \quad (9)$$

or equally

$$|\arg(\lambda)| < \alpha \frac{\pi}{2} \quad (10)$$

where \Re indicates the real part of a complex number. Controller stability for different values of α and ζ_f is depicted in Figure 4.

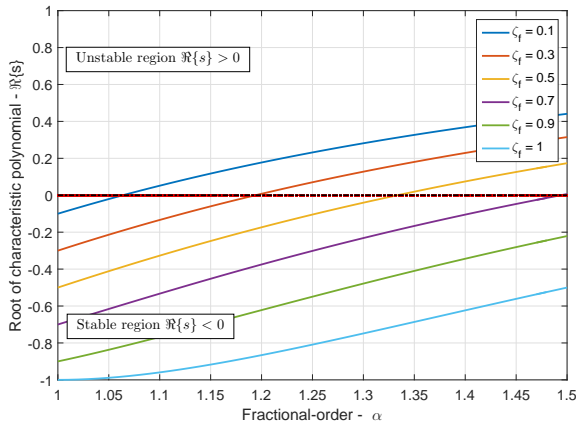


Figure 4. Stable and unstable regions for fractional-order PPF controller $C_{F_1}(s)$ for different values of ζ_f .

A closed-loop stability analysis is instead more difficult to conduct. Unlike the integer-order PPF, where the stability condition is simply given by $g < 1$, for the fractional-order PPF stability does not depend only on g , but also on ζ_f and α . Thus, a full mathematical derivation of the stability condition is very extensive to obtain. Therefore, an alternative approach based on Nichols stability criterion is proposed.

The Nichols criterion states that closed-loop stability is guaranteed if the Nichols plot of the stable open-loop transfer function $L(s)$ does not intersect the line where $\angle L(s) = -180^\circ$ and $|L(s)| \geq 0$ dB. Therefore, by imposing this condition to the open-loop $L(s) = -gC_{F_1}(s)G(s)$, stable and unstable regions for the closed-loop transfer

function $T_1(s)$ can be depicted for different values of α , g and ζ_f (see Figure 5), where $T_1(s)$ is defined as

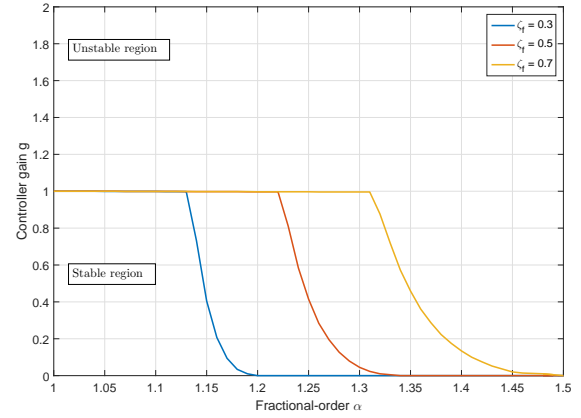
$$T_1(s) = \frac{G(s)}{1 - gC_{F_1}(s)G(s)}.$$


Figure 5. Stability and instability regions for the closed-loop $T_1(s)$ for different values of ζ_f .

As shown in Figure 5, for a fixed value of ζ_f the stability region is defined by the relation between the fractional-order α and the gain g , where the curve indicates the stability limit. Values of $g = 0$ indicate that the controller $C_{F_1}(s)$ becomes unstable, as seen in Figure 4. For different values of ζ_f the stability region changes: as ζ_f increases, the stable region increases towards higher values of α ; moreover for $\alpha = 1$ the stability condition for the integer-order PPF is recovered ($g < 1$).

It is important to notice that the tuning frequency of the filter ω_f does not affect the stability analysis, since ω_f is assumed to be always tuned around the resonance frequency of the plant ω , whose value lies in the stable region of the closed-loop.

2.3.2 Filter #2

A second fractional-order PPF filter is proposed by adding another fractional-order design parameter β . The new filter transfer function $C_{F_2}(s)$ is rewritten as follows:

$$C_{F_2}(s) = \frac{1}{\left(\left(\frac{s}{\omega_f}\right)^{2\alpha} + 2\zeta_f\left(\frac{s}{\omega_f}\right)^\alpha + 1\right)\left(\left(\frac{s}{\omega_f}\right)^\beta + 1\right)} \quad (11)$$

This filter has the advantage of being always stable if $0 < \alpha < 1$ and $0 < \beta < 1$, with $\alpha, \beta \in \mathbb{R}$, being the two polynomials at the denominator of order < 1 . It is very similar to $C_{F_1}(s)$ both for performance and behaviour, however it has an extra parameter to tune.

2.3.2.1 Stability Analysis

Here, since the controller $C_{F_2}(s)$ is always stable, only a stability analysis for the closed-loop

$T_2(s) = \frac{G(s)}{1 - gC_{F_2}(s)G(s)}$ is required. In this case the extra parameter β also has to be taken into account.

Similar to what was already mentioned for $C_{F_1}(s)$, stable and unstable regions for $T_2(s)$ are found for different values of α , β , g and ζ_f which satisfy Nichols stability criterion.

It can be found that for $g < 1$, $T_2(s)$ is always stable irrespective of the choice of the other parameters, whereas for $g \geq 1$ instability is manifested depending on the values of α , β and ζ_f .

In Figure 6, stable and unstable regions are shown for constant ζ_f and different values of α , β and g . The plot shows unstable regions for different values of g , starting from the limit value $g = 1$. The unstable area increases for increasing g . Therefore, for a constant g , the closed-loop is stable for any point outside the corresponding coloured area. In Figure 7, stable and unstable regions are shown instead for constant g and different values of α , β and ζ_f . In this case the unstable area increases for decreasing values of ζ_f .

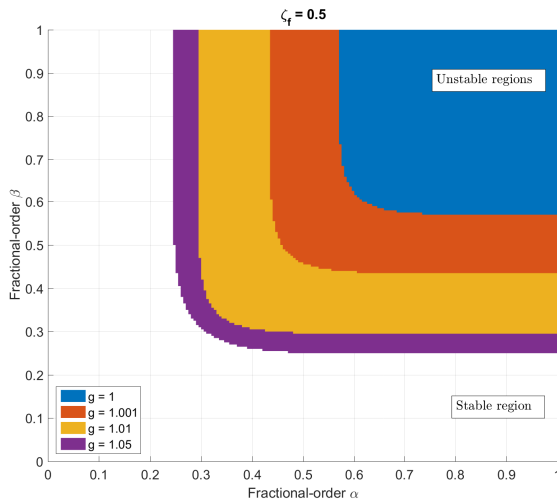


Figure 6. Stable and unstable regions for the closed-loop $T_2(s)$ for different values of g and constant $\zeta_f = 0.5$.

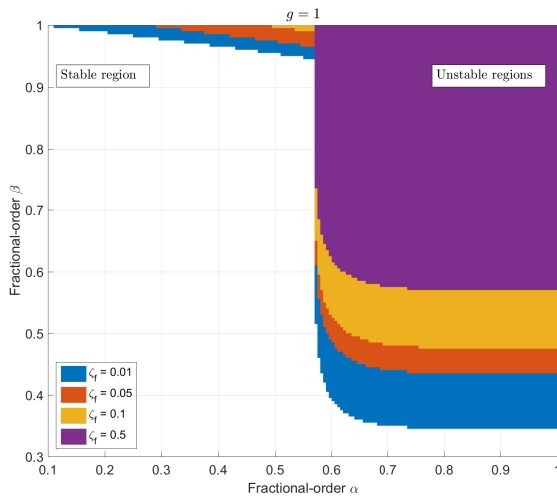


Figure 7. Stable and unstable regions for the closed-loop $T_2(s)$ for different values of ζ_f and constant $g = 1$.

For $\alpha = 1$ and $\beta = 0$, the filter becomes of integer-order. However, differently from the standard PPF which is stable for $g < 1$, stability condition is $g < 2$ because the polynomial $((\frac{s}{\omega_f})^\beta + 1)$ at the denominator of Equation (11) is equal to 2 for $\beta = 0$, resulting in the filter $C(s)$ of Figure 1 being multiplied by $\frac{1}{2}$.

The addition of α (and β) as design parameters makes a full mathematical derivation of the performance of the two fractional-order PPFs very challenging to conduct. That is why an optimization approach is proposed to find the optimal filter parameters.

2.4 Filter Optimization

The fractional-order PPF filters of Equations (6) and (11) have additional design parameters with respect to the standard integer-order PPF, represented by the fractional order α and β , which provide more freedom for the choice of the other tuning parameters ω_f , ζ_f and g . Therefore, an optimality problem is defined to find the mentioned parameters for a fractional-order PPF filter which can effectively control a chosen vibration mode. This is done by improving both phase and magnitude response of the closed-loop transfer function $T(s)$ (here indicating either $T_1(s)$ or $T_2(s)$).

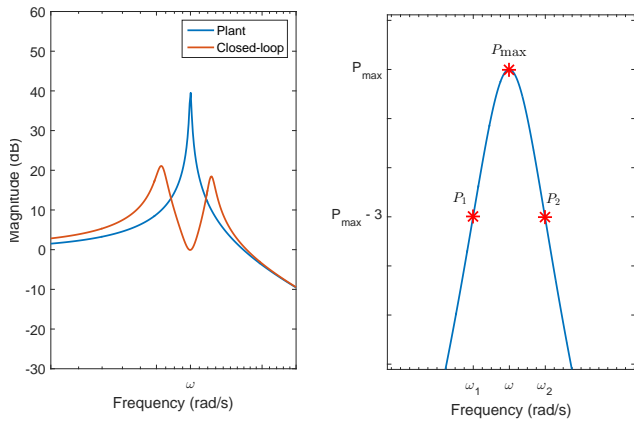
The objective function h to be minimized is:

$$\begin{aligned}
 h = & w_1(P_{\max} - S_G) + w_2 \sum (\angle T(s) - \angle G(s)) \\
 & + p \left(\max \left(0, \frac{P_1}{P_{\max}} - 1 \right) \right)^2 \\
 & + p \left(\max \left(0, \frac{P_2}{P_{\max}} - 1 \right) \right)^2 \\
 & + p \left(\max \left(0, \frac{S_G}{P_1} - 1 \right) \right)^2 \\
 & + p \left(\max \left(0, \frac{S_G}{P_2} - 1 \right) \right)^2 \\
 & + p (\max(0, \zeta_T))^2
 \end{aligned} \tag{12}$$

where the magnitude of the closed-loop $T(s)$ is optimized by the difference between the magnitude P_{\max} at the resonance ω and static gain S_G of the plant $G(s)$, so as to impose maximal peak reduction; the phase is optimized instead by minimization of the difference between phase of the closed-loop $T(s)$ and phase of the plant $G(s)$; two weights w_1 and w_2 are used to give more importance either to the magnitude or phase optimization.

The objective is also enhanced by adding penalization functions, in order to make sure that the resonance peak is always reduced without creating two additional peaks around ω due to the presence of extra zeros in the closed-loop (Kwak, Moon K. and Han, Sang-Bo and Heo 2004) (see Figure 8a). In Figure 8b, P_1 and P_2 are the so-called *half-power* points at 3 dB down from the resonance peak and are used to compute the closed-loop damping ζ_T at resonance with the half-power bandwidth method. Moreover, in Equation (12) p is the penalization factor. Closed-loop stability is also added as an equality constraint by setting the number of unstable poles equal to 0.

A Global-Search algorithm using a constrained non-linear optimization is chosen to solve the optimality problem because the objective h is highly non-linear and presents several local optima. The algorithm is implemented in MATLAB by means of the 'GlobalSearch' and 'fmincon' functions. The plant $G(s)$ is chosen to represent a simple 1-DOF system as in Equation (1), and the outcome



(a) Closed-loop zero causing two extra peaks around resonance. This effect is limited by the addition of proper penalization functions.

(b) Half-power points P_1 and P_2 at 3 dB down from the resonance peak. These points are used to compute the closed-loop damping ζ_T by the half-power bandwidth method:

$$\zeta_T = \frac{\omega_2 - \omega_1}{2\omega}$$

Figure 8. Conditions for closed-loop damping ζ_T .

of the optimization gives the four tuning parameters for the filter $C_{F_1}(s)$ (or $C_{F_2}(s)$). Optimization results depend mainly on the choice of the two weights w_1 and w_2 , from which a fractional filter that has either a stronger effect on the magnitude or on the phase of the closed-loop can be obtained. In the next section a simple example showing the potential benefit of using a fractional-order PPF rather than an integer-order PPF is presented.

2.5 Optimization results

Performances of the standard integer-order PPF and the optimized fractional-order PPFs are compared first on a simple plant representing a MDOF system. Comparison is made by tuning the integer-order PPF such that both integer and fractional-order compensators provide the same magnitude reduction of the resonance peak to be controlled. Tuning parameters for the filters are listed in Table 1. In both cases, the tuning parameters identify a point which is well within the closed-loop stable regions seen in Figures 5, 6 and 7. It is important to highlight that controllers are normally not tuned to achieve 100% peak reduction, and that is mainly done to avoid performance losses in multi-mode control.

In Figure 9, the filters' bode plots tuned according to Table 1 are shown. Both fractional PPF filters have a very similar behaviour and therefore a similar performance is expected. In Figure 10, the 2nd peak of the plant is controlled. The same magnitude reduction of the controlled resonance is achieved by all controllers, but less spillover is present both at lower and higher frequencies compared to the controlled resonance when fractional-order PPFs are used. This is due to the fact that they maintain the phase response much closer to the plant response rather than what the integer-order PPF does. Both fractional controllers provide an almost identical performance.

The benefits of using a fractional-order PPF filter to control a chosen vibration mode are evident from the

simulation results. The next step is the implementation on a complete AVC setup, which is discussed in sections 3 and 4.

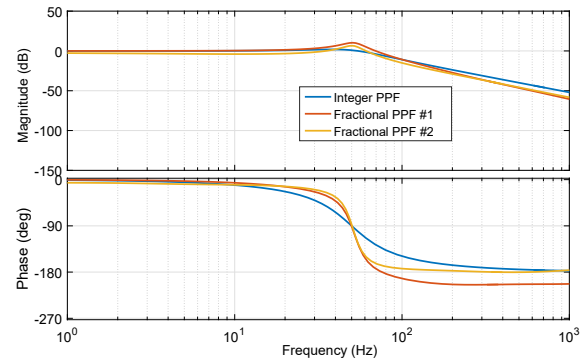


Figure 9. Bode plots of integer and fractional-order PPF filters #1 and #2 tuned according to Table 1. The slope in the quasi-static region of filter #2 is due presence of the second denominator term with order β , although each filter starts from the same 0 dB gain at 0 Hz.

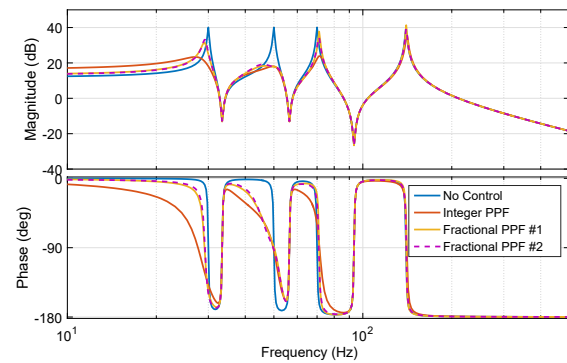


Figure 10. Simple plant representing a MDOF system controlled by integer-order PPF and fractional-order PPF #1 and #2 tuned according to Table 1.

3 Experimental Setup

An experimental set up is built to conduct modal analysis and active vibration control of a rectangular carbon fibre/epoxy composite plate (see Figure 11). This setup is part of the Engineering Dynamics Laboratory of the Department of Precision and Microsystems Engineering (PME) at Delft University of Technology (TU Delft).

The plate has been produced at the Delft Aerospace Structures and Materials Laboratory by vacuum infusion process (VIP), using 6 layers of 0-90° carbon fibres and epoxy resin 04980 type. Plate dimensions and resulting material properties are listed in Table 2. An aluminium frame is used to suspend the plate vertically, with the longest dimension perpendicular to the ground. From the plate corners, suspension with nylon wires is used to approximate free edge boundary conditions. The length of the nylon wires is chosen such that plate rigid body modes have a much lower natural frequency compared to flexural modes. In particular,

Table 1. Tuning parameters for integer and fractional-order PPF filters, all providing same magnitude reduction of the resonance peak at ω .

Parameter	Integer PPF	Fractional PPF #1	Fractional PPF #2
g	0.1	0.0365	0.0559
ω_f	ω	1.0366ω	1.0202ω
ζ_f	0.45	0.4227	0.0267
α	1	1.1844	0.9386
β	-	-	0.2457

Table 2. Carbon fibre/epoxy plate material properties.

Property	Symbol	Value [Unit]
Length	l	0.450 [m]
Width	b	0.250 [m]
Thickness	t	0.0013 [m]
Density	ρ	1504.27 [kg/m ³]
Young's modulus	$E_1 = E_2$	57.5 [GPa]
Poisson's ratio	ν_{12}	0.1 [-]
Shear modulus	G_{12}	3.8 [GPa]

small holes are drilled in proximity of the plate corners where thin carbon fibre wires are used to connect to the nylon wires via a double hook.

The plate is subjected to an orthogonal excitation at a point located 3 cm from the plate center, both horizontally and vertically. The Bruel & Kjaer Vibration Exciter Type 4809 is used to provide random excitation by means of a metal stinger located between the exciter and the PCB Impedance Head 288D01 measuring the force at the excitation point.

Experimental modal analysis of the plate has been conducted by using a Polytec Laser Doppler Vibrometer (LDV) system, consisting of a PSV-400 Scanning Vibrometer Head, OFV-5000 Vibrometer Controller, PSV-400 Junction Box and host PC with Polytec Scanning Vibrometer Software 9.2. The LDV system scans the plate surface and takes hundreds of non-contact velocity measurements. Vibrometer software records time signals for laser vibrometer and impedance head, then computes frequency response functions (FRF) for every measurement point and allows for the visualization of the plate operational deflection shapes at every measured frequency. The same software has been used to generate the excitation signal and drive the vibration exciter. The measured data are then exported to ME'Scope software from Vibrant Technology to conduct modal analysis and to compute natural frequencies, mode shapes and damping ratios.

3.0.1 Experimental Modal Analysis Results

Figure 12 shows the plate average spectrum obtained as the sum of the measured FRFs after scanning the plate surface. Peaks in the frequency response correspond to the natural frequencies of the plate. The measurements taken with the Polytec system were then imported into ME'Scope software, where natural frequencies, damping ratios and mode shapes were calculated with Global Polynomial curve fitting method.

Experimental results are also validated by the finite element software COMSOL Multiphysics 5.2. The carbon fibre/epoxy plate is modelled with orthotropic material

properties according to Table 2. The 'Structural Mechanics' module has been used and an 'Eigenfrequency Analysis' is performed to obtain natural frequencies and mode shapes.

Natural frequencies of the first four natural modes obtained from simulations and experiments are compared in Table 3, where corresponding damping ratios are also included. Mode shapes of the first four natural modes obtained from simulations and experiments are instead shown in Table 4. After validation with the finite element model, the peak at about 45 Hz which can be seen in Figure 12 has been found to be spurious due to non-ideal boundary conditions.

3.1 Active Vibration Control Setup

The complete AVC setup consists of the experimental dynamics setup presented previously, interfaced with an active vibration controller comprised of MFC actuator, sensor and control system.

In Figure 13, a schematic representation of the complete setup is depicted, whereas in Figure 14 the real setup is shown.

The Smart Material transducer type M8557S1 is chosen both for actuation and sensing since it comes as a unique patch with actuator and collocated sensor. The bigger transducer is the actuator which has an active area of 85×47 mm², whereas the sensor has an active area of 85×5 mm². The active layer of these MFC transducers is composed of a mixture between epoxy resin and piezoceramic fibres, which are perpendicular and interdigitated with the electrodes, creating an electric field aligned with the fibres' direction, and thus making the transducers work as elongators (MFC). Araldite 2012 epoxy adhesive has been used to bond the transducers to the plate surface.

A dSPACE DS1005 real-time control system is used for implementation of the control algorithm which is built in Simulink and then compiled into the dSPACE ControlDesk software. The sensor signal is directly sent to the analog-to-digital converter (ADC) of the dSPACE, whereas the signal sent to the actuator from the dSPACE digital-to-analog converter (DAC) is first amplified by the Smart Material High Voltage Amplifier HVA 1550/50-1. This amplifier provides the required voltage to drive the MFC actuator (from -500 V to +1500 V) and amplifies the actuation signal by a factor 200.

Piezoelectric transducers can be easily mounted on different type of structures, but their size, orientation and location play a significant role when active control has to be performed. A badly positioned or misplaced sensor/actuator pair can result in a poor control performance or even cause

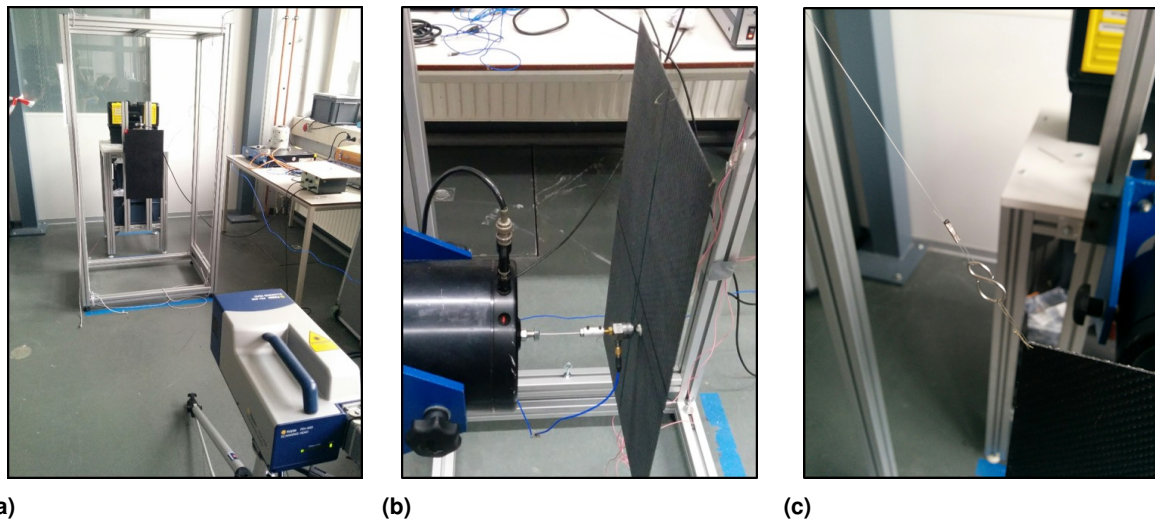


Figure 11. Experimental dynamics setup: (a) Front view of the carbon fibre composite plate and Polytec PSV-400 Scanning Vibrometer Head. (b) Plate backside with Bruel & Kjaer Vibration Exciter Type 4809, stinger connection and PCB Impedance Head 288D01 (force sensor). (c) Detail of boundary conditions realised with suspension on nylon wires.

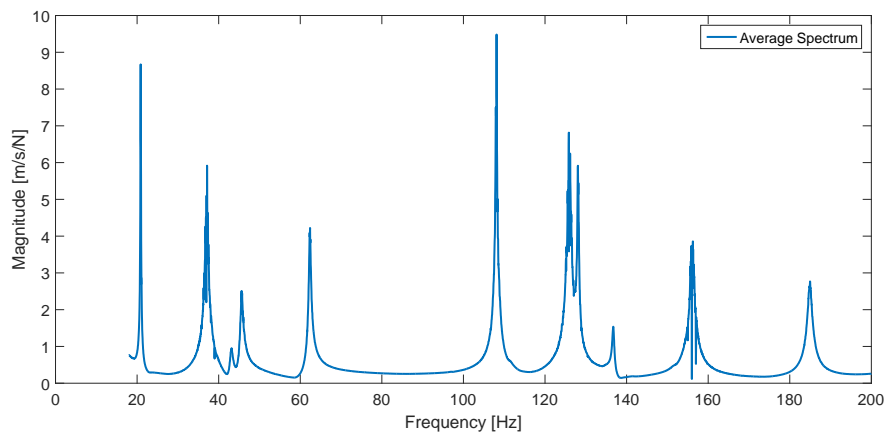


Figure 12. The average of the measured frequency response functions with random excitation.

Table 3. Natural frequencies and damping ratios of the first four natural modes of the composite plate.

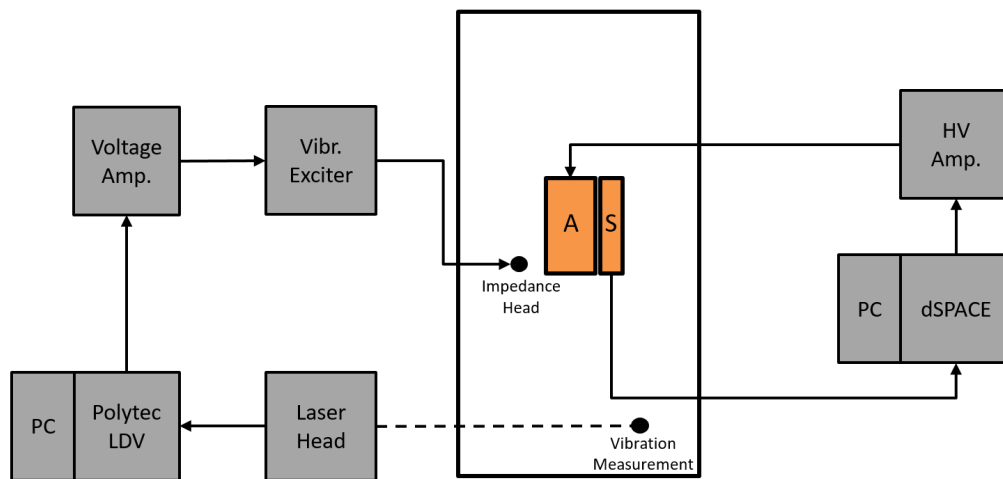
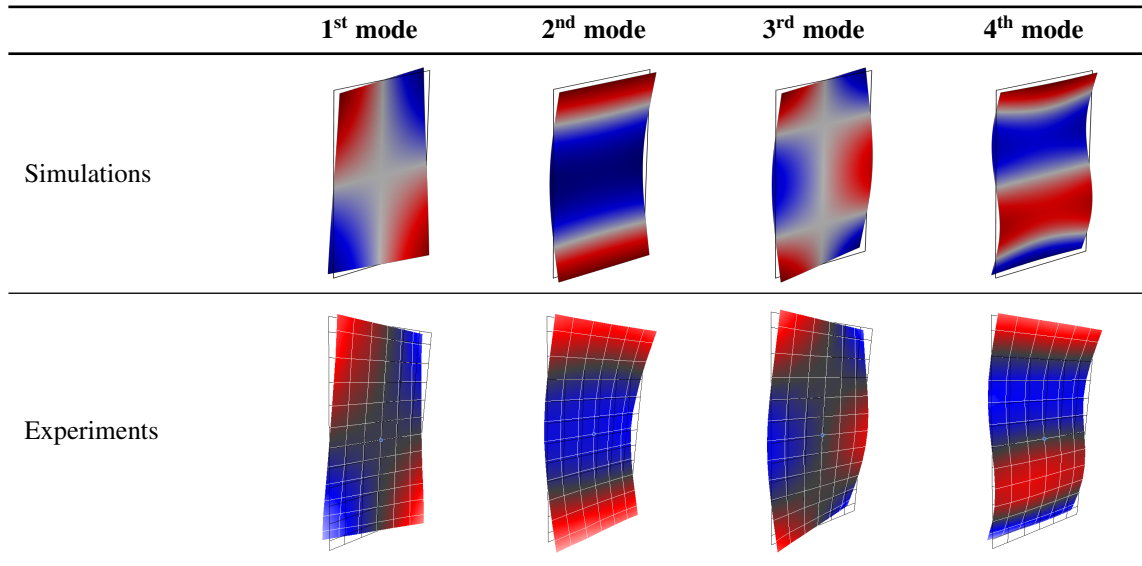
Mode	Simulations - (Hz)	Experiments - (Hz)	Damping ratio - (%)
1	20.51	20.88	0.13
2	42.34	37.16	0.20
3	59.60	62.41	0.37
4	116.54	108.10	0.04

instability. Therefore, the maximal modal force criterion proposed by Bin et al. (Bin et al. 2000) is chosen here as a rule for optimal placement of the MFC sensor and actuator on the carbon fibre/epoxy plate. This criterion states that a piezoelectric actuator exerts maximum force if placed in a region of maximum modal strain for the specific vibration mode to be controlled. In this work, the 2nd vibration mode (1st bending mode (Alijani and Amabili 2013)) is selected as the mode to be controlled. Therefore, actuator and sensor are placed in the middle of the plate, where strain for that particular mode is maximum. This optimal location has been found by looking at the surface strain energy density plot of the 2nd mode shape, as shown in Figure 15.

Before application of the MFC transducers, a finite element analysis of the plate including the bonded

transducers is performed in order to estimate the variation of the plate dynamics, which only resulted in a small increase of the natural frequencies. Only the active area of the transducers is modelled according to the orthotropic material properties given by Smart Material (MFC). After that, an experimental modal analysis is conducted as a further validation. In Figure 16 the plate average spectrum before and after transducer application is shown. In Table 5 the first four natural frequencies and damping ratios after transducer attachment are listed.

Experimental results show that the transducers are both slightly stiffening the plate, as predicted by simulations, and increasing the overall damping ratios of the system. Mode shapes are instead not affected.

Table 4. Comparison between simulation and experimental results of the first four natural modes of the carbon fibre composite plate.**Figure 13.** Scheme representing the AVC setup: MFC actuator and sensor are labelled as 'A' and 'S', respectively.**Table 5.** Natural frequencies and damping ratios after application of piezoelectric transducers.

Mode	Simulations - (Hz)	Experiments - (Hz)	Damping ratio - (%)
1	21.35	25.72	0.38
2	44.27	38.53	0.38
3	59.75	66.38	0.79
4	116.93	108.30	0.45

After this analysis, the resulting dynamic behaviour of the plate with bonded transducers is considered as reference for the AVC implementation.

4 Implementation of AVC

The integer and fractional-order PPF controllers presented in section 2 are first implemented in a Simulink model which is then compiled and built in the dSPACE ControlDesk environment.

Figure 17 shows the Simulink model used for experiments. Controller transfer function is the same as the one of the controllers explained in section 2. The controller can be

activated by means of the gain block 'ON_OFF_switch' which is loaded as a switch button in the dSPACE environment. 'Gain_IN' and 'Gain_OUT' represent hardware gains required from the dSPACE system. In fact, the sensor signal must be multiplied by 10 because it gets internally divided by 10 by the dSPACE DAC, and similarly the signal to the actuator must be multiplied by 0.1 because it gets multiplied by 10 by the dSPACE ADC. A 2.5 V offset voltage is used to provide full operating range to the MFC actuator because the HV amplifier accepts input signals from -2.5 V to 7.5 V, and a saturation block is used to avoid out-of-range signals to the HV amplifier.

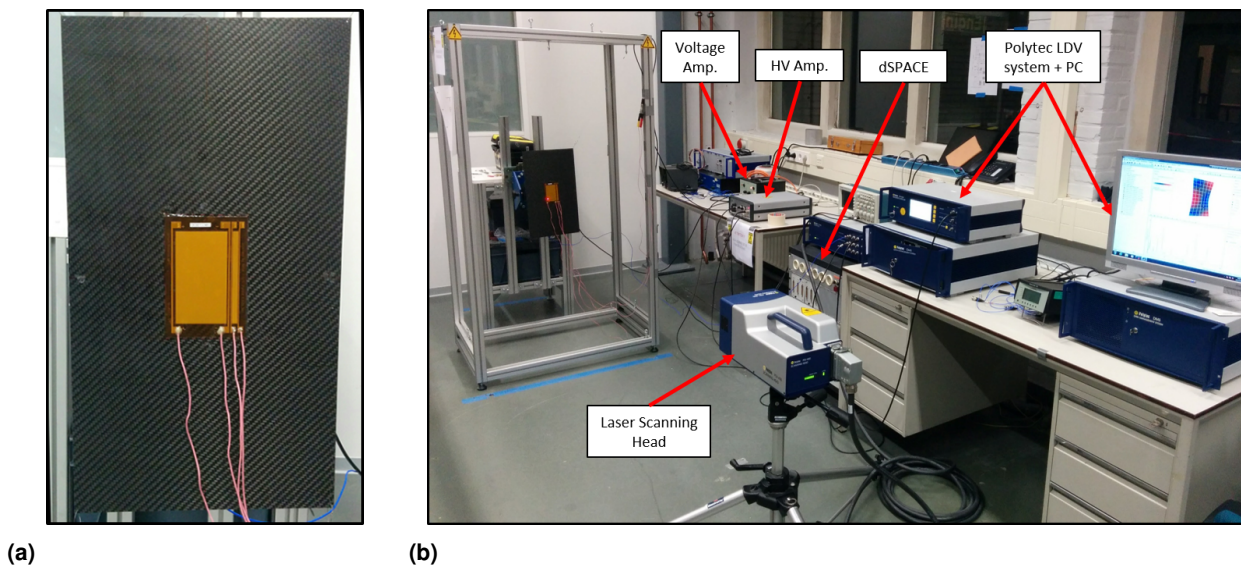


Figure 14. Complete AVC setup: (a) Carbon fibre composite plate with bonded Smart Material MFC transducer type M8557S1 (actuator and collocated sensor). (b) Labels indicating: Polytec PSV-400 Scanning Vibrometer Head; Bruel & Kjaer Voltage Amplifier Type 2718; Smart Material High Voltage Amplifier HVA 1500/50-1; dSPACE DS1005 system; Polytec LDV system comprises OFV-5000 Vibrometer Controller, PSV-400 Junction Box and host PC with Scanning Vibrometer Software 9.2 .

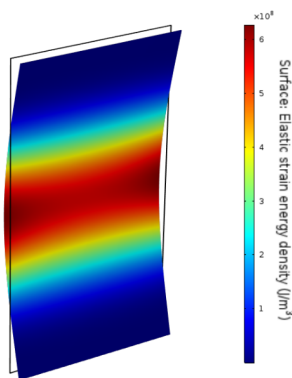


Figure 15. Surface strain energy density plot for the 2nd mode shape: red area indicates maximum strain energy and it is considered as optimal location for actuator placement.

Controllers are implemented one at a time. Tuning parameters from Table 1 are kept the same in order to be able to compare the controllers' performance when they all provide the same magnitude reduction of the controlled resonance peak, as already seen in section 2.

CRONE approximation is used in order to approximate the transfer functions of the fractional-order PPF filters. The Ninteger toolbox for MATLAB by D. Valério (Valério and Sá Da Costa 2004) is used for the CRONE implementation. For both fractional-order PPF filters, the orders α and β are approximated by choosing a frequency range $[10^{-5}\text{rad/s}, 10^{+5}\text{rad/s}]$ and approximation order $N = 10$. The resulting transfer functions for controllers $C_{F_1}(s)$ and $C_{F_2}(s)$ have orders 30 and 40, respectively. Such approximation order, $N = 10$, has been chosen in order to approximate as closely as possible the theoretical fractional-order transfer function of the filters. Orders $N < 10$ do not produce the expected performance.

In order to properly interface control algorithm with the MFC sensor and actuator and to provide the required control

performance, a controller correction gain γ had to be used in addition to the gain g , as seen in the Simulink diagram of Figure 17. The overall controller gain can thus be considered as the multiplication $g\gamma$. From Table 1, it can be noted that the fractional-order PPFs require a much lower g than the integer-order PPF. This is due to the fact that their low-pass filter transfer functions behave differently in the resonance region (see Figure 9). In fact, the resonance peak of the fractional-order filters is more pronounced than the peak of the integer-order filter which is almost flat. This accounts for the need of a lower g for the fractional-order filters in order to provide the same control action as the integer-order filter, which instead requires a much higher g .

In the actual experimental implementation, this effect is more evident and therefore, different correction gains γ have been used for integer and fractional-order controllers. In particular, for the integer-order PPF a correction gain $\gamma = 6$ is used, whereas for both fractional-order PPFs a value of $\gamma = 2.5$ is chosen. These values have been found by trial and error procedure when tuning the controllers to provide an approximately equal magnitude reduction of the controlled resonance peak.

Similar to what has been done for experimental modal analysis, also for AVC measurements random excitation is used as the excitation signal for the vibrating plate.

4.1 AVC results

The center and the bottom-left corner of the vibrating plate are chosen as reference locations for laser measurements of the vibration amplitude. In fact, vibration response of the 2nd mode is maximum at both locations, and therefore it is interesting to measure vibration reduction at those points.

In Figure 18, uncontrolled and controlled FRFs for both reference locations are shown. In both cases integer and fractional-order controllers are applied one at a time.

In Figures 18a and 18b, uncontrolled and controlled FRFs measured at the center and bottom-left corner of the plate

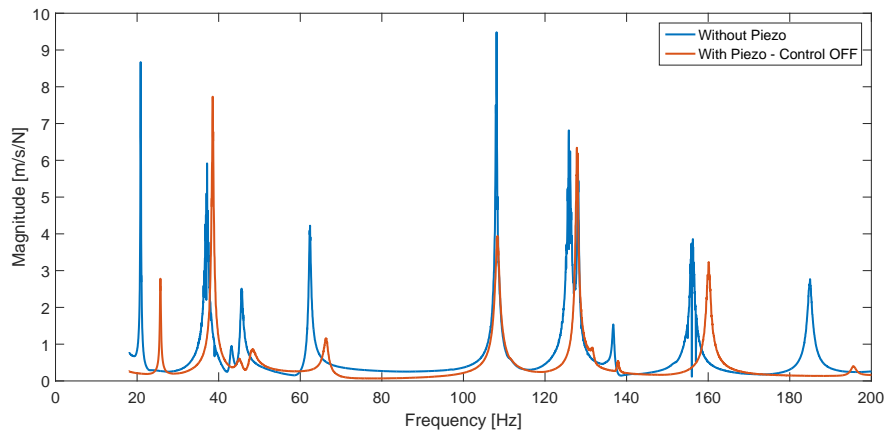


Figure 16. The average of the measured frequency response functions before and after application of piezoelectric transducers.

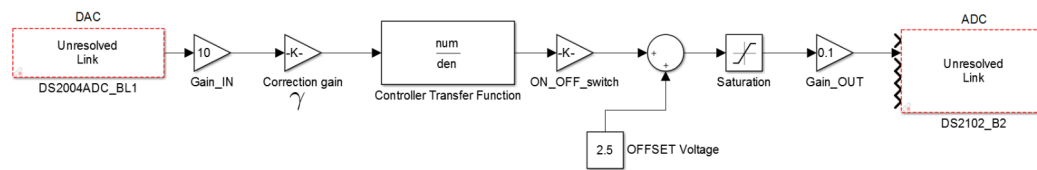


Figure 17. Simulink block diagram: controller transfer function is the same as the one of the controllers explained in section 2; 'Gain.IN' and 'Gain.OUT' represent hardware gains required from the dSPACE system; 2.5 V offset voltage provides full operating range to the MFC actuator; saturation block avoids out-of-range signals to the HV-amplifier.

are shown, respectively. The frequency peak at 38.5 Hz corresponding to the 2nd mode is effectively reduced by each controller, all providing approximately the same peak reduction of 12 dB. Only the fractional-order PPF#2 is reducing the peak slightly less, but the difference is considered to be negligible. As expected, both fractional-order controllers perform almost exactly the same, as also seen in the example of section 2. Each controller causes a frequency shift of the controlled peak towards higher frequencies, and this shift is bigger when integer-order PPF is used. This stiffening effect is caused by the mechanical action of the MFC actuator and it is more evident in the case of integer-order PPF, but it does not represent a problem in this particular case. However, it might become problematic in other situations when, for instance, the stiffening effect influences the frequency of other modes to be controlled, causing a mistuning in the controller. Moreover, in each case the controller is found to be extremely effective in reducing the chosen vibration mode, leaving the other peaks barely affected by the control action. Therefore, it can be mentioned that spillover effect is not observed in this specific application.

Experimental modal analysis is conducted again in order to compare mode shapes and damping ratios, before and after control activation. Mode shapes have not been affected, meaning that the control action of the MFC actuator neither added complexity to the shapes nor triggered other motions.

Figure 19 shows the average spectrum (in dB scale) of the plate before and after control activation. From now on, Fractional-order PPF#1 is chosen as reference for simplicity, because both fractional filters present an almost equal performance. The plot shows an average reduction of 12 dB for the controlled mode, while other modes

remain barely affected. In Table 6, natural frequency and damping ratio of the controlled mode before and after control activation are listed. Damping has been increased from 0.38% of the uncontrolled case to 0.80% in the controlled case.

Another interesting result has been found by looking at the HV amplifier output control signal sent to the MFC actuator during random excitation of the plate. In Figure 20, time history and corresponding fast Fourier transform (FFT) of the control signals in the case of integer-order PPF and fractional-order PPF are shown. Controllers are tuned to provide the same performance in terms of resonance peak reduction, as already seen before. From the time history, it can be noted that the control signal in the case of fractional-order PPF has a much lower amplitude than the one of integer-order PPF. This means that less actuation voltage is required to control the MFC actuator when fractional-order PPF is used. In Figure 20, the FFT of the recorded time signals is taken and corresponding amplitudes are normalized to make the resulting data comparable. From the FFT plot, it is possible to see at which frequencies the control action takes effect. Until the tuning frequency of 38.5 Hz, the FFT content is very similar for both signals, whereas for higher frequencies the frequency content has a much lower amplitude in the case of fractional-order PPF. This effect is due to the steeper roll-off of the fractional-order filter with respect to the integer-order filter, and it confirms that the fractional-order PPF has a greater filtering action, as already shown in Figure 2, and thus is found to be more promising in reducing spillover effect due to uncontrolled modes.

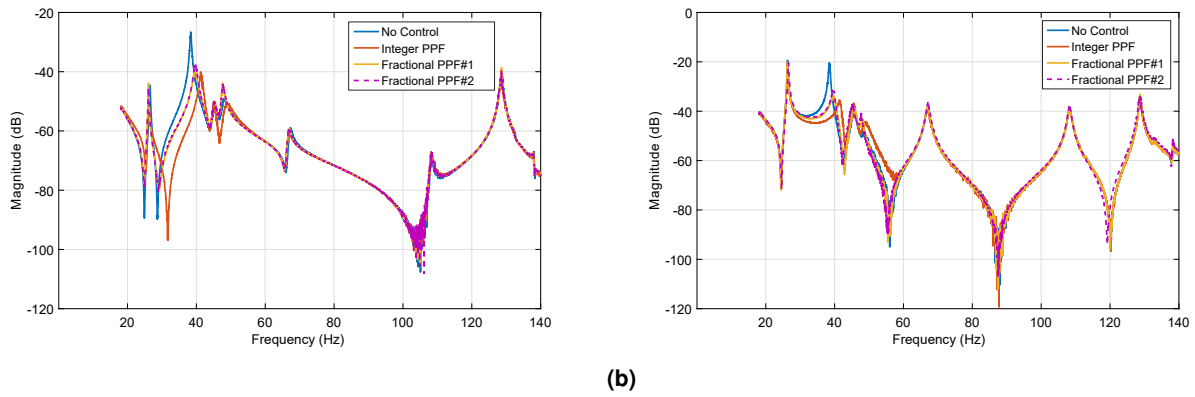


Figure 18. 2nd mode at 38.5 Hz controlled by integer-order PPF and fractional-order PPF #1 and #2: FRFs are measured at center (a) and bottom-left corner (b) of the plate.

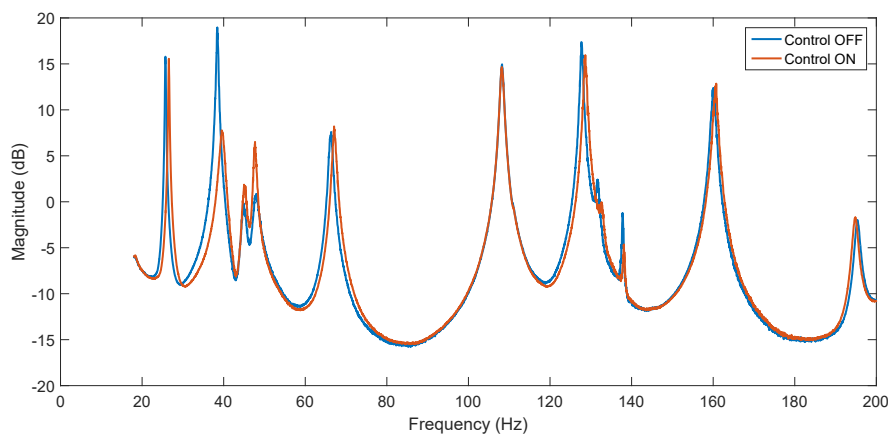


Figure 19. Average spectrum before and after fractional-order PPF #1 activation: an average reduction of 12 dB is achieved for the 2nd mode at 38.5 Hz.

Table 6. Natural frequency and damping ratio of the controlled mode before and after fractional-order PPF #1 control activation.

Mode	Experiments, Control OFF - (Hz)	Experiments, Control ON - (Hz)	Damping ratio, Control OFF - (%)	Damping ratio, Control ON - (%)
2	38.53	39.53	0.38	0.80

5 Conclusions

In this paper active vibration control of a rectangular carbon fibre/epoxy composite plate with free edges has been presented. Two novel fractional-order compensators based on Positive Position Feedback have been proposed, analysed, and successfully applied in practice for the first time.

Both fractional-order controllers have shown comparable performances, although controller #2 has the advantage of being always internally stable. Numerical simulation has shown the benefit of using fractional-order PPF with respect to reduction of spillover effect, compared to the standard integer-order PPF. Controllers have been tested in an experimental setup to control the 2nd mode of the composite plate. The setup was composed of a Laser Doppler Vibrometer system, vibration exciter, MFC actuator and sensor and dSPACE real-time control system. MFC transducers have been positioned on the plate based on

maximal modal strain criterion. Both the integer and fractional-order PPF allowed for the effective control of the second mode, although the newly proposed fractional-order controllers are found to be more efficient in achieving the same performance with less actuation voltage, and more promising in reducing the spillover effect due to uncontrolled modes.

It can thus be concluded that the use of fractional-order transfer functions is very promising to improve the performance of commonly used active vibration control strategies since they can provide response characteristics that would not be achievable by standard integer-order transfer functions.

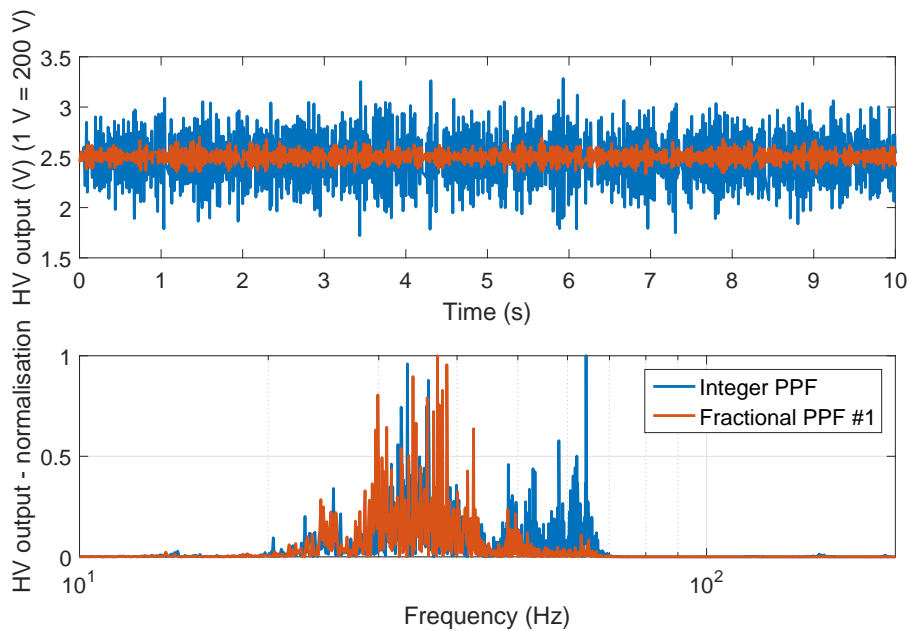


Figure 20. Time history and corresponding FFT of the HV amplifier output control signal sent to the MFC actuator in case of integer-order PPF and fractional-order PPF #1 control both tuned at 38.5 Hz.

References

- Alijani F and Amabili M (2013) Theory and experiments for nonlinear vibrations of imperfect rectangular plates with free edges. *Journal of Sound and Vibration* 332(14): 3564–3588.
- Alijani F, Amabili M, Ferrari G and D'Alessandro V (2013) Nonlinear vibrations of laminated and sandwich rectangular plates with free edges. Part 2: Experiments & comparisons. *Composite Structures* 105: 437–445.
- Aphale SS, Fleming AJ and Moheimani SOR (2007) Integral resonant control of collocated smart structures. *Smart Materials and Structures* 16(2): 439–446.
- Balas MJ (1978) Feedback control of flexible systems. *IEEE Transactions on Automatic Control* 23(4): 673–679.
- Bin L, Yugang L, Xuegang Y and Shanglian H (2000) Maximal Modal Force Rule for Optimal Placement of Point Piezoelectric Actuators for Plates*. *Journal of Intelligent Material Systems and Structures* 11(7): 512–515.
- Butler H and de Hoon C (2013) Fractional-order filters for active damping in a lithographic tool. *Control Engineering Practice* 21(4): 413–419.
- Fanson JL (1987) *An Experimental Investigation of Vibration Suppression in Large Space Structures Using Positive Position Feedback*. Phd thesis, California Institute of Technology.
- Ferrari G and Amabili M (2015) Active vibration control of a sandwich plate by non-collocated positive position feedback. *Journal of Sound and Vibration* 342: 44–56.
- Goh, C.J. and Caughey, T.K. (1985). On the stability problem caused by finite actuator dynamics in the collocated control of large space structures. *International Journal of Control*, 41(3), 787–802.
- Hosseinnia SH, Tejado I, Milanes V, Villagra J and Vinagre BM (2014) Experimental Application of Hybrid Fractional-Order Adaptive Cruise Control at Low Speed. *IEEE Transactions on Control Systems Technology* 22(6): 2329–2336.
- Hosseinnia SH, Tejado I and Vinagre BM (2013) Fractional-order reset control: Application to a servomotor. *Mechatronics* 23(7): 781–788.
- Kwak MK and Heo S (2007) Active vibration control of smart grid structure by multiinput and multioutput positive position feedback controller. *Journal of Sound and Vibration* 304(1-2): 230–245.
- Kwak, Moon K and Han, Sang-Bo and Heo S (2004) The Stability Conditions, Performance and Design Methodology for the Positive Position Feedback Controller. *Transaction of the Korean Society for Noise and Vibration Engineering* 14(3): 208–213.
- Macro Fiber Composite - MFC, in: *S.M. Corporation (Ed.)* <http://www.smart-material.com/MFC-product-main.html>.
- Moheimani, SOR, and Fleming A (2006) *Piezoelectric Transducers for Vibration Control and Damping*. Advances in Industrial Control. London: Springer-Verlag. ISBN 1-84628-331-0.
- Monje CA, Calderon AJ, Vinagre BM, Chen Y and Feliu V (2004) On Fractional PI^λ Controllers: Some Tuning Rules for Robustness to Plant Uncertainties. *Nonlinear Dynamics* 38(1-4): 369–381.
- Monje Ca, Chen YQ, Vinagre BM, Xue D and Feliu V (2010) *Fractional-order Systems and Controls. Fundamentals and Applications*. ISBN 978-1-84996-334-3.
- Monje CA, Vinagre BM, Feliu V and Chen Y (2008) Tuning and auto-tuning of fractional order controllers for industry applications. *Control Engineering Practice* 16(7): 798–812.
- Oustaloup A (1991) *La commande CRONE: commande robuste d'ordre non entier*. Hermes.
- Podlubny I (1999) Fractional-order systems and PI/sup λ/spl lambda/D/sup λ/spl lambda-mu//-controllers. *IEEE Transactions on Automatic Control* 44(1): 208–214.
- Preumont A (2011) *Vibration Control of Active Structures*, volume 179.
- Tejado I, HosseinNia SH and Vinagre BM (2012) Comparing Fractional Order PI Controllers With Variable Gain and Gain-Order for the Networked Control of a Servomotor. *IFAC*

Proceedings Volumes 45(3): 655–660.

Valério D and Sá Da Costa J (2004) Ninteger: a non-integer control toolbox for Matlab. *Proceedings of the Fractional Differentiation and its Applications, Bordeaux* .

Vinagre B, Podlubny I, Hernandez A and Feliu V (2000) Some Approximations of Fractional Order Operators Used in Control Theory and Applications. *Fractional calculus and applied analysis* 3(3): 231–248.

Zippo A, Ferrari G, Amabili M, Barbieri M and Pellicano F (2015) Active vibration control of a composite sandwich plate. *Composite Structures* 128: 100–114.

5

Discussion

In this chapter, further discussion and remarks about the research and results obtained in this thesis work are elaborated. In particular, the discussion is split into different sections discussed below.

5.1 Why PPF and Why Fractional-order control?

The main goal of this thesis was to propose and apply a novel active vibration control strategy which could perform better than current state-of-the-art techniques. Most of these techniques presented some limitations, of which frequency spillover was identified as the most critical when it comes to control performance. In this sense, PPF was found to be one of the best controllers, although still sensitive to frequency spillover, especially when multiple modes with close resonance frequencies have to be controlled at the same time. Therefore, it has been decided to start from the already appealing properties of PPF to design an even better controller.

Fractional-order calculus has been applied in many cases as a tool for modelling already established control systems and making them 'more optimal'. In fact, fractional-order transfer functions present a behaviour which cannot be found in any integer-order transfer functions. And since a strict relation between spillover and plant phase response has been identified, it has been decided to make a fractional-order version of the PPF, and optimize it to give optimal magnitude and phase behaviour, with aim to reduce spillover and further improve control performance.

5.2 Fractional-order PPF #1 and #2

Fractional-order PPF #1 has been presented in chapter 3, and it is intuitively the direct fractional-order version of the standard PPF. In fact, by tuning the fractional-order to value 1, the integer-order PPF is recovered. Fractional-order PPF #2 is instead more of a generalization of the standard PPF, where the addition of a second fractional-order provides even more freedom in tuning the controller, and makes it internally stable too.

The effect which the controller parameters g , ζ_f and ω_f , in case of integer-order PPF, have on the closed-loop response, is known and extensively studied in literature [17]. The introduction of fractional-orders makes instead the tuning process more challenging, because the parameters' value to provide optimal control performance strongly depends on the choice of the fractional-orders. Therefore, an optimization approach has been chosen to properly tune the proposed controllers,

and provide better control performance against spillover as already explained in the previous section.

After optimization, both fractional-order PPFs were found to provide almost exactly the same performance. This was expected, since their formulation was very similar and the resulting filter bode plots were almost identical in the resonance region, where the control action takes place.

5.3 Spillover: from simulation to practice

In simulations, spillover effect has been greatly reduced by the introduction of fractional-order PPFs with respect to the standard integer-order PPF. However, it was not observed in laboratory experiments. The reason for this is probably due to the specific setup used: indeed the transducers' placement was specifically optimal to suppress the 2nd mode of vibration, and it was found to have very limited influence on the other vibration modes.

Nevertheless, it does not mean that spillover is not a real problem in practice. In fact, in many studies of AVC with piezoelectric transducers, spillover have been observed and studied [12].

5.4 Correction gain effect

In chapter 4, it has been seen that a correction γ for the controllers' gain g was needed in the case of experimental implementation. This correction was used to properly interface the control algorithm with MFC sensor and actuator, since the actuator and sensor effects are not taken into account with the standard PPF formulation, as seen in Equation (2.9).

The use of such correction gain is normal practice in every AVC implementation. However, the need to use different correction gains for integer and fractional-order controllers was not expected. Since they have been tuned to provide the same peak reduction, it was expected to use the same correction gain γ for each controller. In particular, a correction gain $\gamma = 2.5$ was used for the fractional-order PPFs, whereas $\gamma = 6$ was used for the integer-order PPF. From Table 1 of chapter 4, as already explained, it can indeed be noted that fractional-order PPFs require a much lower gain g than the integer-order PPF. This is due to the fact that their low-pass filter transfer functions have a more pronounced resonance peak than the peak of the integer-order PPF filter. This accounts for the the need of a lower g for the fractional-order filters in order to provide the same control action as the integer-order filter, which instead requires a much higher g . In actual implementation this effect is more evident, and different corrections gains had to be used. This effect accounted for the use of less actuation voltage to drive the MFC actuator with fractional-order controllers.

However, before this effect could be detected, the same correction gain $\gamma = 6$ was used for each controller and different performances were observed. In Figure 5.1, controllers performance is compared in the case of different correction gains, as shown in chapter 4, and in the case of the same correction gain.

It can be noted that when the same $\gamma = 6$ is used (Figure 5.1b), each controller provides the same shift in frequency of the controlled peak, although the fractional-order controllers reduce the peak more than the integer-order controller. In this case, the amplitude of the control voltage signal sent to the MFC actuator is very similar for each controller. In Figure 5.1a, the same results already seen in chapter 4 are shown, where it can be noted that fractional-order controllers perform the same as the integer-order controller in terms of peak reduction when a smaller correction gain (and thus lower actuation voltage) is used.

This is to emphasize that with the introduction of fractional-order control, a much lower actuation voltage (lower control effort) is required by the actuator to provide the same performance as

the standard integer-order PPF controller, or even better performance when the same actuation voltage is used.

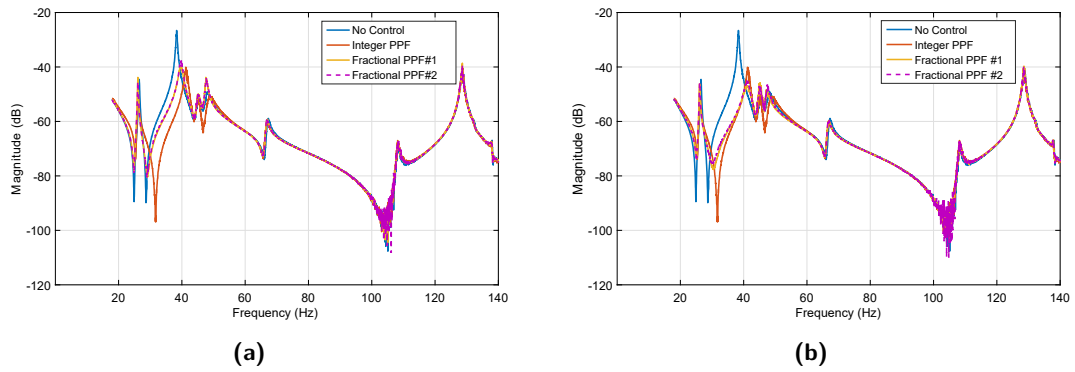


Figure 5.1: 2nd mode at 38.5 Hz controlled by integer-order PPF and fractional-order PPF #1 and #2. In (a), correction gain $\gamma = 2.5$ is used for fractional-order PPFs and $\gamma = 6$ for integer-order PPF. In (b), same correction gain $\gamma = 6$ is used for each controller. FRFs are measured at the center of the plate.

6

Conclusions & Recommendations

6.1 General conclusions

With the motivation of improving on the limitations of state-of-the-art controllers, in this thesis a novel AVC strategy based on fractional-order calculus is proposed, developed, and successfully applied in practice.

First, a fractional-order Positive Position Feedback (PPF) compensator is proposed to overcome the limitations of the commonly used integer-order PPF. Tuning parameters of the controller are obtained by optimizing both magnitude and phase response of the controlled plant. Results are shown by comparing performances of the standard integer-order PPF and the optimized fractional-order PPF on simple plants representing 1-DOF and multi-DOF systems.

Concerning the results obtained from the first part of the work, it can be concluded that the proposed fractional-order controller succeeded in controlling a chosen resonance peak with better performance than the standard integer-order PPF. In particular, frequency spillover and amplitude amplification in the quasi-static region of the closed-loop response have been effectively reduced, making the fractional-order PPF a preferred choice over the integer-order PPF when multiple-modes have to be controlled at the same time.

Secondly, a second version of the fractional-order PPF is proposed, and compared to the other controllers for the AVC of a rectangular carbon fibre composite plate with free edges. The plate is excited orthogonally by a modal vibration exciter and controlled by Macro Fibre Composite (MFC) transducers. Vibration measurements are taken with a Laser Doppler Vibrometer (LDV) system. MFC actuator and sensor are positioned on the plate based on maximal modal strain criterion, in order to control the second natural mode of the plate. Both fractional controllers are tuned with the same optimization process, and in both cases their tuning parameters identify a point well within the closed-loop stability region.

Concerning the results obtained with laboratory experiments, it can be concluded that both integer and fractional-order PPFs allowed for the effective control of the 2nd vibration mode of the plate with approximately the same performance, although the newly proposed fractional-order controllers were found to be more efficient in achieving the same performance with less actuation voltage (lower control effort), and more promising in reducing the spillover effect due to uncontrolled modes. Moreover, the transducers' placement was found to be optimal in specifically controlling the 2nd vibration mode without affecting the others and thus not causing any spillover.

Finally, it can be stated that the fractional-order PPF should be preferred over the integer-order PPF. As overall conclusion, it can be said that the use of fractional-order transfer functions is found

to be very promising to improve the performance of commonly used active vibration control strategies since they can provide in-between response characteristics that would not be achievable by standard integer-order transfer functions, and therefore their use is strongly recommended.

6.2 Recommendations for future research

Concerning a possible continuation of the research presented in this thesis in the field of AVC of smart flexible structures, some recommendations are here proposed.

One of the main benefits of using a fractional-order PPF controller is the reduction of the spillover effect due to uncontrolled vibration modes. However, this particular aspect, already seen in simulations, could not be validated in practice. Therefore, possible steps that can be undertaken to show this effect and still use the same experimental setup with the composite plate are:

- Application of multi-SISO and MIMO control by adding more transducers, similar to what has been done by Zippo et al. [30].
- Application of non-collocated control, similar to what has been done by Ferrari and Amabili [31].
- Application of transducers with different sizes to check their behaviour with respect to spillover effect.

A further step that can be performed is to check vibration reduction as measured by the piezoelectric strain sensor instead of the laser vibrometer. In fact, as shown by Ferrari and Amabili [31], there is a complex relation between the two measurements, since minimization of the sensor signal is not desirable per se. Composite structures can indeed present local vibration modes in correspondence to the location of the control force. Therefore, a full study about this aspect is recommended to better understand the complex interaction of piezoelectric transducers with the controlled structure. In this case, an electro-mechanical model of the entire system would be required. However, this is a very complicated topic.

As a final recommendation, the fractional-order PPF could be applied to control large-amplitude vibrations causing non-linear behaviour in the structure. As shown by Zippo et al. [30], the standard integer-order PPF can deal with weakly non-linear vibrations, so applying the fractional-order PPF in this context could possibly show other benefits of using the proposed controller over the standard PPF. More details about this aspect are given in Appendix A.1.

A

Appendix

A.1 Non-linear Vibrations

Machines and mechanical structures in general are often subjected to multiple and changing dynamic loads, which can vary both in time and amplitude. In practice, the vibration response will not be necessarily linear, whereas it is likely to show non-linear behaviour.

Controllers that can tackle specifically non-linearities in a vibrating structure are not easy to design, both because of the complexity of the problem itself and of the complex dynamics of many structures in today's industry. Therefore a controller, designed to suppress linear vibrations, which can be inherently robust to also deal with a possible non-linear response is preferred in this case.

The initial research approach for this thesis consisted also of the following tasks:

- ▷ Performing Non-Linear Modal Analysis (NLMA) on the structure in order to identify its non-linear dynamic behaviour.
- ▷ Implementing the controller experimentally to suppress non-linear vibrations on the identified structure.

Due to complications with laboratory equipment management which influenced the time planning of the overall thesis work, these tasks could not be entirely completed. The NLMA has been performed to identify the structure non-linear response around the 1st natural frequency. Stepped-sine testing with different forcing loads was used for this task. The measurement system 'PAK MKII VibroAkustik Systeme' from MULLER-BBM was used to implement closed-loop control for the force applied by the shaker during the frequency sweep, and Polytec Laser Doppler Vibrometer was used to measure out-of-plane velocity response. In Figure A.1 experimental results are shown. The figure is made dimensionless by dividing the velocity amplitude by the thickness of the plate and the excitation frequency by the resonance frequency. Hardening response is observed for increasing forcing loads.

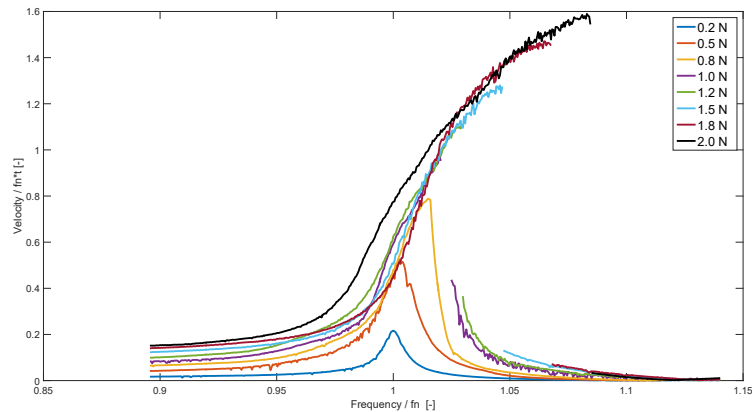


Figure A.1: Non-linear vibration response around the 1st natural frequency obtained using stepped-sine testing with different forcing loads.

Standard PPF controller has been already applied in literature for suppression of non-linear system vibrations (see [19, 30]), and it was proven to be efficient in dealing with weakly non-linear vibrations without substantial modification to the controller itself. So, as a recommendation for future research, it would be interesting to check the performance of the Fractional-order PPF proposed in this thesis in reducing large amplitude vibrations.

A.2 Modal Analysis software

The full experimental modal analysis could be completed with the aid of two software packages. The Polytec PSV software 9.2 has been used to take vibration measurements on the carbon plate. In Table A.1 the acquisition settings applied to take the measurements are listed.

Table A.1: Polytec PSV software acquisition settings.

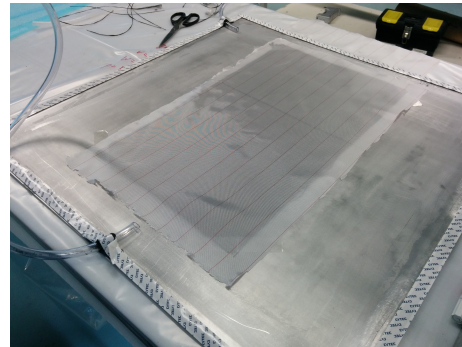
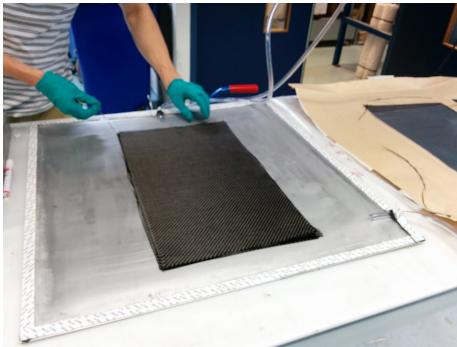
Velocity acquisition	VD-06 50 mm/s/V LP
Tracking filter	Off
Low Pass filter	1.5 MHz
High Pass filter	Off

Damping values and mode shapes validation could instead be obtained with ME'Scope software. The measurements taken with the Polytec system were imported in ME'Scope, where natural frequencies, damping ratios and mode shapes were calculated with Global Polynomial curve fitting method.

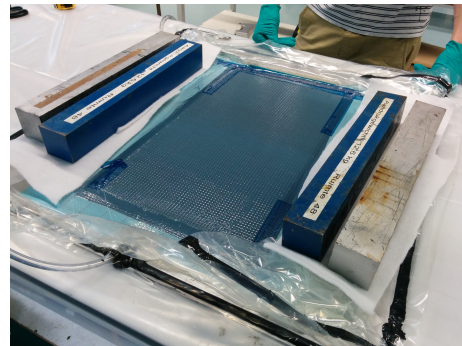
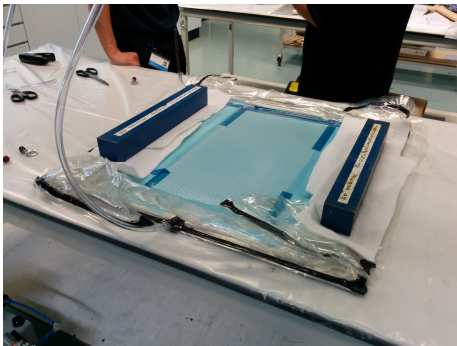
A.3 Carbon fibre/epoxy plate production process

The carbon fibre/epoxy composite plate has been produced at the 'Delft Aerospace Structures and Materials Laboratory' of the TU Delft Aerospace Engineering Department.

Vacuum Infusion Process (VIP) has been used for the panel production. The VIP is a technique that uses vacuum pressure to drive resin into a laminate. Materials are laid dry into the mold and the vacuum is applied before resin is introduced. Once a complete vacuum is achieved, resin is literally sucked into the laminate via carefully placed tubing. This process is aided by an assortment of supplies and materials. In Figure A.2 the production process steps are explained.



(a) 6 layers of 0-90° carbon-fibers are placed on top of an alluminium panel used as a reinforcement layers. It allows to separate other materials from structure. The alluminium panel is coated with the panel and provides a flat and shiny surface to release agent. Resin inlet and vacuum outlet tube the top of the final carbon panel. are placed in position.



(c) Full setup before resin infusion: on top of the peel ply, perforated foil and flow mesh are placed, figure, resin has already flown through the entire and vacuum bagging is applied. The flow mesh helps the resin flowing through the carbon layers. Weights are used to keep the panel straight after vacuum application. Panel edges are loosely secured with tape without applying extra pressure.

(d) Impregnation of tubes with epoxy resin. In this figure, resin has already flown through the entire and vacuum bagging is applied. Epoxy 04908 type is used.

Figure A.2: Carbon fibre/epoxy plate production process.

A.3.1 Material Properties

The carbon fibre/epoxy composite plate resulting from the production process has a length $l = 450$ mm, width $b = 250$ mm and thickness $t = 1.3$ mm.

In order to compute the material properties, the total density of the composite plate should be known. So the so-called *Rule of mixtures* is used. Besides the plate dimensions, the total weight of the plate was measured (0.220 Kg), and the densities of the epoxy glue and carbon fibres were known from datasheets (see B.6). The resulting material properties are listed in Table A.2.

Table A.2: Carbon fibre/epoxy plate material properties.

Property	Symbol	Value [Units]
Length	l	0.450 [m]
Width	b	0.250 [m]
Thickness	t	0.0013 [m]
Density	ρ	1504.27 [kg/m ³]
Young's modulus	$E_1 = E_2$	57.5 [GPa]
Poisson's ratio	ν_{12}	0.1 [-]
Shear modulus	G_{12}	3.8 [GPa]

A.4 MFC transducer bonding procedure

The bonding of the MFC transducer to the structure to be tested is very critical to ensure proper performance both for sensing and actuation. The bond should be as strong as possible, without air bubbles between transducer and structure, and possibly with a small amount of glue.

The MFC transducer has been applied to the composite plate using ARALDITE 2012 epoxy resin (see B.7). Before applying the glue, the gluing area of both structure and transducer are properly polished, then a very thin layer of glue is applied only to the structure and the transducer is pressed against it. A minimum of 2 hours curing time is necessary to have a proper bonding.

A.5 High Voltage wires

For safety reasons, high voltage wires with silicon rubber insulation and 3 kV voltage rating have been used for the application of high voltage to the MFC actuator.

It is important to have also very thin and lightweight wires in order not to add too much mass to the overall structure. Therefore the UL3239 wires from CnC Tech (see B.8) with an overall diameter of 1.55 mm have been selected.

A.6 COMSOL modelling

In this section, the modelling choices used in COMSOL to simulate the dynamic behaviour of the composite carbon fibre plate are explained. 'Structural Mechanics' module and 'Eigenfrequency Analysis' study have been used to obtain natural frequencies and mode shapes.

A.6.1 Carbon fibre/epoxy plate

The plate is modelled with 'Orthotropic' material properties. Geometrical dimensions and total density are the same as seen in Table A.2.

A.6.2 MFC piezoelectric patch transducer

An 'Eigenfrequency Analysis' study has been performed in COMSOL by modelling the effect of the addition of the MFC piezoelectric patch transducer. The MFC transducer is modelled with the 'Orthotropic' material properties given by Smart Material (see B.5). Only the active area of the MFC is modelled, and the epoxy glue used to bond the transducer on the plate is modelled as a 'Die Bond Adhesive'. The piezoelectric effect is not modelled since the purpose of this simulation is just to estimate the mass loading and stiffening effect on the plate due to application of the transducer.

A.7 Signal conditioning piezoelectric sensors

In this work, no conditioning hardware has been used to treat the output signal from the piezoelectric sensor. The signal was directly sent to the ADC of the dSPACE system and used as feedback for the control scheme.

However, in other studies involving vibration control (see [12, 31]), a charge amplifier is generally used to amplify and condition the signal from the piezoelectric sensor, which generates an electrical charge in response to mechanical movement. The reason for this is to have a proper phase behaviour out of the piezoelectric sensor signal.

In this work, phase behaviour problems have not been noticed. However, this appendix is meant as a guide to introduce the reader to all the experimental challenges in active vibration control in a broad sense. Therefore references about studies on signal conditioning piezoelectric sensors are listed here.

- ▶ Karki wrote an application report [35] which discusses the basic concepts of piezoelectric transducers used as sensors and two circuits which are commonly used for signal conditioning their output.
- ▶ Sirohi et al. [36] investigated the fundamental behaviour of piezoelectric strain sensors.
- ▶ Nagata et al. [37] studied instead the structural sensing and actuation properties of MFC transducers.
- ▶ Sathyanarayana et al. [38] proposed a procedure to use PZT sensors in vibration and load measurements.

A.8 Control system robustness against mistuning

In practical applications of Active Vibration Control, it is important to take into consideration possible changes on the structure dynamics due to different effects, like variations in temperature, operating conditions, etc.. These effect could for instance shift the natural frequency to be controlled and the controller would result to be mistuned. Therefore, it is desirable to have a control scheme which is robust to mistuning, or to possible natural frequency changes. The standard PPF compensator is proved to be robust in such circumstances (see [16]), and the fractional compensators proposed in this work have also been tested and compared to the standard PPF.

In Figure A.3 the second mode at 50 Hz of a simple plant is controlled first with controllers tuned at 45 and secondly with controllers tuned at 55 Hz. In both cases all compensators succeeded in controlling the second mode, resulting to be robust to mistuning. Moreover, the performance of the fractional filters results to be better than the one of the standard integer-order PPF regarding the spillover effect, as already shown in this thesis.

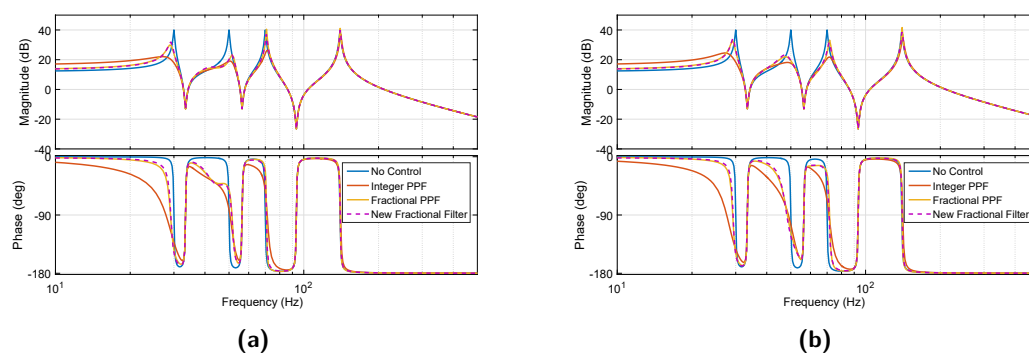


Figure A.3: Effect of filter mistuning on the closed-loop: (a) controlled natural frequency at 50 Hz and filters tuned at 45 Hz; (b) controlled natural frequency at 50 Hz and filters tuned at 55 Hz.

A.9 Controlled time response

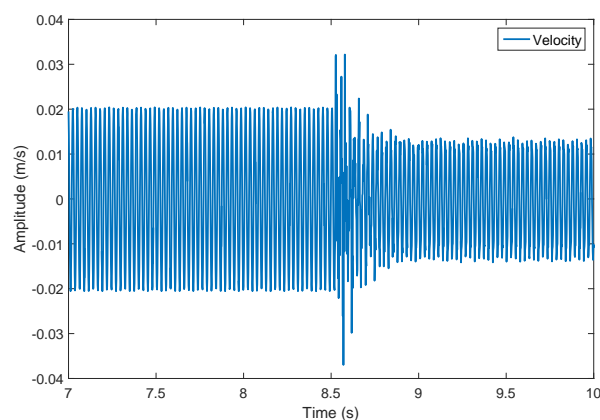


Figure A.4: Time history of velocity response for sinusoidal excitation at second natural frequency (38.5 Hz): fractional-order PPF is activated at approximately 8.6 s .

A.10 Effect of the long-time action of the piezoelectric actuator

The experimental implementation of the Active Vibration Control did not show problems related to spillover effect, as already shown in chapter 4. However a different problem has been found when performing long-time scans with the laser vibrometer: the piezoelectric transducer has been active for a long-time and its continuous mechanical action has caused a stiffening effect in some vibrations modes, as shown in Figure A.5.

This effect is not seen for single-point measurements for which the actuator remains active for a short amount of time, as it can be noticed from the results shown in chapter 4.

It is recommended to investigate better this effect, maybe with the help of a full electromechanical modelling of the interaction between the piezoelectric transducer and the structure.

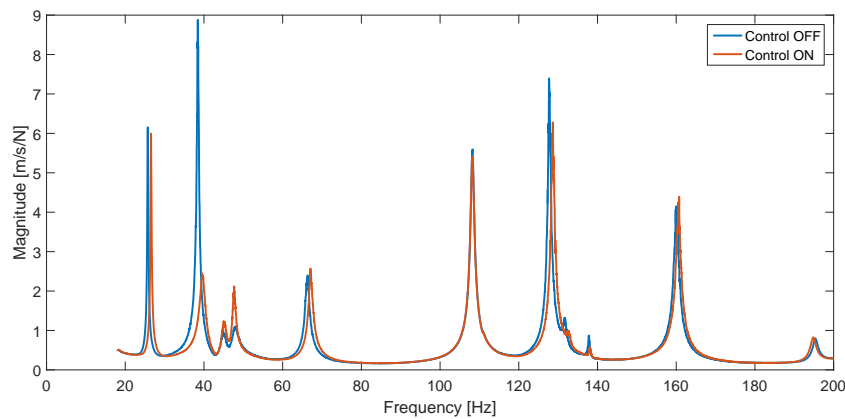


Figure A.5: Average spectrum of carbon fibre plate both with control off and on: the long-time action of the piezoelectric actuator causes frequency shifts in the uncontrolled modes.

In Table A.3, natural frequencies and damping ratios of the first 4 vibrations modes are compared for active and inactive control.

Table A.3: Natural frequencies and damping ratios comparison for active and inactive control.

Mode	Experiments, Control OFF - (Hz)	Experiments, Control ON - (Hz)	Damping ratio, Con- trol OFF - (%)	Damping ratio, Con- trol ON - (%)
1	25.72	26.4	0.38	0.40
2	38.53	39.53	0.38	0.80
3	66.38	66.90	0.79	0.89
4	108.30	108.30	0.45	0.45

A.11 CRONE implementation

The CRONE approximation has been implemented using the 'croneFD' function from the *ninteger* toolbox for MATLAB, by Duarte Valério [39].

The following function returns the CRONE approximation of s^α . Inputs are: fractional order α , frequency range $[\omega_l, \omega_h]$, and approximation order N .

```

1 function G = croneFD(alpha, wl, wh, N)
2 % function G = croneFD(alpha, wl, wh, N)
3 % Crone approximation of s^alpha; alpha may be any complex number.
4 % N poles and N zeros are placed in [wl,wh] rad/s.
5
6 % Duarte Valerio 2009
7
8 zeros = -wl * (wh/wl).^( (2*(1:N)-1-alpha) / (2*N) );
9 poles = -wl * (wh/wl).^( (2*(1:N)-1+alpha) / (2*N) );
10 G = tf(zpk(zeros, poles, 1));
11 wmean = sqrt(wl*wh);
12 if isreal(alpha)
13 G = G * abs((j*wmean)^alpha) / abs(squeeze(freqresp(G, wmean)));
14 else
15 G = G * ((j*wmean)^alpha) / squeeze(freqresp(G, wmean));
16 end

```

A.12 Simulink model

The Simulink model used for the dSPACE implementation is shown in Figure A.6.

Each controller can be activated by means of the gain block 'ON_OFF_switch' which is loaded as a switch button in the dSPACE environment. The sensor signal must be multiplied by 10 because it gets internally divided by 10 by the dSPACE Digital-to-Analog Converter (DAC). Similarly, the signal to the actuator must be multiplied by 0.1 because it gets multiplied by 10 by the dSPACE Analog-to-Digital Converter (ADC). A 2.5 V offset voltage is used to provide full operating range to the MFC actuator because the HV amplifier accepts input signals from -2.5 V to 7.5 V, and a saturation block is used to avoid out-of-range signals to the HV amplifier.

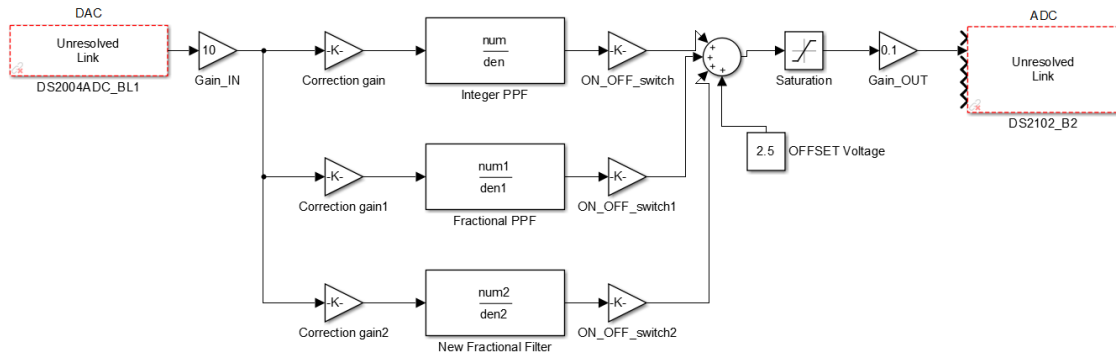


Figure A.6: Simulink block diagram.

A.13 Fractional-order PPF Optimization - MATLAB Code

In this Appendix, the MATLAB code used for optimization of the fractional-order PPF is listed. Only the code for filter #1 is shown for simplicity.

A.13.1 Objective

```

1 function h = objective(x)
2 % Computation of objective function
3 % Input:
4 % x : [1x4] row of design variables (x1, x2, x3, x4)
5 % Output:
6 % h : [...] scalar of objective function value
7 %% Initialization
8 wn = 2*pi*10; % natural frequency of Plant
9 freq = linspace(0,1.3*wn/2/pi,100000); % frequency vector
10 w=2*pi*freq;
11 s=1i*w; % Laplace transform variable
12 zeta = 0.005; % damping ratio of Plant
13 G = wn^2./(s.^2 + 2*zeta*wn*s + wn^2); % 1-DOF Plant
14 %% Assignment of design variables
15 alpha = x(1); % fractional-order
16 wf = x(2); % filter resonance frequency
17 zeta_f = x(3); % filter damping ratio
18 g = x(4); % filter gain
19 CF1 = 1./((s./wf).^(2*alpha)+2*zeta_f*(s./wf).^alpha +1); % Fractional-order PPF#1
20 T = G./(1-g*CF1.*G); % Closed-loop positive feedback
21 %% Objective function definition
22 w1 = 0.9995; w2 = 1-w1; % weights
23 p = 10; % penalization factor (can be chosen differently for each penalization)
24 Sg = 20*log10(abs(G(1))); % Static gain of Plant G at 0 Hz
25 [PK,zeta_HP] = damping_fun(T,freq,wn); % compute closed-loop damping
26 P1 = PK(1); Pmax = PK(2); P2 = PK(3);
27 % Objective + Penalization functions
28 h = w1*(Pmax - Sg) + w2*sum(abs((phase(T)-phase(G)))) + p*(max(0,P1/Pmax-1))^2 + ...
29 p*(max(0,P2/Pmax-1))^2 ...
30 + p*(max(0,Sg/P1-1))^2 + p*(max(0,Sg/P2-1))^2 + p*(max(0,zeta_HP - 1))^2;

```

A.13.2 Constraints

```

1 function [c,c_eq] = constraints(x)
2 % Input:
3 % x : [1x4] row of design variables (x1, x2, x3, x4)
4 % Output:
5 % c : inequality constraints (NONE) , c_eq : equality constraints
6 %% Initialization
7 wn = 2*pi*10; % natural frequency of Plant
8 zeta = 0.005; % damping ratio of Plant
9 s=tf('s'); % Laplace transform variable
10 G = wn^2/(s^2 + 2*zeta*wn*s + wn^2); % 1-DOF Plant
11 %% Assignment of design variables
12 alpha = x(1); % fractional-order
13 wf = x(2); % filter resonance frequency
14 zeta_f = x(3); % filter damping ratio
15 g = x(4); % filter gain
16 %% Fractional-order PPF approximation
17 SD = croneFD(alpha, 1e-5, 1e5, 10); % approximation of s^alpha using CRONE method
18 CF1 = g/(SD^2/wf^(2*alpha)+2*zeta_f*SD/wf^alpha+1); % Fractional-order PPF#1

```

```

19 T = G/(1-g*CF1*G); % Closed-loop positive feedback
20 %% Constraints definition
21 c = []; % no inequality constraints
22 p = length(find(pole(T)>0)); % number of unstable pole in the closed-loop
23 c_eq = p; % Equality constraints

```

A.13.3 Optimization

```

1 %% Fractional-order PPF Optimization
2 % Luca Marinangeli 4420144 - TU Delft - PME
3 % November 2016
4 %% Initialization
5 clear all
6 clc
7 %% Define lower and upper bounds
8 % Fractional-order PPF #1
9 % [ alpha , wf , zeta_f , g ]
10 LB = [0.8, 0.999*2*pi*10, 0.01, 0]; % lower bounds
11 UB = [1.5, 1.1*2*pi*10, 1, 1]; % upperbounds
12 %% starting point
13 x0 = [1, 2*pi*10, 0.5, 0.05]; % Filter #1
14 %% Global Search
15 options = ...
    optimoptions('fmincon','Algorithm','sqp','MaxFunEvals',10000,'MaxIter',1000,...
16 'TolX',1e-09,'TolCon',1e-09,'TolFun',1e-09);
17 % Create Optimization problem
18 problem = createOptimProblem('fmincon',...
19 'objective',@objective,...
20 'x0',x0,'ub',UB,'lb',LB,'nonlcon',@constraints,'options',...
21 options);
22 % Define Global Search
23 gs = GlobalSearch('Display','iter');
24 rng(14,'twister') % for reproducibility
25 [xeq, fval] = run(gs,problem)
26 %% Display results
27 alpha = xeq(1) % fractional-order
28 wf = xeq(2) % filter resonance frequency
29 zeta_f = xeq(3) % filter damping ratio
30 g = xeq(4) % filter gain

```


B

Datasheets

B.1 Vibration Exciter

PRODUCT DATA

Vibration Exciter — Type 4809

USES

- Calibration of accelerometers
- Vibration testing of small objects
- Educational demonstrations
- Mechanical impedance and mobility measurements

FEATURES

- Powered by Power Amplifier Type 2718
- Force rating 45 N (10 lbf) sine peak, 60 N with air cooling
- Frequency range 10 Hz to 20 kHz
- First axial resonance 20 kHz
- Maximum bare table acceleration 736 ms^{-2} (75 g), 981 ms^{-2} with air cooling
- Robust rectilinear guidance system
- Low cross motion and low distortion

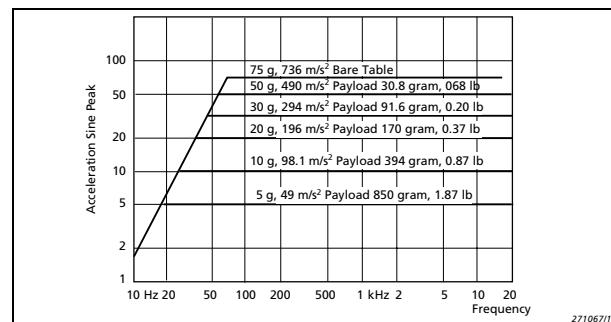


001103w

Description

Vibration Exciter Type 4809 is a small versatile instrument with an impressive performance. High quality materials ensure long term constructional reliability, and strict quality control results in consistent high performance. Type 4809 can be driven by any small power amplifier, with an input current up to a maximum 5 A and a sufficient voltage rating, without assisted cooling. The Brüel & Kjær Power Amplifier Type 2718, rated at 75 VA, has been designed specifically to drive Type 4809.

Fig. 1
Sine performance curves for Type 4809 operating without assisted cooling



4809

Brüel & Kjær

B.2 Impedance Head



MECHANICAL IMPEDANCE SENSOR		Revision: H ECN #: 29479
<p>OPTIONAL VERSIONS Optional versions have identical specifications and dimensions as listed for the standard model except where noted below. More than one option may be used.</p> <p>T - TEDS Capable of Digital Memory and Communication Compliant with IEEE P1451.4 TLA - TEDS LMS International - Free Format TLB - TEDS LMS International - Automotive Format TLC - TEDS LMS International - Aeronautical Format Output Bias Voltage 8 to 15 VDC</p> <p>TLD - TEDS Capable of Digital Memory and Communication Compliant with IEEE 1451.4</p>		
<p>NOTES: [1] Typical. [2] Zero-based, least-squares, straight line method.</p>		
<p>SUPPLIED ACCESSORIES: Model 080A Adhesive Mounting Base (1) Model 081B05 Mounting Stud (10-32 to 10-32) (2) Model HCS-3 NIST Traceable Calibration of Series 298 Impedance head (1) Model M081B05 Mounting Stud 10-32 to M6 X 0.75 (2)</p>		
<p>Entered: LS Engineer: PH Sales: WDC Approved: ESM Spec Number: Date: 10/3/08 Date: 10/21/08 Date: 10/21/08 Date: 10/21/08 6084</p>		
<p>PCB PIEZOTRONICS™ VIBRATION DIVISION 3425 Walden Avenue, Depew, NY 14043 Phone: 716-684-0001 Fax: 716-685-3888 E-Mail: vibration@pcb.com</p>		
<p>Performance Sensitivity(± 10 %)(Acceleration) Sensitivity(± 10 %)(Force) Measurement Range(Acceleration) Measurement Range(Force) Frequency Range(± 5 %)(Acceleration) Frequency Range(± 10 %)(Acceleration) Rise Time(Force) Resonant Frequency(Mounted) Resonant Frequency(Unmounted, no load) Phase Response(± 5 °) Bandwidth Resolution(1 to 10,000 Hz) Broadband Resolution Non-Linearity Transverse Sensitivity(to Acceleration) Maximum Force</p>	<p>ENGLISH 100 mV/g 100 mV/lb ± 50 g pk ± 50 lb pk 1 to 5000 Hz 0.7 to 7000 Hz <10 µsec ≥ 20 kHz >40 kHz 4 to 5000 Hz 0.002 g rms 0.002 lb ± 1 % ± 5 % 500 lb</p>	<p>SI 10.2 mV/(m/s²) 22.4 mV/N ± 480.5 m/s² pk ± 222.4 N pk 1 to 5000 Hz 0.7 to 7000 Hz <10 µ sec ≥ 20 kHz >40 kHz 4 to 5000 Hz 0.02 m/s² rms 0.0089 N ± 1 % ± 5 % 2224 N</p>
<p>Environmental Temperature Range(Operating) Temperature Response(on Acceleration) Temperature Response(on Force) Base Strain Sensitivity Maximum Shock Excitation Voltage Constant Current Excitation Discharge Time Constant(Acceleration) Discharge Time Constant(Force) Output Bias Voltage Output Impedance Output Polarity(Acceleration) Output Polarity(Force) Spectral Noise(1 Hz) Spectral Noise(10 Hz) Spectral Noise(100 Hz) Spectral Noise(1 kHz)</p>	<p>0 to +200 °F ± 0.05 %/F ± 0.03 %/F ≤ 0.0007 g/µe 3000 g pk 22 to 30 VDC 2 to 20 mA 0.4 to 1.5 sec ≥ 60 sec 8 to 14 VDC <250 ohm Positive Positive 200 µg/√Hz 50 µg/√Hz 10 µg/√Hz 3 µg/√Hz</p>	<p>-18 to +95 °C ≤ 0.09 %/°C ≤ 0.05 %/°C ≤ 0.007 (m/s²)/µe 29,430 m/s² pk 22 to 30 VDC 2 to 20 mA 0.4 to 1.5 sec ≥ 60 sec 8 to 14 VDC <250 ohm Positive Positive 1982 (µm/s²)/√Hz 480.5 (µm/s²)/√Hz 98.1 (µm/s²)/√Hz 29.4 (µm/s²)/√Hz</p>
<p>Physical Sensing Element(Acceleration) Sensing Element(Force) Sensing Geometry(Acceleration) Sensing Geometry(Force) Housing Material Sealing Size (hex. x Height) Weight Electrical Connector(Acceleration) Electrical Connector(Force) Mounting Thread(both ends) Mounting Torque End Plate Mass(Force) Stiffness</p>	<p>Ceramic Quartz Shear Compression Titanium Welded Hermelic 11/16 in x 0.820 in 0.68 oz 10-32 Coaxial Jack 10-32 Coaxial Jack 10-32 Female 10 to 20 in-lb 0.16 oz 2.0 lb/in</p>	<p>Ceramic Quartz Shear Compression Titanium Welded Hermelic 11/16 in x 20.83 mm 19.2 gm 10-32 Coaxial Jack 10-32 Coaxial Jack 10-32 Female 1.1 to 2.2 N-m 4.8 gm 0.35 kN/gm</p>
<p><i>All specifications are at room temperature unless otherwise specified. In the interest of constant product improvement, we reserve the right to change specifications without notice. ICP® is a registered trademark of PCB Group, Inc.</i></p>		

B.3 Polytec LDV System



Figure B.1: Polytec Scanning Vibrometer system, [40].

Table B.1: Scanning Head.

Model	PSV-400
Scanning frequency	40 kHz
Scanning range	$\pm 20^\circ R_x$ and R_y
Angular resolution	$< 0.002^\circ$
Angular stability	$< 0.01^\circ/\text{h}$
Working distance	> 0.4 m
Weight	7.5 Kg
Dimensions	365 mm \times 160 mm \times 190 mm

Table B.2: Vibrometer Controller.

Model	OFV-5000
Velocity ranges	2, 10, 50, 100, 1000 mm/s/V
Bandwidth	0.5 - 1.5 MHz
Analog low pass filters	2, 20, 100, 1500 kHz

B.4 dSPACE System

Table B.3: dSPACE system.

Hardware
DS1005 PPC Board
DS2004 High-Speed A/D Board
2× DS2102 D/A Board
DS817 PCI Link Board

B.5 Smart Material MFC

General technical information for the MFC

High-field ($|E| > 1\text{ kV/mm}$), biased-voltage-operation piezoelectric constants:

d_{33}^*	$4.6\text{E} + 02\text{ pC/N}$	$4.6\text{E} + 02\text{ pm/V}$
d_{31}^{**}	$-2.1\text{E} + 02\text{ pC/N}$	$-2.1\text{E} + 02\text{ pm/V}$

Low-field ($|E| < 1\text{ kV/mm}$), unbiased-operation piezoelectric constants:

d_{33}^*	$4.0\text{E} + 02\text{ pC/N}$	$4.0\text{E} + 02\text{ pm/V}$
d_{31}^{**}	$-1.7\text{E} + 02\text{ pC/N}$	$-1.7\text{E} + 02\text{ pm/V}$
Free-strain* per volt (low-field – high-field) for d_{33} MFC (P1)	$\sim 0.75 - 0.9\text{ ppm/V}$	$0.75 - 0.9\text{ ppm/V}$
Free-strain* per volt (low-field – high-field) for d_{31} MFC (P2)	$\sim 1.1 - 1.3\text{ ppm/V}$	$\sim 1.1 - 1.3\text{ ppm/V}$
Free-strain hysteresis*	~ 0.2	~ 0.2
DC poling voltage, V_{pol} for d_{33} MFC (P1)	+1500 V	+1500 V
DC poling voltage, V_{pol} for d_{31} MFC (P2)	+450 V	+450 V
Poled capacitance @ 1kHz, room temp, C_{pol} for d_{33} MFC (P1)	$\sim 0.30\text{ nF/cm}^2$	$\sim 1.94\text{ nF/in}^2$
Poled capacitance @ 1kHz, room temp, C_{pol} for d_{31} MFC (P2)	$\sim 7.8\text{ nF/cm}^2$	$\sim 50\text{ nF/in}^2$

Orthotropic Linear Elastic Properties (constant electric field):

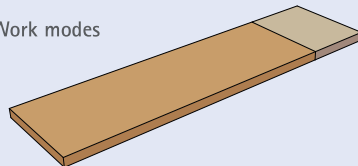
Tensile modulus, $E1^*$	30.336 GPa	4.4E + 06 psi
Tensile modulus, $E1^{**}$	15.857 GPa	2.3E + 06 psi
Poisson's ratio, ν_{12}	0.31	0.31
Poisson's ratio, ν_{21}	0.16	0.16
Shear modulus, G_{12} (rules-of-mixture estimate)	5.515 GPa	8.0E + 05 psi

Operational Parameters:

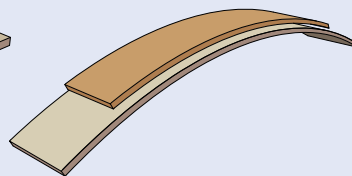
Maximum operational positive voltage, V_{max} for d_{33} MFC (P1)	+1500 V	+1500 V
Maximum operational positive voltage, V_{max} for d_{31} MFC (P2)	+360 V	+360 V
Maximum operational negative voltage, V_{min} for d_{33} MFC (P1)	500 V	-500 V
Maximum operational negative voltage, V_{min} for d_{31} MFC (P2)	-60 V	-60 V
Linear – elastic tensile strain limit	1000 ppm	1000 ppm
Maximum operational tensile strain	< 4500 ppm	< 4500 ppm
Peak work-energy density	1000 in – lb/in ³	$\sim 1000\text{ in – lb/in}^3$
Maximum operating temperature – Standard Version	< 80°C	< 176°F
Maximum operating temperature – HT Version	< 130°C	< 266°F
Operational lifetime (@ 1kVp-p)	> 10E + 09 cycles	> 10E + 09 cycles
Operational lifetime (@ 2kVp-p, 500VDC)	> 10E + 07 cycles	> 10E + 07 cycles
Operational bandwidth as actuator, high electric field	0Hz to 10 kHz	0Hz to 10 kHz
Operational bandwidth as actuator, low electric field	0Hz to 750kHz	0Hz to 750kHz
active Area Density	5.44 g/cm ³	5.44 g/cm ³
Thickness for all MFC Types	approx 0.3mm	approx. 12 mil

* Rod direction
** Electrode direction

Work modes



expansion

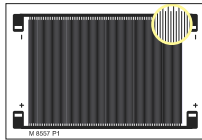


bending

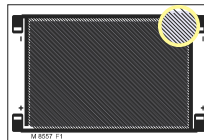


torsion

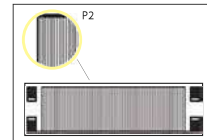
MFC Types specifications



d_{33} Actuators with expanding motion P1



d_{33} Actuators with twisting motion F1



d_{31} Actuators with contracting motion P2

MFC P1 / F1 Types (d_{33} effect actuators)



model	active length mm	active width mm	overall length mm	overall width mm	Capacitance nF	free strain ppm	blocking force N
P1–Types (0° fiber orientation)							
M-2503-P1	25	3	46	10	0.20	1050	28
M-2807-P1	28	7	40	18	0.54	1380	87
M-2814-P1	28	14	38	20	1.15	1550	195
M-4005-P1	40	5	50	11	0.38	1180	51
M-4010-P1	40	10	50	16	1.23	1400	126
M-4312-P1	43	12	60	21	2.03	1500	162
M-5628-P1	56	28	67	37	5.07	1800	450
M-8503-P1	85	3	110	14	0.64	1050	28
M-8507-P1	85	7	101	13	1.76	1380	87
M-8514-P1	85	14	101	20	3.39	1600	202
M-8528-P1	85	28	103	35	6.58	1800	454
M-8557-P1	85	57	103	64	12.84	1800	923
M-14003-P1	140	3	160	10	1.46	1050	28
F1–Types (45° fiber orientation)							
M-8528-F1	85	28	105	35	7.06	1350	485 calc.
M-8557-F1	85	57	105	64	13.26	1750	945 calc.

MFC P2 / P3 Types (d_{31} effect actuators)



model	active length mm	active width mm	overall length mm	overall width mm	Capacitance nF	free strain ppm	blocking force N
P2–Types (anisotropic)							
M-0714-P2	7	14	16	16	7.89	-600	-85
M-2807-P2	28	7	37	10	15.11	-650	-40
M-2814-P2	28	14	37	18	30.78	-700	-85
M-5628-P2	56	28	66	31	113.06	-820	-205
M-8503-P2	85	3	113	8	15.68	-480	-13
M-8507-P2	85	7	100	10	49.84	-670	-42
M-8514-P2	85	14	100	18	84.04	-700	-85
M-8528-P2	85	28	103	31	177.07	-820	-205
M-8557-P2	85	57	103	60	342.93	-840	-430
M-8585-P2	85	85	103	88	520.37	-842	-650
M-17007-P2	170	7	186	12	93.11	-670	-42
P3–Types (orthotropic)							
M-2814-P3	28	14	37	18	33.75	-750	-110
M-5628-P3	56	28	66	31	133.12	-900	-265
M-8528-P3	56	28	103	31	224.06	-900	-265

B.6 Carbon Fibre Properties

Quality Carbon Fibre		Commercial documentation - N°AQ.866 - 1 - Date: April 2006			
TORAYCA®		T 300 / FT 300			
Item	Property	Unit	Filaments	Nominal Value	
TORAYCA® Yarn Properties	Tensile Strength	MPa (kgf/mm ²)		3530 (360)	
	Tensile Modulus	GPa (10 ³ kgf/mm ²)		230 (23.5)	
	Elongation	%		1.5	
	Density		g/cm ³	1000	1.76
			g/cm ³	3000	1.76
			g/cm ³	6000	1.76
			g/cm ³	12000	1.76
	Yield		tex (g/1000 m)	1000	66
			tex (g/1000 m)	3000	198
			tex (g/1000 m)	6000	396
		tex (g/1000 m)	12000	800	
Specific Heat		cal/g.°C		0.19	
	Volume Resistivity	x 10 ⁻³ Ω.cm		1.7	
	0 ° Coef. of Thermal Expansion	x 10 ⁻⁶ °C ⁻¹		- 0.41	
0 ° Thermal Conductivity	cal/cm . s . °C			2.5 x 10 ⁻²	
Cross Sectional Area		mm ²	1000	0.04	
		mm ²	3000	0.11	
		mm ²	6000	0.23	
		mm ²	12000	0.45	
Filament Diameter		µm		7	
Composite Property (Resin System: 3631) (Measured Temp: RT)	0 ° Tensile Strength	MPa (kgf/mm ²)		1760 (180)	
	Tensile Modulus	GPa (10 ³ kgf/mm ²)		132 (13.5)	
	Elongation	%		1.3	
	0 ° Compressive Strength	MPa (kgf/mm ²)		1570 (160)	
	Compressive modulus	GPa (10 ³ kgf/mm ²)		125 (13.0)	
0 ° ILSS		MPa (kgf/mm ²)		110 (11)	

SOFICAR	SOFICAR
Sales Office	Head Office & plant
Sequana II - 87, quai Panhard et Levassor	Route de Lagor
75 634 Paris Cedex 13 - France	64 150 Abidos - France
Tel : 33 (0)1 56 61 12 80	Tel : 33 (0)5 59 60 71 00
Fax : 33 (0)1 53 79 99 01	Fax : 33 (0)5 59 60 71 10
E-mail : info@soficar-carbon.com	E-mail : info@soficar-carbon.com

B.7 Epoxy Adhesive for transducers bonding

Ciba Specialty Chemicals

Performance
Polymers

Structural Adhesives

Araldite® 2012 (AW 2104/HW 2934))

Two component epoxy paste adhesive

Key properties

- High shear and peel strength
- Tough and resilient
- Rapid curing
- Bonds a wide variety of materials

Description

Araldite 2012 is a rapid cure, multipurpose, two component, room temperature curing, high viscosity liquid adhesive of high strength and toughness.

It is suitable for bonding wide variety of metals, ceramics, glass, rubbers, rigid plastics, and most other materials in common use. It is a versatile adhesive for the craftsman as well as most industrial applications.

Product data

	2012/A	2012/B	2012 (mixed)
Colour (visual)	opaque	pale yellow	pale yellow
Specific gravity	1.16-1.18	1.15-1.18	ca 1.18
Viscosity (Pas)	25-45	20-40	typically 25-35
Pot Life (100 gm at 25°C)	-	-	4 minutes
Shelf life (2 - 40°C)	3 years	3 years	-

Processing

Pretreatment

The strength and durability of a bonded joint are dependant on proper pretreatment of the surfaces to be bonded.

At the very least, joint surfaces should be cleaned with a good degreasing agent such as acetone, trichloroethylene or proprietary degreasing agent in order to remove all traces of oil, grease and dirt.

Alcohol, gasoline (petrol) or paint thinners should never be used.

The strongest and most durable joints are obtained by either mechanically abrading or chemically etching ("pickling") the degreased surfaces. Abrading should be followed by a second degreasing treatment.

Mix ratio	Parts by weight	Parts by volume
Araldite 2012/A	100	100
Araldite 2012/B	100	100

Resin and hardener should be blended until they form a homogeneous mix.

Resin and hardener are also available in cartridges incorporating mixers and can be applied as ready-to-use adhesive with the aid of the tool recommended by Ciba.

Application of adhesive

The resin/hardener mix is applied directly or with a spatula, to the pretreated and dry joint surfaces.

A layer of adhesive 0.05 to 0.10 mm thick will normally impart the greatest lap shear strength to the joint.

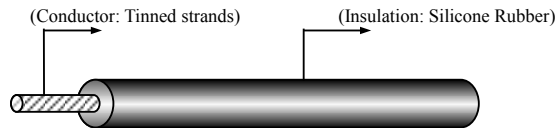
The joint components should be assembled and clamped as soon as the adhesive has been applied. An even contact pressure throughout the joint area will ensure optimum cure.

B.8 High Voltage Wires

CnC Tech
Industrial Cable and Connector Technology



P/N 3239-24-1-0500-0XX-1-TS



UL3239 - Silicone Rubber Wire 150°C 3KV (24 AWG)

CONSTRUCTION:	Tinned Strands, copper conductor, 11/0.16mm strands. Overall Diameter = 1.55mm (+ 0.10mm – 0.03mm) Insulation Thickness: 0.55mm			
CERTIFICATION & APPROVALS:	DUAL-RATED AWM: Can be used in USA and Canada UL Subject 758 UL FILE NO:E108485 CSA Standard CSA FILE NO:LL84687 Printed Markings: <i>"AWM 3239 150°C 3KVDC VW-1 24AWG E108485-S REIHSING CSA TYPE TV-3 150°C 3KVDC 24AWG LL84687 FT1 SILICONE RUBBER"</i> Passes UL VW-1 & CSA FT1 Vertical Flame Test.			
PHYSICAL & ELECTRICAL PROPERTIES:	Rated Temperature: 150°C ~ -50°C Rated Voltage: 3KV Insulation Potential Strength: 6000 VAC/min High flexibility: Soft silicone rubber material. Maximum Conductor Resistance: 88.6Ω/km Resistant to: Oil, extremes of hot & cold, flexing, high Voltage spikes.			
APPLICATIONS:	Silicone rubber wire, has high temperature resistance and high flexibility in confined spaces. Suitable for use in LED TVs, Laptops, Microwaves, Photocopiers, Scanners.			
PACKAGING:	500ft per reel.			
ENVIRONMENTAL APPROVALS:	Conforms to all current RoHS directives as laid out in EU Directive 2011/65/EC. Current SGS reports for this wire are available upon request.			
P/N's & COLORS				
3239-24-1-0500-001-1-TS BLACK	3239-24-1-0500-002-1-TS WHITE	3239-24-1-0500-003-1-TS YELLOW	3239-24-1-0500-004-1-TS RED	3239-24-1-0500-005-1-TS BLUE
3239-24-1-0500-006-1-TS BROWN	3239-24-1-0500-007-1-TS GREEN	3239-24-1-0500-008-1-TS ORANGE	3239-24-1-0500-010-1-TS VIOLET	3239-24-1-0500-011-1-TS GREEN + YELLOW

Bibliography

- [1] A. Preumont. *Vibration Control of Active Structures*, volume 179. 2011.
- [2] Peter Avitabile. Experimental Modal Analysis. *Sound and Vibration*, 35(1):20–31, 2001.
- [3] A.J. Moheimani, S.O.R. , and Fleming. *Piezoelectric Transducers for Vibration Control and Damping*. Advances in Industrial Control. Springer-Verlag, London, 2006.
- [4] M. J. Balas. Active control of flexible systems. *Journal of Optimization Theory and Applications*, 25(3):415–436, jul 1978.
- [5] M. J. Balas. Feedback control of flexible systems. *IEEE Transactions on Automatic Control*, 23(4):673–679, 1978.
- [6] Sang-Myeong Kim Sang-Myeong Kim, S Pietrzko, and M J Brennan. Active Vibration Isolation Using an Electrical Damper or an Electrical Dynamic Absorber. *IEEE Transactions on Control Systems Technology*, 16(2):245–254, 2008.
- [7] Ehsan Omid and S Nima Mahmoodi. Vibration control of collocated smart structures using H modified positive position and velocity feedback. *Journal of Vibration and Control*, (February), 2014.
- [8] Ibrahim Furkan Lüleci. *Active vibration control of beam and plates by using piezoelectric patch actuators*. Master thesis, Middle East Technical University, 2013.
- [9] Sang-Myeong Kim, Semyung Wang, and Michael J Brennan. Comparison of negative and positive position feedback control of a flexible structure. *Smart Materials and Structures*, 20(1):015011, 2010.
- [10] Chuen Jin Goh. *Analysis and Control of Quasi-Distributed Parameter Systems*. Phd thesis, California Institute of Technology, 1983.
- [11] J. L. Fanson. *An Experimental Investigation of Vibration Suppression in Large Space Structures Using Positive Position Feedback*. Phd thesis, California Institute of Technology, 1987.
- [12] Moon K. Kwak and Seok Heo. Active vibration control of smart grid structure by multiinput and multioutput positive position feedback controller. *Journal of Sound and Vibration*, 304(1-2):230–245, 2007.
- [13] S. Poh and A. Baz. Active Control of a Flexible Structure Using a Modal Positive Position Feedback Controller. *Journal of Intelligent Material Systems and Structures*, 1(3):273–288, 1990.
- [14] A Baz, S Poh, and J Fedor. Independent Modal Space Control with Positive Position Feedback. *Journal Of Dynamic Systems Measurement And Control-Transactions of the ASME*, 114(1):96–103, 1992.

- [15] Mark McEver and Donald J. Leo. Autonomous Vibration Suppression Using On-Line Pole-Zero Identification. *Journal of Vibration and Acoustics*, 123(4):487, 2001.
- [16] G. Song, S. P. Schmidt, and B. N. Agrawal. Experimental Robustness Study of Positive Position Feedback Control for Active Vibration Suppression. *Journal of Guidance, Control, and Dynamics*, 25(1):179a–182, 2002.
- [17] Seok Kwak, Moon K. and Han, Sang-Bo and Heo. The Stability Conditions, Performance and Design Methodology for the Positive Position Feedback Controller. *Transaction of the Korean Society for Noise and Vibration Engineering*, 14(3):208–213, 2004.
- [18] Ming Yuan, Jinhao Qiu, Hongli Ji, Weiyinuo Zhou, and Roger Ohayon. Active control of sound transmission using a hybrid/blind decentralized control approach. *Journal of Vibration and Control*, 21(13):2661–2684, 2015.
- [19] W. a. El-Ganaini, N. a. Saeed, and M. Eissa. Positive position feedback (PPF) controller for suppression of nonlinear system vibration. *Nonlinear Dynamics*, 72(3):517–537, 2013.
- [20] Adam K. Smith. *Adaptive Resonant Mode Active Noise Control*. Master’s thesis, University of Pittsburgh, 2006.
- [21] M. a. Creasy, D. J. Leo, and K. M. Farinholt. Adaptive positive position feedback for actively absorbing energy in acoustic cavities. *Journal of Sound and Vibration*, 311(1-2):461–472, 2008.
- [22] M. Austin Creasy, Donald J. Leo, and Kevin M. Farinholt. Adaptive Collocated Feedback for Noise Absorption in Payload Fairings. *Journal of Spacecraft and Rockets*, 45(3):592–599, 2008.
- [23] S N Mahmoodi, M Ahmadian, and D J Inman. Adaptive Modified Positive Position Feedback for Active Vibration Control of Structures. *Journal of Intelligent Material Systems and Structures*, 21(6):571–580, 2010.
- [24] R Orszulik and J J Shan. Multi-Mode Adaptive Positive Position Feedback: An Experimental Study. *2011 American Control Conference*, pages 3315–3319, 2011.
- [25] Sumeet S Aphale, Andrew J Fleming, and S O Reza Moheimani. Integral resonant control of collocated smart structures. *Smart Materials and Structures*, 16(2):439–446, apr 2007.
- [26] Douglas Russell, Student Member, Andres San-millan, Vicente Feliu, Senior Member, and Sumeet S Aphale. Butterworth pattern based simultaneous damping and tracking controller designs for nanopositioning systems. pages 1082–1087, 2015.
- [27] Macro Fiber Composite - MFC, in: *S.M. Corporation (Ed.)* <http://www.smart-material.com/MFC-product-main.html>.
- [28] Piezo Patch Transducers: DuraAct Flexible Piezoelectric Transducers for Energy Harvesting, in: *P. Instrumente (Ed.)* <http://www.duraact.net>.
- [29] Changjoo Shin, Chinsuk Hong, and Weui Bong Jeong. Active vibration control of clamped beams using positive position feedback controllers with moment pair. *Journal of Mechanical Science and Technology*, 26(3):731–740, 2012.
- [30] Antonio Zippo, Giovanni Ferrari, Marco Amabili, Marco Barbieri, and Francesco Pellicano. Active vibration control of a composite sandwich plate. *Composite Structures*, 128:100–114, 2015.
- [31] Giovanni Ferrari and Marco Amabili. Active vibration control of a sandwich plate by non-collocated positive position feedback. *Journal of Sound and Vibration*, 342:44–56, apr 2015.

- [32] V. Gupta, M. Sharma, and N. Thakur. Optimization Criteria for Optimal Placement of Piezoelectric Sensors and Actuators on a Smart Structure: A Technical Review. *Journal of Intelligent Material Systems and Structures*, 21(12):1227–1243, 2010.
- [33] K. D. Dhuri and P. Seshu. Multi-objective optimization of piezo actuator placement and sizing using genetic algorithm. *Journal of Sound and Vibration*, 323(3-5):495–514, 2009.
- [34] Li Bin, Li Yugang, Yin Xuegang, and Huang Shanglian. Maximal Modal Force Rule for Optimal Placement of Point Piezoelectric Actuators for Plates. *Journal of Intelligent Material Systems and Structures*, 11(7):512–515, 2000.
- [35] James Karki. Signal Conditioning Piezoelectric Sensors. *App. rept. on mixed signal products (sloa033a)*, Texas Instruments Incorporated, 48(September):1–6, 2000.
- [36] Jayant Sirohi and Inderjit Chopra. Fundamental Understanding of Piezoelectric Strain Sensors. *Journal of Intelligent Materials Systems and Structures*, 11(4):246–257, 2000.
- [37] Yoshinori Nagata, Seokyong Park, and Aiguo Ming. Structural sensing and actuation utilizing macro fiber composite. *2006 IEEE International Conference on Robotics and Biomimetics, ROBIO 2006*, 0069(4):1275–1280, 2006.
- [38] C. N. Sathyanarayana, S. Raja, and H. M. Ragavendra. Procedure to Use PZT Sensors in Vibration and Load Measurements. *Smart Materials Research*, 2013:1–9, 2013.
- [39] Valério D and Sá Da Costa J (2004) Ninteger: a non-integer control toolbox for Matlab. *Proceedings of the Fractional Differentiation and its Applications, Bordeaux* .
- [40] Polytec Scanning Vibrometer System <http://www.polytec.com/eu/>.

